African Journal of Biotechnology

Volume 17 Number 7, 14 February, 2018

ISSN 1684-5315

Academic Journals

ABOUT AJB

The African Journal of Biotechnology (AJB) (ISSN 1684-5315) is published weekly (one volume per year) by Academic Journals.

African Journal of Biotechnology (AJB), a new broad-based journal, is an open access journal that was founded on two key tenets: To publish the most exciting research in all areas of applied biochemistry, industrial microbiology, molecular biology, genomics and proteomics, food and agricultural technologies, and metabolic engineering. Secondly, to provide the most rapid turn-around time possible for reviewing and publishing, and to disseminate the articles freely for teaching and reference purposes. All articles published in AJB are peer-reviewed.

Contact Us

Editorial Office: ajb@academicjournals.org

Help Desk: helpdesk@academicjournals.org

Website: http://www.academicjournals.org/journal/AJB

Submit manuscript online http://ms.academicjournals.me/

Editor-in-Chief

George Nkem Ude, Ph.D
Plant Breeder & Molecular Biologist
Department of Natural Sciences
Crawford Building, Rm 003A
Bowie State University
14000 Jericho Park Road
Bowie, MD 20715, USA

Editor

N. John Tonukari, Ph.D
Department of Biochemistry
Delta State University
PMB 1
Abraka, Nigeria

Associate Editors

Prof. Dr. AE Aboulata
Plant Path. Res. Inst., ARC, POBox 12619, Giza, Egypt
30 D, El-Karama St., Alf Maskan, P.O. Box 1567,
Ain Shams, Cairo,
Egypt

Dr. S.K Das
Department of Applied Chemistry and Biotechnology, University of Fukui,
Japan

Prof. Okoh, A. I.
Applied and Environmental Microbiology Research Group (AEMREG),
Department of Biochemistry and Microbiology,
University of Fort Hare.
P/Bag X1314 Alice 5700,
South Africa

Dr. Ismail TURKOGLU
Department of Biology Education, Education Faculty, Fırat University, Elazığ, Turkey

Prof T.K.Raja, PhD FRSC (UK)
Department of Biotechnology
PSG COLLEGE OF TECHNOLOGY (Autonomous)
(Affiliated to Anna University)
Coimbatore-641004, Tamilnadu, INDIA.

Dr. George Edward Mamati
Horticulture Department,
Jomo Kenyatta University of Agriculture
and Technology,
P. O. Box 62000-00200,
Nairobi, Kenya.

Dr. Gitonga
Kenya Agricultural Research Institute,
National Horticultural Research Center,
P.O Box 220,
Thika, Kenya

Editorial Board

Prof. Sagadevan G. Mundree

Department of Molecular and Cell Biology
University of Cape Town
Private Bag Rondebosch 7701
South Africa

Dr. Martin Fregene

Centro Internacional de Agricultura Tropical (CIAT)
Km 17 Cali-Palmira Recta
AA6713, Cali, Colombia

Prof. O. A. Ogunseitan

Laboratory for Molecular Ecology
Department of Environmental Analysis and Design
University of California,
Irvine, CA 92697-7070. USA

Dr. Ibrahima Ndoye

UCAD, Faculte des Sciences et Techniques
Departement de Biologie Vegetale
BP 5005, Dakar, Senegal.
Laboratoire Commun de Microbiologie
IRD/ISRA/UCAD
BP 1386, Dakar

Dr. Bamidele A. Iwalokun

Biochemistry Department
Lagos State University
P.M.B. 1087. Apapa – Lagos, Nigeria

Dr. Jacob Hodeba Mignouna

Associate Professor, Biotechnology
Virginia State University
Agricultural Research Station Box 9061
Petersburg, VA 23806, USA

Dr. Bright Ogheneovo Agindotan

Plant, Soil and Entomological Sciences Dept
University of Idaho, Moscow
ID 83843, USA

Dr. A.P. Njukeng

Département de Biologie Végétale
Faculté des Sciences
B.P. 67 Dschang
Université de Dschang
Rep. du CAMEROUN

Dr. E. Olatunde Farombi

Drug Metabolism and Toxicology Unit
Department of Biochemistry
University of Ibadan, Ibadan, Nigeria

Dr. Stephen Bakiamoh

Michigan Biotechnology Institute International
3900 Collins Road
Lansing, MI 48909, USA

Dr. N. A. Amusa

Institute of Agricultural Research and Training
Obafemi Awolowo University
Moor Plantation, P.M.B 5029, Ibadan, Nigeria

Dr. Desouky Abd-El-Haleem

Environmental Biotechnology Department &
Bioprocess Development Department,
Genetic Engineering and Biotechnology Research
Institute (GEBRI),
Mubarak City for Scientific Research and Technology
Applications,
New Burg-Elarab City, Alexandria, Egypt.

Dr. Simeon Oloni Kotchoni

Department of Plant Molecular Biology
Institute of Botany, Kirschallee 1,
University of Bonn, D-53115 Germany.

Dr. Eriola Betiku

German Research Centre for Biotechnology,
Biochemical Engineering Division,
Mascheroder Weg 1, D-38124,
Braunschweig, Germany

Dr. Daniel Masiga

International Centre of Insect Physiology and Ecology,
Nairobi,
Kenya

Dr. Essam A. Zaki

Genetic Engineering and Biotechnology Research
Institute, GEBRI,
Research Area,
Borg El Arab, Post Code 21934, Alexandria
Egypt

Dr. Alfred Dixon
International Institute of Tropical Agriculture (IITA)
PMB 5320, Ibadan
Oyo State, Nigeria

Dr. Sankale Shompole
Dept. of Microbiology, Molecular Biology and Biochemisty,
University of Idaho, Moscow,
ID 83844, USA.

Dr. Mathew M. Abang
Germplasm Program
International Center for Agricultural Research in the Dry Areas
(ICARDA)
P.O. Box 5466, Aleppo, SYRIA.

Dr. Solomon Olawale Odemuyiwa
Pulmonary Research Group
Department of Medicine
550 Heritage Medical Research Centre
University of Alberta
Edmonton
Canada T6G 2S2

Prof. Anna-Maria Botha-Oberholster
Plant Molecular Genetics
Department of Genetics
Forestry and Agricultural Biotechnology Institute
Faculty of Agricultural and Natural Sciences
University of Pretoria
ZA-0002 Pretoria, South Africa

Dr. O. U. Ezeronye
Department of Biological Science
Michael Okpara University of Agriculture
Umudike, Abia State, Nigeria.

Dr. Joseph Hounhouigan
Maître de Conférence
Sciences et technologies des aliments
Faculté des Sciences Agronomiques
Université d'Abomey-Calavi
01 BP 526 Cotonou
République du Bénin

Prof. Christine Rey
Dept. of Molecular and Cell Biology,
University of the Witwatersand,
Private Bag 3, WITS 2050, Johannesburg, South Africa

Dr. Kamel Ahmed Abd-Elsalam
Molecular Markers Lab. (MML)
Plant Pathology Research Institute (PPathRI)
Agricultural Research Center, 9-Gamma St., Orman, 12619,
Giza, Egypt

Dr. Jones Lemchi
International Institute of Tropical Agriculture (IITA)
Onne, Nigeria

Prof. Greg Blatch
Head of Biochemistry & Senior Wellcome Trust Fellow
Department of Biochemistry, Microbiology & Biotechnology
Rhodes University
Grahamstown 6140
South Africa

Dr. Beatrice Kilel
P.O Box 1413
Manassas, VA 20108
USA

Dr. Jackie Hughes
Research-for-Development
International Institute of Tropical Agriculture (IITA)
Ibadan, Nigeria

Dr. Robert L. Brown
Southern Regional Research Center,
U.S. Department of Agriculture,
Agricultural Research Service,
New Orleans, LA 70179.

Dr. Deborah Rayfield
Physiology and Anatomy
Bowie State University
Department of Natural Sciences
Crawford Building, Room 003C
Bowie MD 20715,USA

Dr. Marlene Shehata
University of Ottawa Heart Institute
Genetics of Cardiovascular Diseases
40 Ruskin Street
K1Y-4W7, Ottawa, ON, CANADA

Dr. Hany Sayed Hafez
The American University in Cairo,
Egypt

Dr. Clement O. Adebooye
Department of Plant Science
Obafemi Awolowo University, Ile-Ife
Nigeria

Dr. Ali Demir Sezer
Marmara Üniversitesi Eczacilik Fakültesi,
Tibbiye cad. No: 49, 34668, Haydarpasa, Istanbul,
Turkey

Dr. Ali Gazanchain
P.O. Box: 91735-1148, Mashhad,
Iran.

Dr. Anant B. Patel
Centre for Cellular and Molecular Biology
Uppal Road, Hyderabad 500007
India

Prof. Arne Elofsson
Department of Biophysics and Biochemistry
Bioinformatics at Stockholm University,
Sweden

Prof. Bahram Goliaei
Departments of Biophysics and Bioinformatics
Laboratory of Biophysics and Molecular Biology
University of Tehran, Institute of Biochemistry and Biophysics
Iran

Dr. Nora Babudri
Dipartimento di Biologia cellulare e ambientale
Università di Perugia
Via Pascoli
Italy

Dr. S. Adesola Ajayi
Seed Science Laboratory
Department of Plant Science
Faculty of Agriculture
Obafemi Awolowo University
Ile-Ife 220005, Nigeria

Dr. Yee-Joo TAN
Department of Microbiology
Yong Loo Lin School of Medicine,
National University Health System (NUHS),
National University of Singapore
MD4, 5 Science Drive 2,
Singapore 117597
Singapore

Prof. Hidetaka Hori
Laboratories of Food and Life Science,
Graduate School of Science and Technology,
Niigata University.
Niigata 950-2181,
Japan

Prof. Thomas R. DeGregori
University of Houston,
Texas 77204 5019,
USA

Dr. Wolfgang Ernst Bernhard Jelkmann
Medical Faculty, University of Lübeck,
Germany

Dr. Moktar Hamdi
Department of Biochemical Engineering,
Laboratory of Ecology and Microbial Technology
National Institute of Applied Sciences and Technology.
BP: 676. 1080,
Tunisia

Dr. Salvador Ventura
Department de Bioquímica i Biologia Molecular
Institut de Biotecnologia i de Biomedicina
Universitat Autònoma de Barcelona
Bellaterra-08193
Spain

Dr. Claudio A. Hetz
Faculty of Medicine, University of Chile
Independencia 1027
Santiago, Chile

Prof. Felix Dapare Dakora
Research Development and Technology Promotion
Cape Peninsula University of Technology,
Room 2.8 Admin. Bldg. Keizersgracht, P.O. 652, Cape Town 8000,
South Africa

Dr. Geremew Bultosa
Department of Food Science and Post harvest Technology
Haramaya University
Personal Box 22, Haramaya University Campus
Dire Dawa,
Ethiopia

Dr. José Eduardo Garcia
Londrina State University
Brazil

Prof. Nirbhay Kumar
Malaria Research Institute
Department of Molecular Microbiology and Immunology
Johns Hopkins Bloomberg School of Public Health
E5144, 615 N. Wolfe Street
Baltimore, MD 21205

Prof. M. A. Awal
Department of Anatomy and Histplogy,
Bangladesh Agricultural University,
Mymensingh-2202,
Bangladesh

Prof. Christian Zwieb
Department of Molecular Biology
University of Texas Health Science Center at Tyler
11937 US Highway 271
Tyler, Texas 75708-3154
USA

Prof. Danilo López-Hernández
Instituto de Zoología Tropical, Facultad de Ciencias,
Universidad Central de Venezuela.
Institute of Research for the Development (IRD),
Montpellier,
France

Prof. Donald Arthur Cowan
Department of Biotechnology,
University of the Western Cape Bellville 7535 Cape Town, South Africa

Dr. Ekhaise Osaro Frederick
University Of Benin, Faculty of Life Science
Department of Microbiology
P. M. B. 1154, Benin City, Edo State,
Nigeria.

Dr. Luísa Maria de Sousa Mesquita Pereira
IPATIMUP R. Dr. Roberto Frias, s/n 4200-465 Porto
Portugal

Dr. Min Lin
Animal Diseases Research Institute
Canadian Food Inspection Agency
Ottawa, Ontario,
Canada K2H 8P9

Prof. Nobuyoshi Shimizu
Department of Molecular Biology,
Center for Genomic Medicine
Keio University School of Medicine,
35 Shinanomachi, Shinjuku-ku
Tokyo 160-8582,
Japan

Dr. Adewunmi Babatunde Idowu
Department of Biological Sciences
University of Agriculture Abia
Abia State,
Nigeria

Dr. Yifan Dai
Associate Director of Research
Revivicor Inc.
100 Technology Drive, Suite 414
Pittsburgh, PA 15219
USA

Dr. Zhongming Zhao
Department of Psychiatry, PO Box 980126,
Virginia Commonwealth University School of Medicine,
Richmond, VA 23298-0126,
USA

Prof. Giuseppe Novelli
Human Genetics,
Department of Biopathology,
Tor Vergata University, Rome,
Italy

Dr. Moji Mohammadi
402-28 Upper Canada Drive
Toronto, ON, M2P 1R9 (416) 512-7795
Canada

Prof. Jean-Marc Sabatier
Directeur de Recherche Laboratoire ERT-62
Ingénierie des Peptides à Visée Thérapeutique,
Université de la Méditerranée-Ambrilia
Biopharma inc.,
Faculté de Médecine Nord, Bd Pierre Dramard,
13916,
Marseille cédex 20.
France

Dr. Fabian Hoti
PneumoCarr Project
Department of Vaccines
National Public Health Institute
Finland

Prof. Irina-Draga Caruntu
Department of Histology
Gr. T. Popa University of Medicine and Pharmacy
16, Universitatii Street, Iasi,
Romania

Dr. Dieudonné Nwaga
Soil Microbiology Laboratory,
Biotechnology Center. PO Box 812,
Plant Biology Department,
University of Yaoundé I, Yaoundé,
Cameroon

Dr. Gerardo Armando Aguado-Santacruz
Biotechnology CINVESTAV-Unidad Irapuato
Departamento Biotecnología
Km 9.6 Libramiento norte Carretera
Irapuato-León Irapuato,
Guanajuato 36500
Mexico

Dr. Abdolkaim H. Chehregani
Department of Biology
Faculty of Science
Bu-Ali Sina University
Hamedan,
Iran

Dr. Abir Adel Saad
Molecular oncology
Department of Biotechnology
Institute of graduate Studies and Research
Alexandria University,
Egypt

Dr. Azizul Baten
Department of Statistics
Shah Jalal University of Science and Technology
Sylhet-3114,
Bangladesh

Dr. Bayden R. Wood
Australian Synchrotron Program
Research Fellow and Monash Synchrotron
Research Fellow Centre for Biospectroscopy
School of Chemistry Monash University Wellington
Rd. Clayton,
3800 Victoria,
Australia

Dr. G. Reza Balali
Molecular Mycology and Plant Pthology
Department of Biology
University of Isfahan
Isfahan
Iran

Dr. Beatrice Kilel
P.O Box 1413
Manassas, VA 20108
USA

Prof. H. Sunny Sun
Institute of Molecular Medicine
National Cheng Kung University Medical College
1 University road Tainan 70101,
Taiwan

Prof. Ima Nirwana Soelaiman
Department of Pharmacology
Faculty of Medicine
Universiti Kebangsaan Malaysia
Jalan Raja Muda Abdul Aziz
50300 Kuala Lumpur,
Malaysia

Prof. Tunde Ogunsanwo
Faculty of Science,
Olabisi Onabanjo University,
Ago-Iwoye.
Nigeria

Dr. Evans C. Egwim
Federal Polytechnic,
Bida Science Laboratory Technology Department,
PMB 55, Bida, Niger State,
Nigeria

Prof. George N. Goulielmos
Medical School,
University of Crete
Voutes, 715 00 Heraklion, Crete,
Greece

Dr. Uttam Krishna
Cadila Pharmaceuticals limited ,
India 1389, Tarsad Road,
Dholka, Dist: Ahmedabad, Gujarat,
India

Prof. Mohamed Attia El-Tayeb Ibrahim
Botany Department, Faculty of Science at Qena,
South Valley University, Qena 83523,
Egypt

Dr. Nelson K. Ojijo Olang'o
Department of Food Science & Technology,
JKUAT P. O. Box 62000, 00200, Nairobi,
Kenya

Dr. Pablo Marco Veras Peixoto
University of New York NYU College of Dentistry
345 E. 24th Street, New York, NY 10010
USA

Prof. T E Cloete
University of Pretoria Department of Microbiology
and Plant Pathology,
University of Pretoria,
Pretoria,
South Africa

Prof. Djamel Saidi
Laboratoire de Physiologie de la Nutrition et de Sécurité
Alimentaire Département de Biologie,
Faculté des Sciences,
Université d'Oran, 31000 - Algérie
Algeria

Dr. Tomohide Uno
Department of Biofunctional chemistry,
Faculty of Agriculture Nada-ku,
Kobe., Hyogo, 657-8501,
Japan

Dr. Ulises Urzúa
Faculty of Medicine,
University of Chile Independencia 1027, Santiago,
Chile

Dr. Aritua Valentine
National Agricultural Biotechnology Center,
Kawanda
Agricultural Research Institute (KARI)
P.O. Box, 7065, Kampala,
Uganda

Prof. Yee-Joo Tan
Institute of Molecular and Cell Biology 61 Biopolis Drive,
Proteos, Singapore 138673
Singapore

Prof. Viroj Wiwanitkit
Department of Laboratory Medicine,
Faculty of Medicine, Chulalongkorn University,
Bangkok
Thailand

Dr. Thomas Silou
Universit of Brazzaville BP 389
Congo

Prof. Burtram Clinton Fielding
University of the Western Cape
Western Cape,
South Africa

Dr. Brnčić (Brncic) Mladen
Faculty of Food Technology and Biotechnology,
Pierottijeva 6,
10000 Zagreb,
Croatia.

Dr. Meltem Sesli
College of Tobacco Expertise,
Turkish Republic, Celal Bayar University 45210,
Akhisar, Manisa,
Turkey.

Dr. Idress Hamad Attitalla
Omar El-Mukhtar University,
Faculty of Science,
Botany Department,
El-Beida, Libya.

Dr. Linga R. Gutha
Washington State University at Prosser,
24106 N Bunn Road,
Prosser WA 99350-8694

Dr Helal Ragab Moussa
Bahnay, Al-bagour, Menoufia,
Egypt.

Dr VIPUL GOHEL
DuPont Industrial Biosciences
Danisco (India) Pvt Ltd
5th Floor, Block 4B,
DLF Corporate Park
DLF Phase III
Gurgaon 122 002
Haryana (INDIA)

Dr. Sang-Han Lee
Department of Food Science & Biotechnology,
Kyungpook National University
Daegu 702-701,
Korea.

Dr. Bhaskar Dutta
DoD Biotechnology High Performance Computing
Software Applications
Institute (BHSAI)
U.S. Army Medical Research and Materiel Command
2405 Whittier Drive
Frederick, MD 21702

Dr. Muhammad Akram
Faculty of Eastern Medicine and Surgery,
Hamdard Al-Majeed College of Eastern Medicine,
Hamdard University,
Karachi.

Dr. M. Muruganandam
Departtment of Biotechnology
St. Michael College of Engineering & Technology,
Kalayarkoil,
India.

Dr. Gökhan Aydin
Suleyman Demirel University,
Atabey Vocational School,
Isparta-Türkiye,

Dr. Rajib Roychowdhury
Centre for Biotechnology (CBT),
Visva Bharati,
West-Bengal,
India.

Dr Takuji Ohyama
Faculty of Agriculture, Niigata University

Dr Mehdi Vasfi Marandi
University of Tehran

Dr FÜgen DURLU-ÖZKAYA
Gazi Üniversity, Tourism Faculty, Dept. of
Gastronomy and Culinary Art

Dr. Reza Yari
Islamic Azad University, Boroujerd Branch

Dr Zahra Tahmasebi Fard
Roudehen branche, Islamic Azad University

Dr Albert Magrí
Giro Technological Centre

Dr Ping ZHENG
Zhejiang University, Hangzhou, China

Dr. Kgomotso P. Sibeko
University of Pretoria

Dr Greg Spear
Rush University Medical Center

Prof. Pilar Morata
University of Malaga

Dr Jian Wu
Harbin medical university , China

Dr Hsiu-Chi Cheng
National Cheng Kung University and Hospital.

Prof. Pavel Kalac
University of South Bohemia, Czech Republic

Dr Kürsat Korkmaz
Ordu University, Faculty of Agriculture, Department
of Soil Science and Plant Nutrition

Dr. Shuyang Yu
Department of Microbiology, University of Iowa
Address: 51 newton road, 3-730B BSB bldg. Iowa City,
IA, 52246, USA

Dr. Mousavi Khaneghah
College of Applied Science and Technology-Applied Food Science, Tehran, Iran.

Dr. Qing Zhou
Department of Biochemistry and Molecular Biology, Oregon Health and Sciences University Portland.

Dr Legesse Adane Bahiru
Department of Chemistry,
Jimma University,
Ethiopia.

Dr James John
School Of Life Sciences,
Pondicherry University,
Kalapet, Pondicherry

African Journal of Biotechnology

Table of Content: Volume 17 Number 7 14 February, 2018

ARTICLES

Isolation, purification and partial characterization of thermostable serine alkaline protease from a newly isolated *Bacillus thuringinsis*-SH-II-1A 178
Sunil L. Harer, Manish S. Bhatia and Neela M. Bhatia

Cucurbit yellow stunting disorder virus and watermelon chlorotic stunt virus induced gene silencing in tobacco plants 189
Ahmed Mohamed Soliman, Adel Abdelsabour Rezk and Khalid Abdallah Alhudaib

***Tomato yellow leaf* curl virus: Diagnosis and metabolites** 198
Ahmed Mohamed Soliman and Maged Elsayed Mohamed

Polymerase chain reaction amplification of 16S rDNA from three nosocomial bacterial isolates in Kaduna State, Northern Nigeria 206
Richard, R., Denwe, S. D.., Yerima, M. B. and Olatunde, S. K.

The nitrogen-fixing *Frankia* significantly increases growth, uprooting resistance and root tensile strength of *Alnus formosana* 213
Jung-Tai Lee and Sung-Ming Tsai

Characterization of biodiesel obtained from atemoya (*Annona squamosa* × *A. cherimola*) seed oil 226
Luciana Soares Da Cruz, Bárbara Lemes Outeiro Araújo, Luiz Roberto Marques Albuquerque, Pedro Castro Neto, Angelita Duarte Corrêa and Luciana de Matos Alves Pinto

academicJournals

Vol. 17(7), pp. 178-188, 14 February, 2018
DOI: 10.5897/AJB2015.14831
Article Number: 54A8DD255913
ISSN 1684-5315
Copyright © 2018
Author(s) retain the copyright of this article
http://www.academicjournals.org/AJB

African Journal of Biotechnology

Full Length Research Paper

Isolation, purification and partial characterization of thermostable serine alkaline protease from a newly isolated *Bacillus thuringinsis*-SH-II-1A

Sunil L. Harer*, Manish S. Bhatia and Neela M. Bhatia

Department of Pharmaceutical Chemistry, Bharati Vidyapeeth College of Pharmacy, Near Chitranagri, Kolhapur-416013 (MS) India.

Received 2 July, 2015; Accepted 5 November, 2015

In the present study, the isolation, purification and partial characterization of thermostable serine alkaline protease produced from *Bacillus thuringinsis* SH-II-1A was reported. The culture was isolated from soil of slaughter house waste and identified further from ribosomal sequence. The crude enzyme was purified by ammonium sulfate precipitation, dialysis and Sephadex G-200 gel permeation chromatography up to 17.04 fold with recovery of 8.47%. Relative molecular weight (67 kDa) of purified enzyme was observed by sodium dodecyl sulfate-polyacrylamide gel electrophoresis (SDS-PAGE). Maximum production of enzyme and cell biomass was observed for 48 h of incubation period at 45°C. Strong activity of enzyme was observed at pH 10 to 11; also stability of up to 2 and 20 h incubation at the same pH range confirms alkaline protease. Optimum temperature recorded for protease activity was 45°C, and 100% thermal stability up to 350 min of incubation was recorded. Among different natural substrates tried, casein was found as ideal substrate. Enzyme activity was strongly enhanced by metal ions like Ca^{2+}, Mg^{2+} and Mn^{2+} whereas, 100% enzyme activity was inhibited by phenylmethylsulphonyl fluoride (PMSF), and up to 92% inhibition by diisopropyl fluorophosphates (DFP) confirmed serine protease. Detergent compatibility of the enzyme was studied in the presence of 10 mM $CaCl_2$ and 1 M glycine at 45°C. This indicates 80 to 100% stability for a period of 0.5 to 2.5 h incubation. Improved washing performance and removal of blood stains from the cotton cloth was observed when detergent Surf excel was used with enzyme. Overall, the observed properties of isolated protease conclude its commercial application in detergent and leather industries.

Key words: Thermostable serine alkaline protease, *Bacillus thuringinsis,* purification, partial characterization.

INTRODUCTION

Among the large number of microbial enzymes, proteases occupy a pivotal position owing to their wide applications. The current estimated value of the worldwide sales of microbial enzymes is $ 1 billion; proteases alone account for about 60% of the total worldwide sales (Immaculate and Jamila, 2014) and were the first enzymes to be produced in bulk (Beg et al., 2003; Ellaiah et al., 2003). Alkaline proteases are a physiologically and commercially important group of enzymes used primarily as detergent additives. They play

*Corresponding author: E-mail: sunil.harer5@rediffmail.com. Tel: +91-9405141021. Fax: +91-231-2638833.

Author(s) agree that this article remains permanently open access under the terms of the Creative Commons Attribution License 4.0 International License

a specific catalytic role in the hydrolysis of proteins. This enzyme accounts for 40% of the total worldwide enzyme sales. It is expected to be an upward trend in the use of alkaline proteases in the future (Adinarayana et al., 2003; Moreira et al., 2003). Proteases are used in laundry detergents for over 50 years to facilitate release of proteinaceous materials in stains (blood and milk) and account for approximately 25% of total worldwide sales of enzymes (Ahmed et al., 2011). Thermostable alkaline proteases are having application in detergent industry as additive (Lagzian et al., 2012)

In the present study, the authors produced protease enzyme from *Bacillus thuringinsis* SH-II-1A (Foda et al., 2013). The bacillus strain was obtained from natural source of slaughter house waste drainage soil of different locations (Joachim et al., 2008). Maximum growth of culture and production of enzyme was observed at 48 h of incubation period. Isolation and purification of the enzyme was carried out by sequential steps of ammonium sulphate precipitation, DEAE-cellulose dialysis and Sephadex G-200 gel permeation chromatography. Isolated protease enzyme was identified as serine type after maximum inhibition of enzyme activity by phenyl methyl sulfonyl fluoride (PMSF) and di-isopropyl fluoro phosphate (DFP). Maximum hydrolysis of casein as a substrate and maximum stability was observed at pH 10 to 11, which supports alkaline type protease. Proteolytic efficiency of the enzyme was observed at 45°C, which supports thermal stability of enzyme at higher temperature. Activity of enzyme was enhanced by the use of metal ions like calcium ($CaCl_2$) supporting cofactor requirement. Enzyme has shown greater compatibility and stability with commercial detergent formulations like surf excel up to 1.5 h of incubation. Improved washing performance and removal of blood stains from the cotton cloth was observed upon incubation of enzyme along with detergent powder. Molecular weight of the purified enzyme was up to 68 kDa estimated with SDS-PAGE and supported by gelatin zymogram activity.

As it was desirable to search for new proteases with novel properties from as many different sources as possible, the present enzyme could become one of the ideal sources to fulfill all the required properties. Overall, the isolated protease enzyme could be considered as an additive for commercial detergent formulations. Commercially, it would have many industrial applications like hair removal property in leather industry, as a laundry additive in detergent industry, and breakdown of X-ray films to remove trapped silver particles. It would have therapeutic applications as a digestive aid, fibrinolytic agent, dissolution of blood clots and treatment of atherosclerosis in the future scope.

MATERIALS AND METHODS

The following chemicals were obtained from Sigma-Aldrich, St. Louis, MO (USA): Casein, Sephadex G-200, bovine serum albumin (BSA), phenylmethylsulfonyl fluoride (PMSF), β-mercaptoethanol (β-ME), DEAE-Cellulose equilibrium dialysis Harvard apparatus. Heavy metal ions, surfactants, organic solvents and chemicals for electrophoresis were purchased from Merck, Germany. Molecular mass markers (20 to 205 kDa) were obtained from Biotech-GeneiPvt Ltd., Bangalore, India. Commercial detergent powder and electrophoresis Vertical Slab Gel System were from Asian Scientific Instruments Ltd. All other chemicals used such as Ariel, Tide, Surf, Surf excel, Nirma and Rin were purchased from local market of high analytical grade.

Isolation and cultivation of microorganisms

The soil samples were collected in the form of soil from the waste drainage areas of slaughter house at six different locations of Pune district region (MS) India, and were diluted in sterile saline solution (Palsaniya et al., 2012). The clear supernatant liquid of the diluted samples was plated onto skim milk agar plates containing peptone (0.1% wt/vol), NaCl (0.5% wt/vol), agar (2.0% wt/vol) and skim milk (10% vol/vol). Plates were incubated at 37°C for 24 h. A clear zone of skim milk hydrolysis gave an indication of protease producing organisms (Shata, 2005; Shieh, 2009). Depending on the maximum zone of hydrolysis, strain SH-II-1A was selected for further experimental studies. The pure isolated proteolytic strain was further subjected to identification of nucleotide sequence at National Centre for Cell Science (NCCS), Pune (MS), India. It was identified as *B. thuringinsis* and it was designated as *B. thuringinsis* SH-II-1A used in further study. Production of protease from *B. thuringinsis* SH-II-1A was carried out in a medium containing the following components; glucose 1% (wt/vol); yeast extract 0.5% (wt/vol); tryptone, 0.5% (wt/vol); casein, l.0% (wt/vol); soluble starch, 1.0% (wt/vol); $NaNO_2$ 1.0% (wt/vol); $CaCl_2$, 1.0% (wt/vol); NH_4Cl_2 1.0% (wt/vol); it was maintained at 45°C for 72 h in a shaker incubator (150 rpm). The pH of the medium was preadjusted with 0. 1 N NaOH or 0.1 N HCl. After the completion of fermentation, the whole fermentation broth was centrifuged at 5000 x*g* at 4°C for 15 min, and the clear supernatant was recovered. The crude enzyme supernatant was subjected to purification and further studies (Amrita et al., 2012; Akolkar 2009).

Enzyme purification

Ammonium sulphate precipitation

As described above, fermentation was carried out for 72 h at 45°C and clear supernatant was separated from the cells by centrifuge at 5000 x*g* for 15 min. Further supernatant was fractionated by precipitation with ammonium sulfate between 40 and 60% of saturation. All subsequent steps were carried out at 5 to 8°C. The protein mass obtained after precipitation was resuspended again in 0.1 M Tris-HCl buffer, pH 10.0, and dialyzed using diethyl amino ethyl (DEAE) cellulose membrane against the buffer having same composition (Asker et al., 2013).

SephadexG-200 gel permeation chromatography

Sephadex G-200 (5 gm) gel was added to 0.1 M Tris-HCl (pH 10.0) and allowed to swell overnight; and column (1.5 × 65 cm) (Sigma-Aldrich, St Louis, MO) was packed. The column (1.5 × 65 cm) was equilibrated with 0.1 M Tris-HCl buffer and pH 10.0. The protein pellet obtained after saturation with ammonium sulphate between 50 and 70% was dissolved in 0.1 M Tris-HCl buffer and pH 10.0, and a total of 5 mL of protein precipitate was loaded onto a column of Sephadex G-200 (1.5 × 65 cm). The column was equilibrated

with Tris-HCl buffer and pH 10.0. The process of elution was started at a flow rate of 1 mL/min with a 1:1 volume gradient flow from 0.1 to 1 M NaCl in the same buffer. Protein concentration from each fraction was determined by Lowry method using bovine serum albumin as standard. Such fractions were pooled, dialyzed and concentrated to be used for further studies (Asker et al., 2013)

Molecular mass determination

Molecular mass of the purified enzyme fractions showing greater activity was determined on sodium dodecyl sulphate polyacrylamide gel electrophoresis (SDS-PAGE) according to the method of Laemmli (1970) and Ali et al. (2014) with 15% acrylamide concentration. Approximately, 10 µg of purified protein was loaded on 15% SDS-PAGE with standard molecular mass markers into two side wells of the gel. The dragging process of loaded protein was started at initial current of 15 mA and then constant current of 30 mA. After electrophoresis, the gel was stained with Co-omassie Brilliant Blue R-250 (CBB R-250) and destained in glacial acetic acid to visualize protein bands.

Determination of proteolytic activity (caseinase determination)

Caseinase activity was assessed by the modified procedure (Tsuchida et al., 1986) using 2% casein substrate dissolved in 0.2 M carbonate buffer pH 10. Casein solution (0.5 ml) with an equal volume of suitably diluted enzyme solution was incubated at 37°C. After 15 min, the reaction was terminated by addition of 1 ml of 10% trichloroacetic acid (TCA). The reaction mixture was centrifuged and 5 ml of 0.44 M Na_2CO_3 was added to the supernatant. Addition of two fold diluted (1 mL) Folin CioCalteu reagent to the mixture resulted in blue color. After 45 min at room temperature, the reaction mixture was subjected to centrifugation (Remi, 4000 rpm, 4°C). The intensity of color developed in the supernatant mixture was measured at 660 nm against a reagent blank prepared in the same manner. Tyrosine served as the reference standard and optical density of colored solution was measured by UV spectrophotometer (Shimadzu, Japan).

Protein assay

Protein was measured by the method of Lowry et al. (1951) with bovine serum albumin (BSA) as the standard. The concentration of protein during purification studies was calculated from the absorbance at 280 nm (Singhal et al., 2012).

Effect of pH on enzyme activity and stability

The activity of the enzyme (10 µl) was measured at different pH values in the presence of 10 mM $CaCl_2$. The pH was adjusted using the following buffers (0.05 M): phosphate buffer (pH 6.0 to 7.0), Tris-HCl buffer (pH 8.0) and glycine-NaOH buffer (pH 9.0 to 12.0). Reaction mixtures containing 0.5% casein (1 mL) were incubated at 45°C for 30 min. The reaction was stopped by addition of 0.5% Tri chloro acetic acid (TCA). Absorbance of TCA soluble peptides was measured at 280 nm. The purified enzyme was diluted in different relevant buffers (pH 6.0 to 12.0) and incubated at 45°C for 2 and 20 h for checking of enzyme stability. The relative activity at each exposure was measured as per assay procedure (Siala et al., 2009).

Effect of temperature on enzyme activity and stability

The activity of the enzyme was determined by incubating the reaction mixture at different temperatures ranging from 35 to 65°C in the presence of 10 mM $CaCl_2$ for 30 min. To determine the enzyme stability with changes in temperature, purified enzyme was incubated at different temperatures (35, 40, 45, 50, 55, 60 and 65°C) in the presence of 10 mM $CaCl_2$ and relative protease activities were assayed at standard assay conditions (Bhunia et al., 2012).

Effect of protease inhibitors on enzyme activity

The effect of different protease inhibitors on purified protease activity was studied using phenyl methyl sulfonyl fluoride (PMSF) (1 mM), ethylene diamine tetra acetic acid (EDTA) (5 mM), *p*-chloro mercuric benzoate (*p*-CMB) (5 mM), Iodoacetate (5 mM), Di-isopropyl fluoro phosphate (DFP) 5 mM and β-mercaptoethanol (β-ME) (5 mM) (Sigma et al., 1975). The reaction mixture was prepared by pre-incubating the purified enzyme with inhibitors without substrate for 10 min at 45°C. The protease assay was performed by addition of casein as a substrate for 30 min. Protease activity obtained without inhibitor was considered as 100% (Usharani et al., 2010).

Effect of various metal ions on enzyme activity

Effect of monovalent (Na^+ and K^+), divalent (Ca^{2+}, Mg^{2+}, Mn^{2+}, Co^{2+}, Cd^{2+}, Zn^{2+} and Hg^{2+}) and trivalent (Al^{+3}, Fe^{+3}) metal ions on enzyme activity at a concentration of 5, 10 and 15 mM was investigated by using casein as substrate (Sigma et al., 1975). The reaction mixture was prepared by pre-incubating the purified enzyme with metal ions at each concentration for 10 min at 45°C and the proteolytic activity was determined for 1 h by the above mentioned method. Enzyme activity in the absence of metal ions was considered as 100% (George et al., 2012).

Hydrolysis of protein substrates

Protease activity with different protein substrates including BSA, casein, egg albumin and gelatin was assayed by mixing 100 ng of the enzyme and 200 µL of assay buffer containing the protein substrates (2 mg/mL). After incubation at 45°C for 30 min, the reaction was stopped by adding 200 µL of 10% (wt/vol) trichloro acetic acid (TCA) and allowed to stand at room temperature for 10 min. The undigested protein was removed by centrifugation and peptides released were assayed. The specific protease activity towards casein as a substrate was considered as a control (Iqbal et al., 2011).

Detergent stability

The compatibility of SH-II-1A protease with local laundry detergents was studied in the presence of 10 mM $CaCl_2$ and 1 M glycine. Detergents used were Nirma (Nirma Chemical, India); Henko (Henkel Spic, India); Surf, Surf Excel, Super Wheel, Rin (Hindustan Lever Ltd, India); and Ariel (Procter and Gamble, India). The detergents were diluted in distilled water (0.7% wt/vol) and incubated with protease for 3 h at 45°C, and the residual activity was determined. The enzyme activity of a control sample (without any detergent) was taken as 100% (Ire et al., 2011).

Washing test with protease preparation

Application of protease (5000 U/mL) as a detergent additive was studied on white cotton cloth pieces (4 × 4 cm) stained with blood.

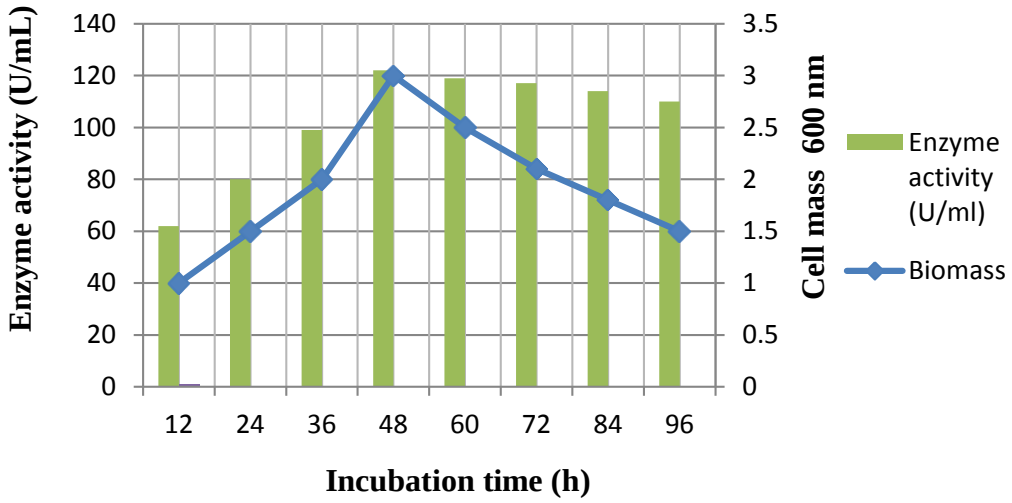

Figure 1. Maximum growth of culture and enzyme production.

The stained cloth pieces were taken in separate flasks. The following sets were prepared and studied: 1. Flask with distilled water (100 mL) + stained cloth (cloth stained with blood); 2. Flask with distilled water (100 mL) + stained cloth (cloth stained with blood) + 1 mL Wheel detergent (7 mg/mL); 3. Flask with distilled water (100 mL) + stained cloth (cloth stained with blood) + 1 mL Wheel detergent (7 mg/mL) + 2 mL enzyme solution.

The above flasks were incubated at 45°C for 15 min. After incubation, cloth pieces were taken out, rinsed with water, and dried. Visual examination of cloth pieces exhibited the effect of enzyme in removal of stains. Untreated cloth pieces stained with blood were taken as control for comparison (Ram et al., 2012).

RESULTS AND DISCUSSION

Identification of bacterial culture

The most significant characteristics of the isolate SH-II-1A are summarized: these are vegetative cells and characterized as large stout rods that are straight or slightly curved with rounded ends (Gopala, 2011). They usually occur in pairs or short chains. It is Gram positive, non-capsulated and motile with peritrichous flagella. Classification of *B. thuringinsis* strains has been accomplished by H serotyping the immunological reaction to the bacterial flagellar antigen (Ash et al., 1991). The *hag* gene encodes flagellin, which is responsible for eliciting the immunological reaction in H serotyping. This showed that the isolate belongs to the class of *Bacillus* sp.

Purification of extracellular protease of *B. thuringiensis* SH-II-1A

In *B. thuringiensis*, maximum growth and maximum enzyme production was observed at 48 h (Figure 1). Fermentation was carried out at 45°C and clear supernatant was separated from the cells by centrifuging at 5000 ×*g* for 15 min. Further supernatant was fractionated by precipitation with ammonium sulfate between 40 and 60% of saturation. All subsequent steps were carried out at 5 to 8°C. The protein mass obtained after precipitation was resuspended in 0.1 M Tris-HCl buffer, pH 10; it was dialyzed using diethyl amino ethyl (DEAE) cellulose membrane against the buffer having same composition in order to achieve desired purity of enzyme.

The protein pellet obtained after dialysis using DEAE membrane was loaded onto a column of Sephadex G-200 (1.5 × 65 cm) equilibrated with Tris-HCl buffer, pH 10. The elution profile of gel filtration chromatography is shown in Figure 2. Elution profile of column was monitored and it was observed that the protease enzyme was eluted in the form of well resolved single peak, showing casein hydrolysis (caseinase) activity coinciding with a single protein peak at a NaCl concentration of 0.6 M. Eluted fractions sequence numbers (25 to 30) were observed with high protease activity. The summary of purification steps involved for alkaline protease is presented in Table 1 (Zhou et al., 2009; Fakhfakh et al., 2010).

When the ammonium sulphate precipitation and purified protease was analyzed by SDS-PAGE, seven bands were observed in the presence of ammonium sulphate precipitation (Figure 3); while purified protease showed a single band on SDS-PAGE, indicating a homogenous preparation. The molecular weight of the protease was determined by comparison of the migration distances of standard markers protein. The molecular mass standards were bovine serum albumin (67 kDa), ovalbumin (45 kDa), carbonic anhydrase (30 kDa), trypsinogen (24 kDa) and α-lactalbumin (14 kDa) on SDS-PAGE. The molecular mass was determined by extrapolation from a linear semi logarithmic plot of

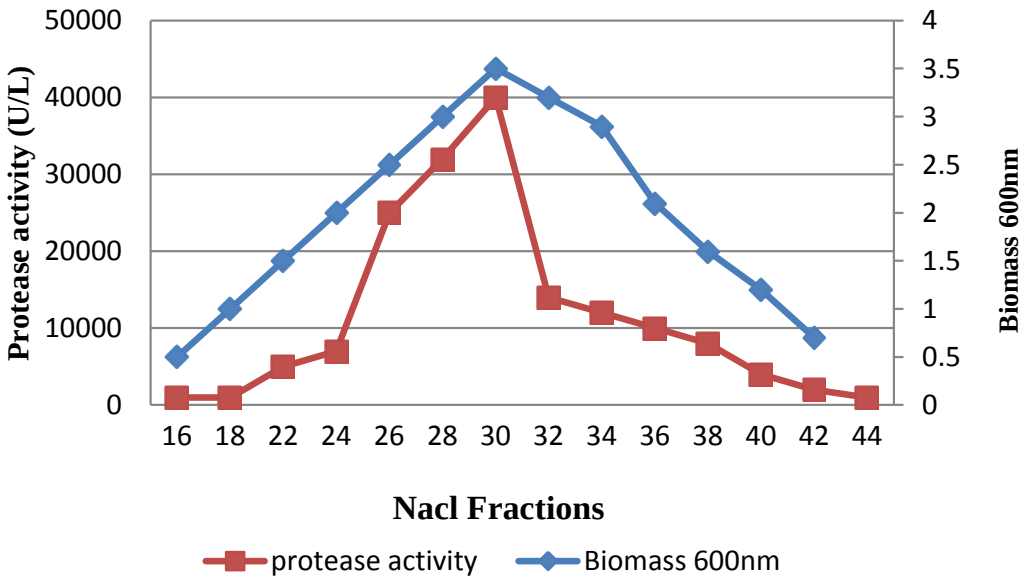

Figure 2. Elution profile of protease SH-II-1A by Sephadex G-200 column chromatography.

Table 1. Summary of purification steps for isolated enzyme.

Purification step	Total enzyme activity (U)	Total protein (mg)	Specific activity (U/mg)	Purification folds	Recovery (%)
Crude enzyme	105000	6025	17.4	1	100
Ammonium sulphate ppt. and dialysis	90500	4000	22.62	1.29	86.19
Sephadex G-200	8900	30	296.66	17.04	8.47

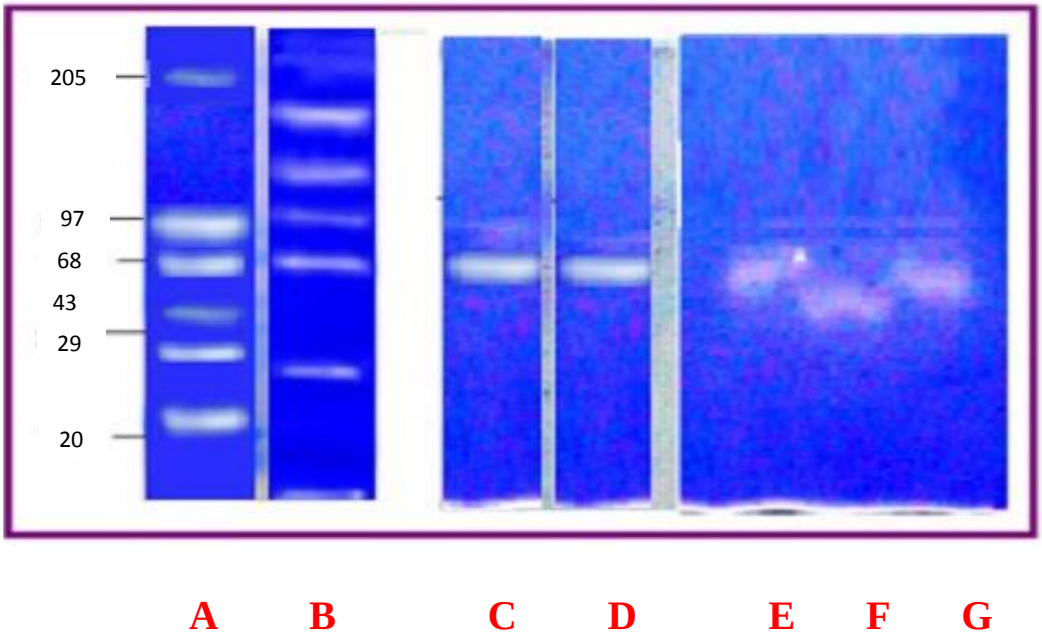

Figure 3. SDS-PAGE and Gelatin zymogram for enzyme. Lane A, Molecular mass marker; Lane B, crude enzyme; Lane C, purified enzyme; Lane D, standard BSA; Lane E and G, gelatin zymogram for standard BSA; Lane F, gelatin zymogram for purified enzyme. The molecular mass markers are- myosin 205 kDa, phosphorylaseB-97 kDa, bovine serum albumin- 68 kDa, ovalbumin-43 kDa, carbonic anhydrase-29 kDa, tyrosine-20 kDa.

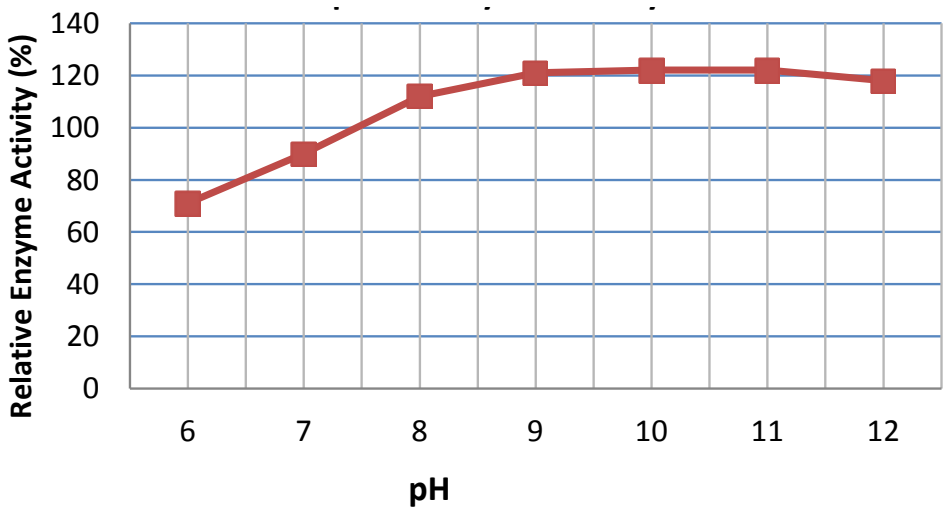

Figure 4. Relative enzyme activity (%) observed at different pH level.

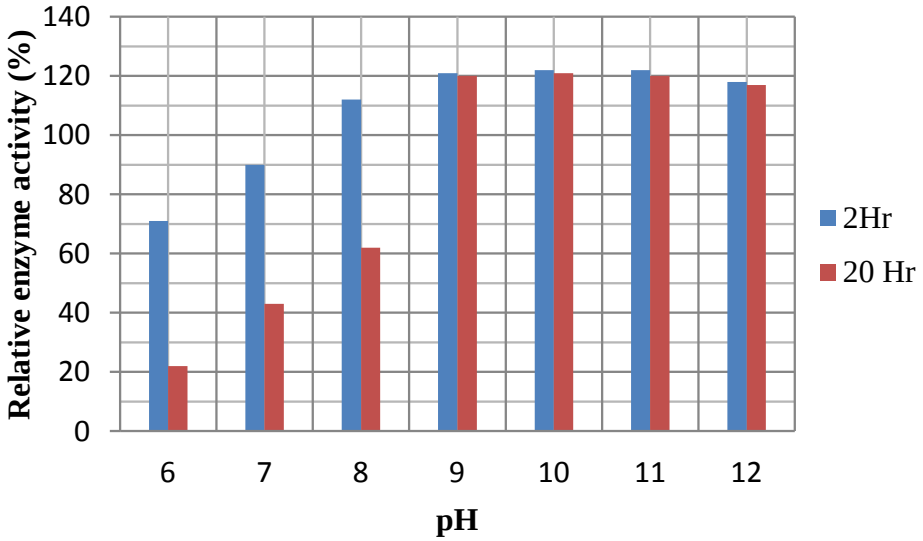

Figure 5. Stability of enzyme at different pH level.

relative molecular mass versus the Rf value (relative mobility). Depending on the relative mobility, the molecular weight of the protein band was calculated to be 68 kDa, which coincided with the band of bovine serum albumin (BSA) marker protein (Prashant et al., 2013).

Characterization of purified enzyme

For the determination of the pH optimum, phosphate (pH 6 to 7), Tris-HCl (pH 8), and glycine-NaOH (pH 9 to 12) buffers were used in the absence and presence of 10 mM $CaCl_2$. The highest protease activity was found to be at pH 10 to 11 using glycine-NaOH buffer (Figure 4). These findings are in line with several earlier reports showing pH optima of 10 to 10.5 for protease from *Bacillus* sp., *Thermus aquaticus*, *Xanthomonas maltophila* and *Vibrio metscnikovii.* The important detergent enzymes, subtilisin Carlberg and subtilisin Novo or BPN (Dhandapani et al., 1994) also showed maximum activity at pH 10.5. The stability of enzyme was checked at various pH 6 to 12. 100% stability was achieved at pH 9 to 11 for a period of 2 and 20 h incubation (Figure 5).

The activity of the crude and purified enzyme was determined at different temperatures ranging from 35 to 65°C in the absence and presence of 10 mM $CaCl_2$. The optimum temperature recorded was at 45°C for protease activity. The enzyme activity gradually declined at

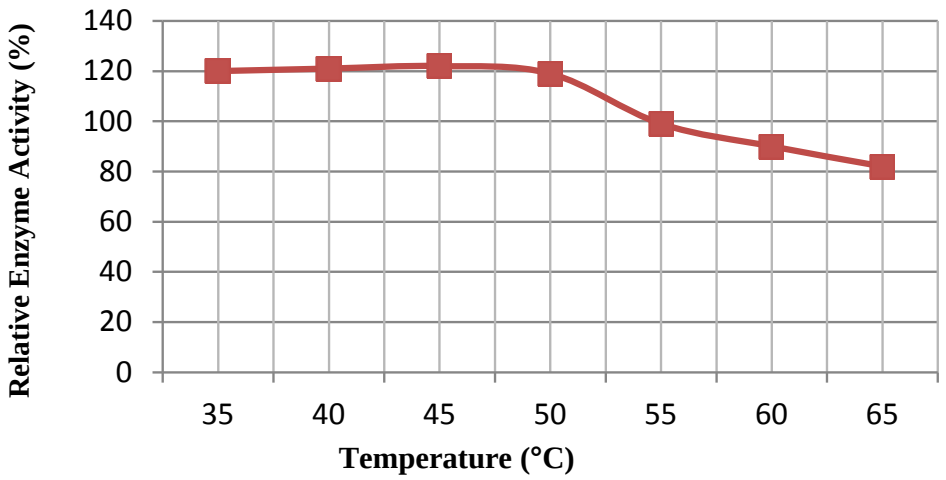

Figure 6. Effect of temperature on protease activity.

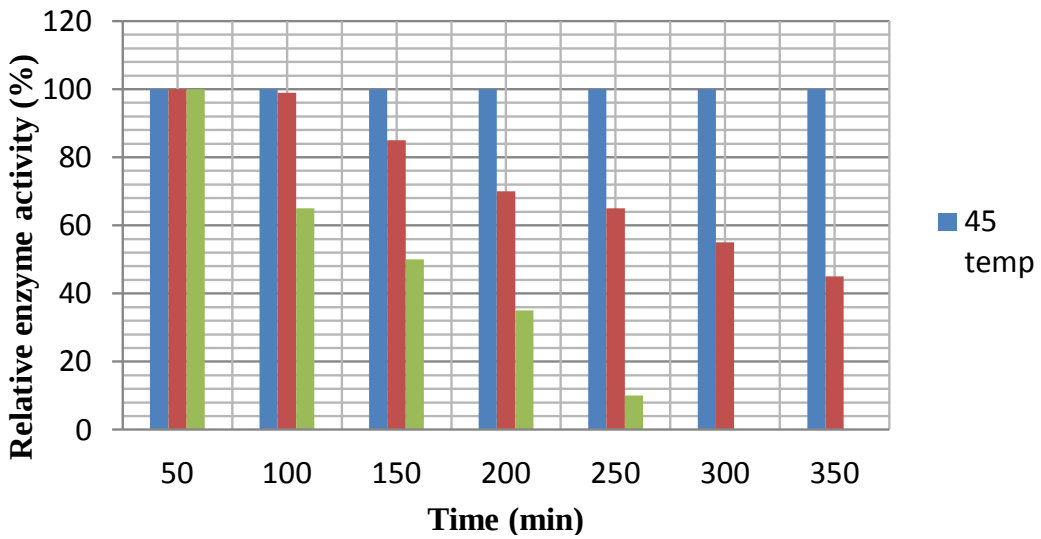

Figure 7. Thermal stability of enzyme at different temperature.

temperatures beyond 50°C (Figure 6). A similar type of result was observed by other investigators where a maximum temperature of 55°C was recorded for an alkaline protease from *Bacillus stearothermophilus* AP-4 and 60°C for a protease (Jellouli et al., 2009) derived from *Bacillus* sp B21-2. The thermal stability of the purified protease was tested at different temperatures of 45, 50 and 55°C for different periods (50 to 350 min) in the presence of 10 mM $CaCl_2$. The enzyme was almost 100% stable at 45°C even after 350 min of incubation (Figure 7). Previous reports on thermostability have shown half-lives of >200 min at 50°C and 2 to 22 min at 60°C for heat stable serine proteases, and half-lives of 3.4 and 2.4 min at 50°C have been recorded for subtilisin Carlsberg and subtilisin BPN, respectively.

Effect of protease inhibitors on enzyme activity

Inhibition studies primarily give an insight into the nature of an enzyme, its cofactor requirements, and the nature of the active center. The effect of different inhibitors on the enzyme activity of the purified protease was studied. Among the inhibitors tested (at 5 mM concentration), PMSF was able to inhibit the protease completely, while DFP exhibited 94% inhibition. In this regard, PMSF sulphonates, the essential serine residue in the active site of the protease and has been reported to result in the complete loss of enzyme activity. Relative enzyme activity by different inhibitors is described in Figure 8. Our findings are similar to those of Tsuchida et al. (1986) where the protease was completely inhibited by PMSF.

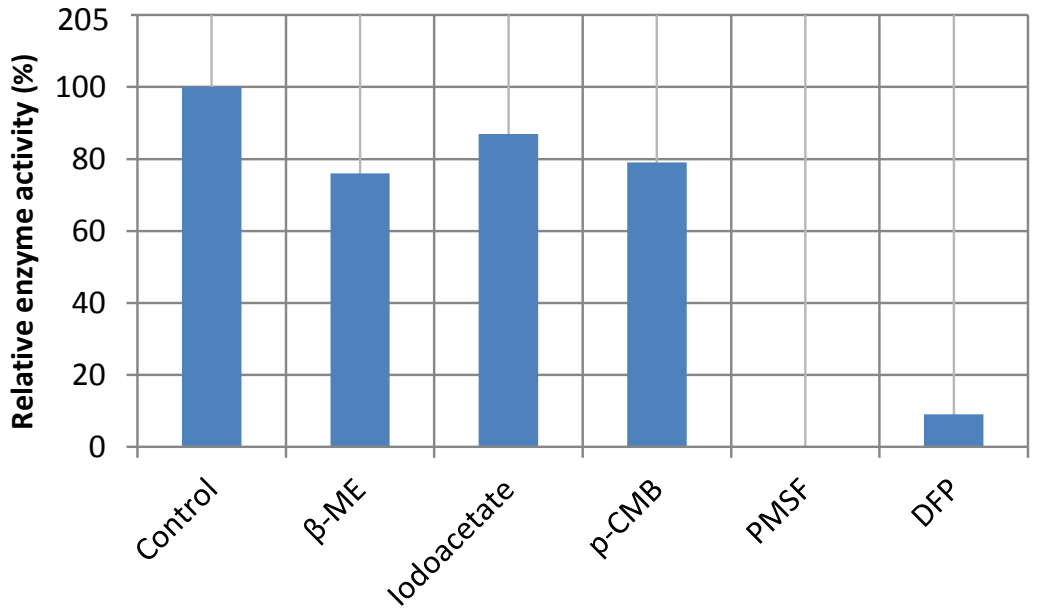

Figure 8. Effect of various enzyme inhibitors on enzyme activity. *β-ME indicates β-mercaptoethanol; *p*-CMB, *p*-Chloro mercuric benzoate; PMSF, Phenyl methyl sulfonyl fluoride; DFP, di-isopropyl fluoro phosphate.

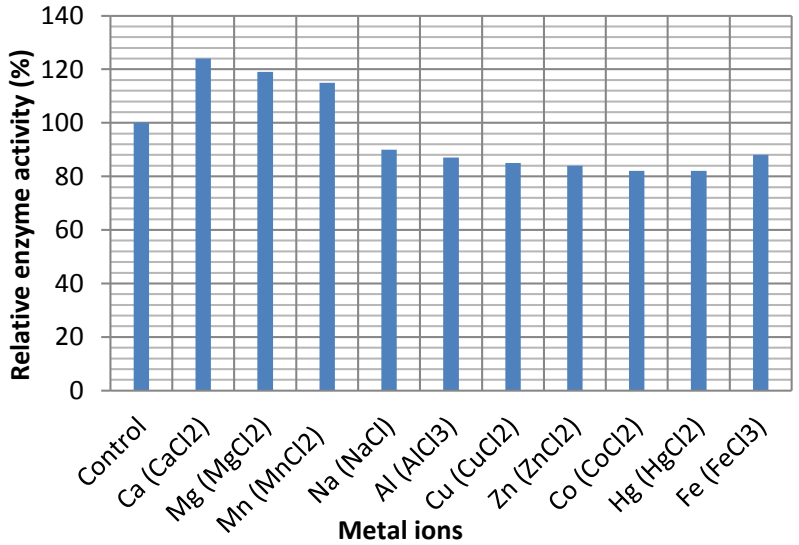

Figure 9. Effect of various metal ions on enzyme activity.

This indicated that it is a serine alkaline protease. Slight inhibition was observed with other inhibitors like iodoacetate, *p*-CMB and β-ME.

Effect of various metal ions on enzyme activity

Most of the metal ions tested had a stimulatory effect (Ca^{2+}, Mg^{2+} and Mn^{2+}) or a slight inhibitory effect (other ions) on enzyme activity. Some of the metal ions such as Ca, Mg^{2+} and Mn^{2+} increased and stabilized the protease activity of the enzyme; this is possible because of the activation by the metal ions. These cations also have been reported to increase the thermal stability of other *Bacillus* alkaline proteases. These results suggest that concerned metal ions apparently protected the enzyme against thermal denaturation and played a vital role in maintaining the active confirmation of the enzyme at high temperatures. Other metal ions such as Zn^{2+}, Cu^{2+}, Hg^{2+}, Co^{2+}, N^{2+}, Cd^{2+}, Al^{3+} and Fe^{3+} did not show any appreciable effect on enzyme activity. Relative enzyme activity is described in Figure 9.

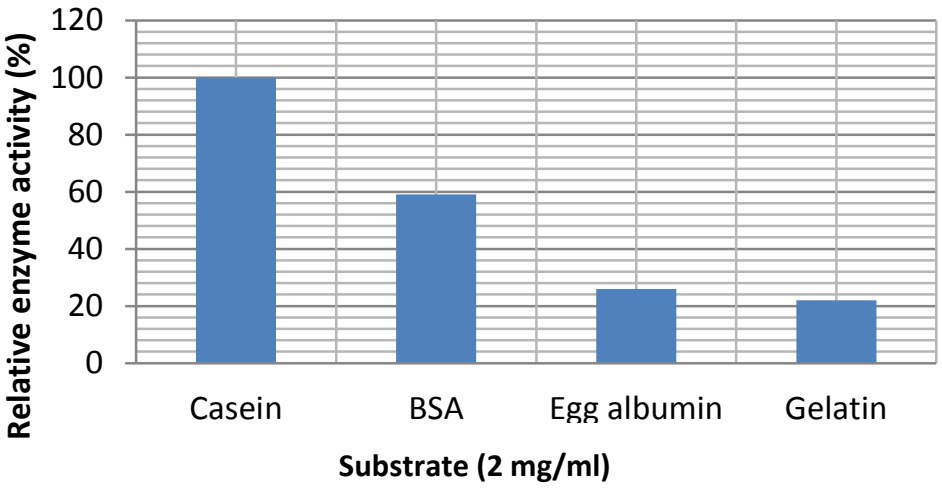

Figure 10. Hydrolysis of different natural substrates.

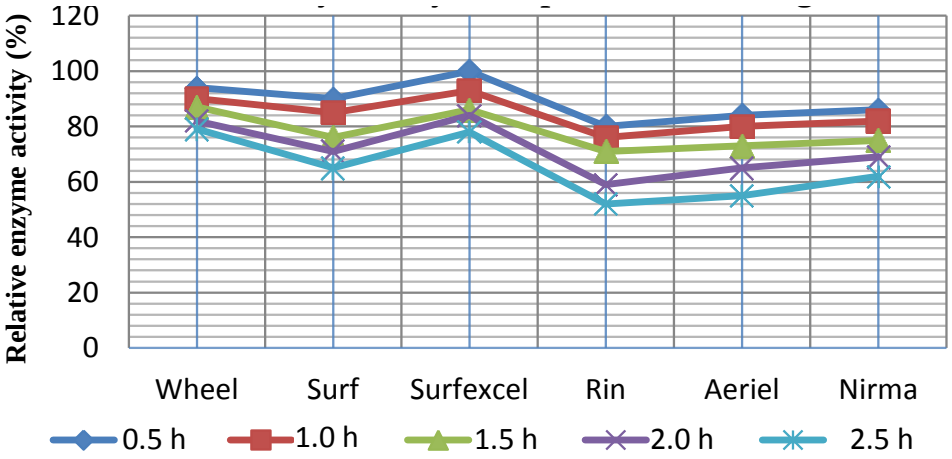

Figure 11. Compatibility and stability of enzyme with various detergent formulations.

Hydrolysis of protein substrates

When assayed with native proteins as substrates, the protease showed a high level of hydrolytic activity against casein and poor to moderate hydrolysis of BSA and egg albumin; although the hydrolysis was hardly observed with gelatin (Figure 10) (Loops et al., 2003).

Compatibility with detergents

Besides pH, a good detergent protease is expected to be stable in the presence of commercial detergents. Protease from *B. thuringinsis* SH-II-1A showed stability and compatibility with a wide range of commercial detergents at 45°C in the presence of $CaCl_2$ and glycine as stabilizers using distilled water. Isolated protease has shown good stability and compatibility in the presence of detergent Surf excel. The enzyme retained more than 60% activity with most of the detergents tested even after 2.5 h incubation at 45°C after the supplementation of $CaCl_2$ and glycine (Annamalai et al., 2013). High activity alkaline protease was reported from *Conidiobolus coronatus* showing compatibility at 50°C, in the presence of 25 mM $CaCl_2$, with a variety of commercial detergents. Also, 16% activity was reported in Revel, 11.4% activity in Aerial and 6.6% activity in Wheel. Comparing these results, the *Bacillus subtilis* PE-11 enzyme was significantly more stable in commercial detergents. The compatibility of alkaline protease was studied with Surf excel in the presence of 10 mM $CaCl_2$ and 1 M glycine for different periods (0.5 to 2.5 h) at 45°C. The enzyme retained about 82% activity after 1.5 h in the presence of surf excel at 45°C and was almost inactivated after 2.5 h in the absence of any stabilizer (Figure 11). However, the addition of $CaCl_2$ (10 mM) and glycine (1 M), individually

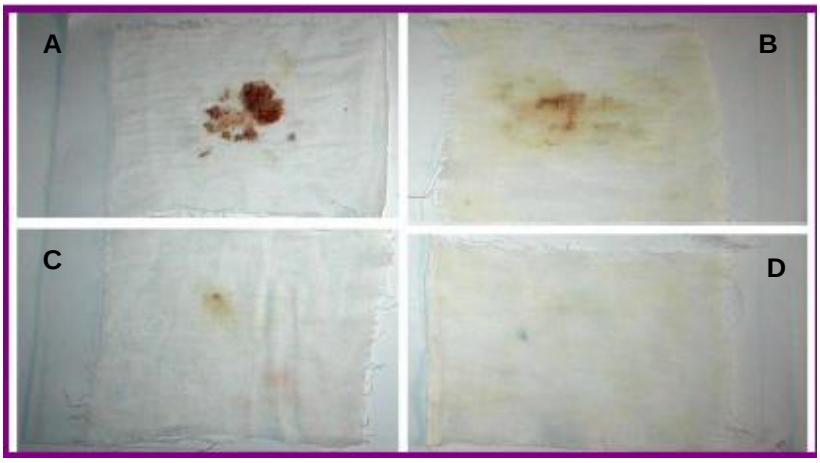

Figure 12. Washing performance of protease in presence of detergent (Surf excel). **A.** Cotton cloth stained with blood; **B.** cloth stained with blood and washed with distilled water only; **C.** cloth stained with blood and washed with detergent only; **D.** cloth stained with blood and washed with the detergent and enzyme solution.

and in combination, was very effective in improving the stability, where it retained 60% activity even after 2.5 h. As the protease produced by our isolate *B. thuringinsis* SH-II-1A was stable over a wide range of pH values and temperatures and also showed compatibility with various commercial detergents tested in the presence of $CaCl_2$ and glycine, it was used as an additive in detergent to check the contribution of the enzyme in improving the washing performance of the detergent. The supplementation of the enzyme preparation in detergent (that is, Surf excel) could significantly improve the cleansing of the blood stains (Figure 12).

Conclusion

The alkaline protease isolated from *B. thuringinsis* SH-II-1A is a thermostable serine protease. It is stable at alkaline pH, at high temperatures, and in the presence of commercial detergents and is compatible with commercial and local detergents. These properties indicate the possibilities for use of the protease in the detergent industry. This enzyme can be exploited commercially.

CONFLICT OF INTERESTS

The authors have not declared any conflict of interests.

Abbreviations

NCCS, National Centre for Cell Sciences; **DEAE,** di ethyl amino ethyl; **CBB,** co-ommassie brilliant blue; **SDS-PAGE,** sodium dodecyl sulphate poly-acrylamide gel electrophoresis; **TCA,** tri-chloro acetic acid; **UV,** ultra violet; **BSA,** bovine serum albumin; ***p*-CMB,** para chloro mercuric benzoate; **PMSF,** phenyl methyl sulfonyl fluoride; **β-ME,** β-mercapto ethanol; **DFP,** di isopropyl fluoro phosphate.

REFERENCES

Adinarayana K, Ellaiah P (2003). Production of alkaline protease by immobilized cells of alkalophilic*Bacillus* sp. J. Sci. Ind. Res. 62:589-592.

Ahmed I, Anjum ZM, Iftikar T, Iqbal N (2011). Characterization and detergent compatibility of purified protease produced from *Aspergillus niger* by utilizing agrowastes. BioResources. 6(4):4505-4522.

Akolkar AV (2009). Isolation and characterization of halophilic archaea: Production, characterization and application of extracellular protease from *Halobacterium* sp. 1(1), Ph.D. Thesis Dissertation, Maharaja Sayajirao University of Baroda.

Ali SS, Vidhale NN (2013). Protease production by *Fusarium oxysporum* in solid- state fermentation using rice bran. Am. J. Microbiol.l Res. 1(3):45-47.

Amrita R, Nancy K, Namrata P, Souray B, Arjita D, Subbaramaiah S (2012). Enhancement of protease production by *Pseudomonas aeruginosa* isolated from dairy effluent sludge and determination of its fibrinolytic potential. Asian Pac. J. Trophical Biomed. S1485:1845-1851.

Annamalai N, Rajeswari MV, Thavasi R, Vijayalakshmi S, Balasubramanian T (2013). Solvents table protease from Bacillus halodurans CAS6 using marine shellfish wastes:a potential additive for detergent and antioxidant synthesis. Bioprocess Biosyst. Eng. 7:873-883.

Asker MMS, Mahmoud MG, Shebwy KE, Aziz MSA (2013). Purification and characterization of two thermostable protease fractions from *Bacillus megaterium*. J. Genet. Eng. Biotechno. pp.103-109.

Beg KB, Sahai V, Gupta R (2003). Statistical media optimization and alkaline protease production from *Bacillus mojavensis* in a bioreactor. Process Biochem. 39:203-209.

Bhunia B, Apurba D (2012). Statistical approach for optimization of physiochemical requirements on alkaline protease production from *B. licheniformis NCIM 2042*. Enzyme Res. PMCID: PMC3278927.

Dhandapani R, Vijayaragavan R (1994). Production of a thermophilic extracellular alkaline protease by *Bacillus stearothermophilus* AP-4. World J. Microbiol. Biotechnol. 10:33-35.

Ellaiah P, Adinarayana K, Rajlaxmi P, Srinivasulu B (2003). Optimization of process parameters for alkaline protease production under solid state fermentation by alkalophilic *Bacillus* sp. Asian J. Microbiol. Biotechnol. Environ. Sci. 5:49-54.

Fakhfakh ZN, Haddar A, Noomen H, Fakher F, Nasri M (2010). Application of statistical experimental design for optimization of keratinases production by *B. pumilus* A1 grown on chicken feather and some biochemical properties. Process Biochem. 45:617-626.

Foda MS, Safaa MA, Youssef AM, Kahil T, Hoda MS, Amira M (2013). Production physiology of alkaline protease by *Bacillus thuringiensis* spp. under solid-state fermentation conditions. Journal of Applied Sciences Research. 9(3):1975-1984.

George OUO, Mike AEE (2012). Screening and optimal protease production by *Bacillus* sp. Sw-2 using low cost substrate medium. Res. J. Microbiol. 7:327-336.

Gopala KC. (2011). Comprehensive hand held microbiology laboratory manual. B09 Publishers.

Immaculate JK, Jamila P (2014). Enhancement of alkaline protease production by *bacillus* species through random mutagenesis. International Journal of Microbiol. Res. 5(2):130-139.

Iqbal HMN, Ahmed I, Asif KM (2011). Partial characterization of purified protease produced from *Rhizopus oligosporus* using a by-product of oil industry. World Appl. Sci. J. 13(3):600-605.

Ire FS, Bartholomew NO, Anene AM (2011). Purification and characterization of an acid protease from *Aspergillus carbonarius*. Afr. J. Food Sci. 5(12):695-709.

Jellouli K, Bougatef A, Manni L, Agrebi R, Siala R, Younes I, Nasri M (2009). Molecular and biochemical characterization of an extracellular serine-protease from *Vibrio metschnikovii* J. J. Ind. Microbiol. Biotechnol. 36:939-948.

Joachim HJRM, Patrick AN (2008). Selected soil enzymes: Examples of their potential roles in the ecosystem. African Journal of Biotechnology. 7(3):181-191.

Laemmli UK (1970). Cleavage of structural proteins during the assembly of the head of bacteriophage T4. Nature. 227:680-685.

Lagzian M, Asoodeh A (2012). An extremely thermotolerant, alkaliphilic subtilisin- like protease from hyperthermophilic *Bacillus* sp. MLA64. Int. J. Biol. Macromol. 51:960-967.

Loops AR, Terra WR (2003). Purification, properties and substrate specificity of a digestive trypsin from *Periplaneta americana* (Dictyoptera). Insect Biochem. Mol. Biol. 33:407-415.

Lowry OH, Rosebrough NJ, Farr AL, Randall JR (1951). Protein measurement with the Folin phenol reagent. J. Biol. Chem. 193:265–275.

Moreira KA, Porto TS, Teixeira MFS, Porto ALF, Lima Filho JL (2003). New alkaline protease from *Nocardiopsis*sp: partial purification and characterization. Process Biochem. 27:69-78.

Palsaniya P, Mishra R, Beejawat N, Sethi S, Gupta, B (2012). Optimization of alkaline protease production from bacteria isolated from soil. J. Microbiol. Biotechnol. Res. 6: 858-865.

Prashant T, Sanatan P, Lomate R, Ashok P, Hivrale K (2013). Characterization of a chemostable serine alkaline protease from *Periplaneta americana*. BMC Biochemistry. 14(32); 1-9.

Ram KP, Satish R, Hemant T (2012). Studies on compatibility of fungal alkaline protease with commercially available detergents. Int. J. Modern Biochem. 1(1):41-56.

Shata HMA (2005). Extraction of milk-clotting enzyme produced by solid state fermentation of *Aspergillus oryzae*. Polish Journal of Microbiology. 3:241-247.

Shieh CJ, Lan-Anh Phan, TL, Shih I (2009). Milk-clotting enzymes produced by culture of *Bacillus subtilis* natto. Biochem. Eng. J. 43:85-91.

Siala R, Alya SK, Hajji M, Abid I, Neji G, Moncef N (2009). Extracellular acid protease from *Aspergillus niger* I1: purification and characterization. Afr. J. Biotechnol. 8(18):4582-4589.

Sigma DS, Mooser G (1975). Chemical studies of enzyme active sites. Annual Rev. Biochem. 44:889-931.

Singhal P, Nigam KV, Vidyarthi S (2012). Studies on production, characterization and applications of microbial alkaline proteases. Int. J. Adv. Biotechnol. Res. 3(3):653-669.

Tsuchida O, Yamagota Y, Ishizuka J, Arai J, Yamada J, Ta-keuchi M, Ichishima E (1986). An alkaline proteinase of an alkalophilic *Bacillus* sp. Curr. Microbiol. 14:7-12.

Usharani B, Muthuraj M (2010). Production and characterization of protease enzyme from *Bacillus Laterosporus*. Afr. J. Microb. Res. 4(11):1057-1063.

Zhou LH, Yi-Qiong Z, Ruo JW, Shen X, Yong QL, Wen J (2009). Optimization of mycelial biomass and protease production by *Laccocephalum mylittae* in submerged fermentation. Afr. J. Biotechnol. 8(8):1591-1601.

academicJournals

Vol. 17(7), pp. 189-197, 14 February, 2018
DOI: 10.5897/AJB2017.16314
Article Number: 79F699955915
ISSN 1684-5315
Copyright © 2018
Author(s) retain the copyright of this article
http://www.academicjournals.org/AJB

African Journal of Biotechnology

Full Length Research Paper

Cucurbit yellow stunting disorder virus and *Watermelon chlorotic* stunt virus induced gene silencing in tobacco plants

Ahmed Mohamed Soliman[1,3*], Adel Abdelsabour Rezk[2,3] and Khalid Abdallah Alhudaib[1]

[1]Department of Arid Land Agriculture, College of Agriculture and Food Sciences, King Faisal University, Saudi Arabia.
[2]Department of Biotechnology, College of Agriculture and Food Sciences, King Faisal University, Saudi Arabia.
[3]Virus and Phytoplasma Research Department, Plant Pathology Research Institute, Agricultural Research Center, Egypt.

Received 11 November, 2017; Accepted 26 January, 2018

***Cucurbit yellow stunting disorder virus* (CYSDV) and *Watermelon chlorotic stunt virus* (WmCSV) are the most widespread and damaging viruses to cucurbits in the Middle East. CYSDV and WmCSV are cucurbit-infecting bipartite whitefly-transmitted viruses. Post-transcriptional gene silencing (PTGS) is a universal mechanism by which plants are able to systemically switch off the expression of targeted genes via the reduction of steady-state levels of specific RNAs. PTGS was used in this study to control the two viruses. In this study, the efficiency of the dsRNA for the ability to trigger resistance against the CYSDV and WmCSV was investigated. Three regions of three genes of CYSDV genome were selected; the coat protein gene (CP), heat shock gene (Hsp70) and ORF3, while the two regions of two genes of WmCSV genome were selected; CP gene and rep gene. Bioassay, dot-blot hybridization and polymerase chain reaction (PCR) methods were capable to evaluate the resistance against viruses. Clear symptoms on tobacco plants took two to three weeks to appear and all non-infiltrating tobacco plants (positive control) showed viral symptoms after inoculation. Most of the agro-infiltrating sense/antisense constructs did not yield symptoms of the viruses. Dot-blot hybridization, showed that negative hybridization was obtained with infiltrating tobacco plants with prepared constructs compared to those non-infiltrating tobacco plants used as the control. Only one out of five gave positive signals with the construct pasCYSDV-Hsp70. Using PCR, positive reactions of the expected size of 500 bp fragment with WmCSV and 800 bp with CYSDV were obtained with the infiltrating tobacco plants with sense constructs, which pointed out the existence of viral genome in challenging tobacco plants. Infiltrating tobacco plants with sense/antisense constructs gave negative PCR pointed out the lack of the viral genome.**

Key words: Cucurbit yellow stunting disorder virus (CYSDV), watermelon chlorotic stunt virus (WmCSV), Post-transcriptional gene silencing (PTGS), coat protein (CP), Hsp70, ORF3, Rep, dot-blot, hybridization.

INTRODUCTION

Cucurbit crops are widely grown in the Middle East and consumed in large quantities in the traditional diet. The warm climate permits the nearly year-round development of insect vectors such as the whiteflies, which are the main vector for the viruses that infect cucurbits. The most widespread and damaging viruses are members of the

genus Begomovirus (*Geminiviridae*) and Crinivirus (*Closteroviridae*). The most important time of the year for whitefly infestation of cucurbit crops in Saudi Arabia is the autumn (Raja Al-Zahrani, 2010). During 2001, two new viral diseases were detected in cucurbits: watermelon (*Citrullus lanatus*), squash (*Cucurbita pepo*) and cucumber (*Cucumis sativus* L.*)* in the Middle East region. Sequence analysis revealed that the diseases were caused by the native *Watermelon chlorotic stunt virus* and *Squash leaf curl virus* (Abdel-Salam et al., 2006; Abudy et al., 2010; Ali-Shtayeh et al., 2014; Idris et al., 2006). WmCSV was first identified in Yemen (Jones et al., 1988) and after that, in the following years, it was reported through the Middle East and also in North Africa as the following: Sudan (Kheyr-Pour et al., 2000), Jordan (Al-Musa et al., 2011), Oman (Khan et al., 2012) and Palestine (Ali-Shtayeh et al., 2014). The symptoms caused by WmCSV are chlorotic mottling, vein yellowing, stunting and severe decrease of yield, generally in watermelon (*Citrullus* species) crops. WmCSV host range covers the most cucurbits including squash, cucumber, melons, and pumpkin.

The first detection of CYSDV in the Middle East was reported in the United Arab Emirates in 1982 (Hassan and Duffus, 1991). In subsequent years, it was identified throughout the Mediterranean region, in Europe, and in North America (Abou-Jawdah et al., 2000; Brown et al., 2007; Kuo et al., 2007; Papayiannis et al., 2009; Sweiss et al., 2007). CYSDV is a bunchy crinivirus, which has had a main negative impact on the production of cucumbers in several regions of the world, a phenomenon increased by the absence of effective preventive arrangements against the whitefly (Owen et al., 2016). WmCSV and CYSDV infect all cultivated cucurbits, some legumes (alfalfa, bean), and malvaceous species. CYSDV causes severe symptoms in cucurbit plants, green spots on the oldest leaves, severe interveinal chlorosis, and spot appears between 14 and 22 days' post-inculcation and severe symptoms including leaf rolling, complete leaf lamina yellowing, brittleness, severe stunting of young leaves and a drastic reduction of yield (Célix et al., 1996).

One of the primary aspects of virus-plant host interactions is derived from plant natural defenses through RNA silencing (Ding and Voinnet, 2007; Ruiz-Ferrer and Voinnet, 2009). Through infection, plants process viral double-stranded RNAs (dsRNAs) into small interfering RNAs (siRNAs) and use the siRNAs to guide specific antiviral silencing activities (Li et al., 2015). siRNAs guide members of the Argonaute protein family to specific mRNAs for cleavage, a process referred to as post-transcriptional gene silencing (PTGS), which is a universal defense mechanism against RNA viruses and transcripts produced by DNA viruses such as geminiviruses (Li et al., 2015). The lack of natural sources of resistance to WmCSV and CYSDV and the need to reduce pesticide application motivates us to develop multiple virus resistance through the development of transgenic cucurbit plants. This study was conducted to improve the socioeconomic status of the Saudi Arabia farmers and the local economy by the accurate diagnosis of cucurbit virus diseases and development of transgenic plant resistant to those viruses' adapted to local conditions. In the present study, infiltrating tobacco plants with sense/antisense constructs gave negative PCR which pointed out the lack of the viral genome while the infiltrating tobacco plants with sense constructs pointed out the existence of viral genome in challenging tobacco plants.

MATERIALS AND METHODS

The present work was conducted at Pest and Plant Diseases Unit (PPDU), College of Agriculture and Food Sciences, King Faisal University, Saudi Arabia.

Extraction of total nucleic acids from cucurbit tissues

The total RNA (for CYSDV) was extracted from infected cucurbit plants using the RNeasy® Plant Mini Kit (Qiagen, Germany) according to the instructions of the manufacturer w`hile the total DNA (for WmCSV) was extracted from infected cucurbit plants using the DNeasy® Plant Mini Kit (Qiagen, Germany) according to the instructions of the manufacturer.

Design and synthesis of oligonucleotide primers

Specific primers were designed for parts (selected fragments) of the coat protein gene (CP) of CYSDV (176 bp), heat shock gene (Hsp70) of CYSDV (232 bp), ORF3 of CYSDV (198 bp), CP gene of WmCSV (160 bp) and rep gene of WmCSV (230 bp) (Table 1) according to the sequences obtained from GenBank. The sense primers are CYcpf, Hsp702f, CYorf3f, Wmcp1 and Wmrep1 with *Asc*I and *Xba*I sites (underlined), respectively at the 5` end (Table 1). The antisense primers are CYcpr, Hsp702r, CYorf3r, Wmcp2 and Wmrep2 with *Swa*I and *Bam*HI sites (underlined) respectively, at the 5` end (Table 1). The restriction sites were inserted at the 5` end of the prepared primers to ease the cloning of the selected fragments into the binary vector.

One-step reverse transcriptase-polymerase chain reaction (RT-PCR) for the selected fragments of CYSDV

Platinum Quantitative RT-PCR Thermo Script One Step System experiment. The RT reaction started with incubation for 30 min at 50°C, then denaturation for 5 min at 95°C. Thirty-five cycles of PCR started with denaturation for 1 min at 95°C, primer annealing for 1 min at 55°C, and extension for 1 min at 72°C with a final extension

*Corresponding author. E-mail: amsma33@hotmail.com or amohamed@kfu.edu.sa.

Author(s) agree that this article remains permanently open access under the terms of the Creative Commons Attribution License 4.0 International License

for 7 min at 72°C.

PCR for the selected fragments of WmCSV

PCR cycle parameters were as follows: 2 min at 94°C, after that, 35 cycles of 1 min at 94°C, 2 min at 55°C and 2 min at 72°C, then the final extension for 10 min at 72°C.

Cloning and sequencing of the amplified fragments of CYSDV and WmCSV

PCR products of CYSDV and WmCSV pGEM®T-Easy vector (Promega, USA) were ligated together. The insertion of recombinant plasmids in strain DH5α of *E. coli* occurred according to the instructions of the manufacturer. The Wizard® Plus SV Minipreps DNA Purification System (Promega, USA) was applied for the isolation of DNA from different white colonies. Then the digestion of DNA was done using *Eco*RI and electrophoresed on agarose gels. The orientation of these inserts in the plasmid was determined using two different primers for sequencing, the first one was T7 forward primer in the promoter region (5' TAATACGACTCACTATAGGG '3) and the second was SP6 reverse in promoter region (5'ATTTAGGTGACACTATAG '3). The clones having inserts of accurate sizes were selected for sequencing using an automated instrument for DNA sequencing (ABI 377XL). Sequencing Analysis Software, ABI™ version 3.0 was used to analyze the data. All sequencing was carried out in Macrogen Company, Seoul, South Korea.

Sub-cloning of the selected fragments into a binary vector

The selected fragments for gene silencing (CYSDV-CP, CYSDV-Hsp70, CYSDV-ORF3, WmCSV-CP and WmCSV-rep*)* were re-amplified from the clones into pGEM-Teasy and sub-cloned into the binary vector pFGC5941 (kindly provided from the University of Arizona, USA) in both orientations once to give the sense orientation by restriction enzymes *Asc*I and *Swa*I and another one to give the antisense orientation with *Xba*I and *Bam*HI departing the intron *Chalcon Synthase* (*ChaS*) in the middle (Rezk et al., 2006; Soliman et al., 2008).

Preparation of sense, antisense and sense/antisense constructs

The sense constructs were prepared through the digestion of the DNA plasmids (pCYSDV-CP, pCYSDV-Hsp70, pCYSDV-ORF3, pWmCSV-CP and pWmCSV-rep) with *Asc*I (Thermo Fisher Scientific, USA) and *Swa*I (Thermo Fisher Scientific, USA) as the following: 50 U of *Swa*I and 10 µl of 10X buffer O were used to digest 50 µl of each DNA plasmid and dH_2O were added to reach 100 µl. The tubes were incubated at 30°C for 4 h and 50 U of *Asc*I and 10 µl of 10X buffer Tango™ were added, and incubated at 37°C for 4 h. The antisense constructs were prepared through the digestion of the plasmids with *Xba*I (Promega, USA) and *Bam*HI (Promega, USA) as the following: 50 U of each of *Xba*I and *Bam*HI, 5 µl of BSA (100 µg/µL), 10 µl of multicore buffer (PROMEGA) were used to digest 50 µl of DNA plasmids and dH_2O was added to reach 100 µl. The tubes were incubated at 37°C for 4 h. The sense/antisense constructs were prepared through the digestion of the plasmids with *Xba*I and *Bam*HI as described in antisense preparation and the tubes were incubated at 37°C in water bath for 4 h. The digested DNAs were electrophoresed in 2% agarose gel. A clean sharp scalpel was used to cut out the digested bands for gene cleaning. The restriction enzymes (the same enzymes) were used to digest the binary vector as described in each case of sense and antisense constructs. At the same time, the prepared sense constructs (psCYSDV-CP, psCYSDV-Hsp70, psCYSDV-ORF3, psWmCSV-CP and psWmCSV-rep) were digested in another reaction with *Xba*I and *BamH*I. The digested vector (100 ng) was added with 15 ng of the digested DNA of the selected fragment to a clean tube (both of them were digested with the same restriction enzymes). 1 U of T_4 DNA ligase, 1 µl of 10X ligase buffer and final volume of the 10 µl of the ligation mixture was obtained using nuclease-free water, and finally incubated overnight at 4°C.

Transformation of the constructs into *E. coli* competent cells

Competent cells *E. coli* (strain DH5α) were thawed on ice for 30 min and 100 µl was transferred to a pre-chilled 5 ml tube and 5 µl of ligated DNA was added and incubated on ice for another 30 min. Cells were heat-shocked for 2 min at 42°C by immersing the tube into a water bath for 2 min and then incubated on ice for 2 min. One milliliter of Luria-Bertani (LB) medium was added and cells grown for 1 h at 37°C in shaking water bath. Transformed cells were plated on the surface of prepared plates (LB solid medium with 50 µg/ml kanamycin) for overnight at 37°C and bacterial colonies containing recombinant plasmids were selected for further characterization. The enzyme digestion for the DNA minipreps of the selected colonies of constructs (sense, anti-sense, sense/anti-sense) were carried out using the restriction enzymes *Swa*I and *Asc*I (sense), *BamH*I and *Xba*I (anti-sense) and *Asc*I and *Xba*I (sense/anti-sense) as described earlier.

Nucleotide sequence analysis

Two primers were designed in the binary vector pFGC5941; one in the p35S promoter location (pFGC35SF, 5'AAGATGGACCCCCACCCACGAGG3') and the other in the OCS location (pFGC-OCSR, 5`AGGATCTGAGCTACACATGCTCAGG3`).

Transformation into *Agrobacterium tumefaciens* LBA4404

One microgram of plasmid DNA was added to the cells. Freezing the cells in liquid nitrogen was performed. The cells were thawed by incubating the tubes in a 37°C water bath for 5 min. 1 ml of YEP medium was added to the tube and incubated at 28°C for 2 to 4 h with gentle shaking. This period allowed the bacteria to express the antibiotic resistance genes. The tubes were centrifuged for 30 s in a table centrifuge. The supernatant solution was discarded and the cells were resuspended in 0.1 ml YEP medium. The cells were spread on a YEP agar plate containing 50 µg/ml kanamycin and 50 µg/ml streptomycin. The plate was incubated at 28°C. Transformed colonies should appear in 2 to 3 days.

Gene delivery using the syringe-spotting technique (SST)

After *A. tumefaciens* LBA4404 has been transformed with vectors harboring different constructs using chemical transformation, 5 ml culture was grown overnight at 28°C in the appropriate antibiotic selection medium. The next day, the culture was inoculated into a 50 ml LB medium containing the selective antibiotics. The culture was grown overnight in a 28°C shaker. *Agrobacterium* cells were harvested and resuspended in infiltration media [10 mM $MgCl_2$, 10 mM MES (2-N-morpholino ethane sulfonic acid), and 20 µM acetosyringone (4'-hydroxy-3,5-dimethoxyacetophenone)], adjusted

Table 1. Nucleotide sequences of the prepared primers to amplify the selected fragments of CYSDV and WmCSV.

Viruses'name	Primers' name	Nucleotide sequences (5`----------3`)	Restriction enzymes	Size (bp)
CYSDV	CYcpf	ATATTCTAGAGGCGCGCCACCAACACACTCATGCACGG	*Xba*I, *Asc*I	176
	CYcpr	ATATGGATCCATTTAAATATGTTCATGAGCCCTGGCG	*Bam*HI, *Swa*I	
	CYorf3f	ATATTCTAGA GGCGCGCCACTTGAAGTACAGGGGC	*Xba*I, *Asc*I	198
	CYorf3r	ATATGGATCCATTTAAATATGCCCTAGCCCTTAGAAGATCC	*Bam*HI, *Swa*I	
	Hsp702f	ATATTCTAGA GGCGCGCCAGGTGATTCGTTTTTGGGAGG	*Xba*I, *Asc*I	232
	Hsp702r	ATATGGATCCATTTAAATTCACATTATGAAGTTTGCCTG	*Bam*HI, *Swa*I	
WmCSV	Wmcp1	ATATTCTAGAGGCGCGCCAGATATTCTCATTTCCACTCCCG	*Xba*I, *Asc*I	160
	Wmcp2	ATATGGATCCATTTAAATCCTGTACATCCTCGGCTTCC	*Bam*HI, *Swa*I	
	Wmrep1	ATATTCTAGAGGCGCGCCAAGTGCTTTAGATAGTGCGG	*Xba*I, *Asc*I	230
	Wmrep2	ATATGGATCCATTTAAATACCGCCTGAGCTCGTTGATTGGG	*Bam*HI, *Swa*I	

to OD_{600} of 2.0 and left at room temperature for 3 h. The prepared constructs (pasCYSDV-CP, pasCYSDV-Hsp70, pasCYSDV-ORF3, pasWmCSV-CP, and pasWmCSV-rep) in sense and sense/antisense direction were used to inoculate all experimental plants in this study. Tobacco (*Nicotiana benthamiana*) plants were infiltrated at the stage of seedlings in 2 to 3 leaves (each treatment contains 10 plants) with *Agrobacterium* containing both prepared constructs and the empty binary vector without construct (as a control) using a 5 ml syringe with no needle (Johansen and Carrington, 2001; Abhary, 2003). Fifteen days after the infiltration of the constructs, the challenge with infection viruses was carried out using the syringe spotted technique with infectious clones of WmCSV and CYSDV.

Evaluation of the resistance triggered against viral infection

The agro-infiltrating plants of *N. benthamiana* with different constructs were inoculated with viral infectious clones and the development of the disease symptoms was observed. In addition, RNA for CYSDV and DNA for WmCSV were extracted as described earlier; after that, PCR and non-radioactive hybridization methods were applied to detect the two viruses in the challenged plants.

RESULTS

PCR and RT-PCR analysis of the selected fragments

The designed specific primers CYcpf/CYcpr, Hsp702f/Hsp702r and CYorf3f/CYorf3r (Table 1), were used successfully for the amplification of the selected fragments of the coat protein gene (CP), heat shock 70 (Hsp70) and ORF3, respectively. In addition, the designed specific primers Wmcp1/Wmcp2 and Wmrep1/Wmrep2 (Table 1) were used successfully for the amplification of the selected fragments of coat protein gene (CP) and rep gene. The selected fragments of CYSDV were 176 bp of CP, 232 bp of Hsp70 and 198 bp of ORF3. While the selected fragments of WmCSV were 160 bp of CP and 230 bp of rep gene (Figure 1).

Cloning and sequencing of the selected fragments

The recombinant plasmids were digested with *Eco*RI restriction endonuclease to test for inserts of 176, 232 and 198 bp of CYSDV and 230 and 160 bp of WmCSV. One recombinant plasmid with inserts pCYSDV-*CP*, pCYSDV-*Hsp70*, pCYSDV-*ORF3*, pWmCSV-*CP* and pWmCSV-*rep* were selected for sequencing and sub-cloning in the binary vector pFGC5941.

Nucleotide sequence analysis of the selected fragments

Sequences of the PCR amplified fragments in the recombinant (pCYSDV-*CP*, pCYSDV-*Hsp70*, pCYSDV-*ORF3*, pWmCSV-*CP* and pWmCSV-*rep)* were completed. The sequences obtained with T7 forward, SP6 reverse primers were aligned with CYSDV, and WmCSV sequences available in the GenBank.

Sub-cloning of the selected fragments into the binary vector

Sub-cloning of the selected fragments into the binary vector were done in the two orientations once by the *Asc*I and *Swa*I (sense orientation) and second time with *Xba*I and *Bam*HI (antisense orientation) departing the Chalcon Synthase (*ChaS*) Intron in the middle and finally the third

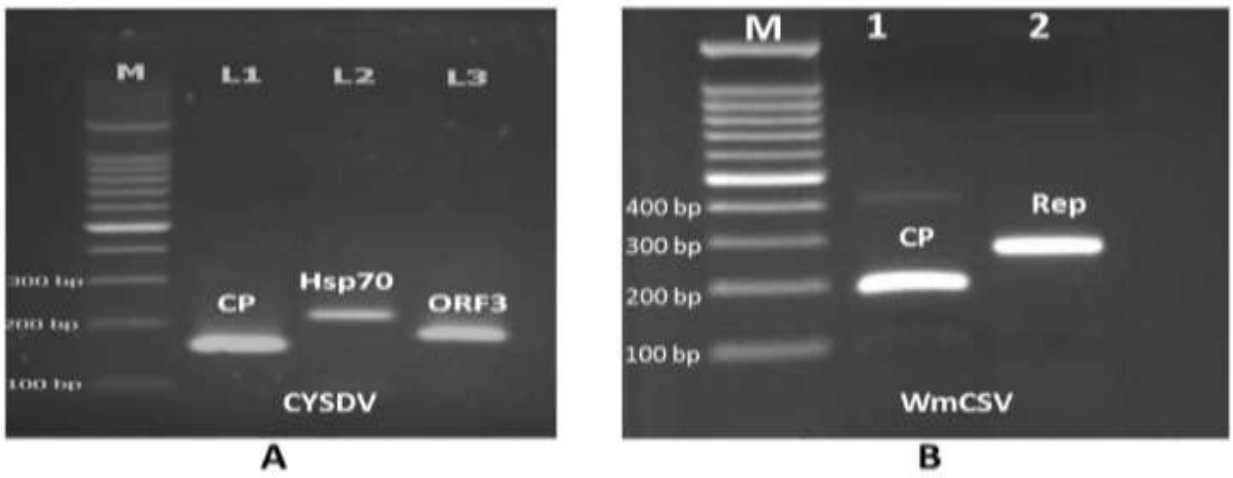

Figure 1. RT-PCR products of CYSDV and PCR products of WmCSV. **(A)** M: 100 bp DNA ladder; L1, 176 bp amplified fragment with primers CYcpf/CYcpr; L2, 232 bp amplified fragment with primers Hsp702f/Hsp702r; L3, 198 bp amplified fragment with primers CYorf3f/CYorf3r. **(B)** M, 100 bp DNA ladder; 1, 160 bp amplified fragment with primers Wmcp1/Wmcp2; 1, 230 bp amplified fragment with primers Wmrep1/Wmrep2.

construct of sense/antisense was prepared.

Nucleotide sequence analysis

The selected clones of the sense/antisense constructs were prepared for sequencing as described earlier. Nucleotide sequencing of the silencing fragments from the sense/anti-sense constructs were completed and the sequences were the same as the sequence obtained earlier.

PCR for the recombinant plasmids

PCR was done on the recombinant plasmids obtained from the Alkaline Lysis Miniprep method as described earlier. Using the previous profile of PCR, it was found that the transformation was carried out successfully and the bands appeared at their expected sizes.

Transformation into *Agrobacterium*

The constructs pasCYSDV-CP, pasCYSDV-Hsp70, pasCYSDV-ORF3, pasWmCSV-CP and pasWmCSV-rep in sense and anti-sense direction and binary vector pFGC5941 without construct as a control were transformed into *A. tumefaciens* LBA4404. Tobacco (*N. benthamiana)* plants were transformed using Syringe-Spotting Technique.

Evaluation of the transgenes

Screening for viral symptoms

The monitoring of symptoms appearance, after inoculation with viral infectious clones, was done daily to record the severity of symptoms. Clear symptoms on tobacco plants (*N. benthamiana*) took two to three weeks to appear (Table 2). All non-infiltrating tobacco plants (positive control) showed viral symptoms after inoculation. Most of the agro-infiltrating sense/antisense constructs did not yield symptoms of the viruses.

Screening with dot-blot hybridization

Tobacco plants inoculated with viral infectious clones were used as sources for DNA in dot-blot hybridization for the detection of viral genome in challenging plants. Total RNA and total DNA were extracted from new leaves using the methods mentioned earlier and blotted into nylon membranes. Hybridization was carried out using probes prepared to detect the viral genome in infiltrating plants with the different constructs. Results presented in Figure 2 showed that negative hybridization was obtained with infiltrating tobacco plants prepared constructs compared to those of non-infiltrating plants used as control. Only one out of five gave positive signals with the construct pasCYSDV-Hsp70.

Screening with RT-PCR and PCR

RT-PCR and PCR were carried out on the extracted RNA and DNA, respectively for the detection of the viral genome in challenging plants, after 15 days of inoculation with infectious clones of CYSDV and WmCSV. RT-PCR was applied using CYSDV-CP1 and CYSDV-CP2 primers to detect CYSDV. While, PCR was done using WmF2 and WmR2 primers to detect WmCSV. Positive reaction of the expected size, 500 bp of WmCSV and 800 bp of CYSDV were obtained with the infiltrating plants in case

Table 2. Viral symptoms severity after challenging with viral infectious clones showed by the number of infected tobacco plants per the number of infiltrating tobacco plants.

Construct's name	No symptoms	Mild symptoms	Severe symptoms
pasCYSDV-CP	5/5	0/5	0/5
pasCYSDV-Hsp70	2/5	2/5	1/5
pasCYSDV-ORF3	4/5	1/5	0/5
pasWmCSV-CP	5/5	0/5	0/5
pasWmCSV-rep	5/5	0/5	0/5
pFGC5941	0/5	0/5	5/5
Untreated plants	0/5	0/5	5/5

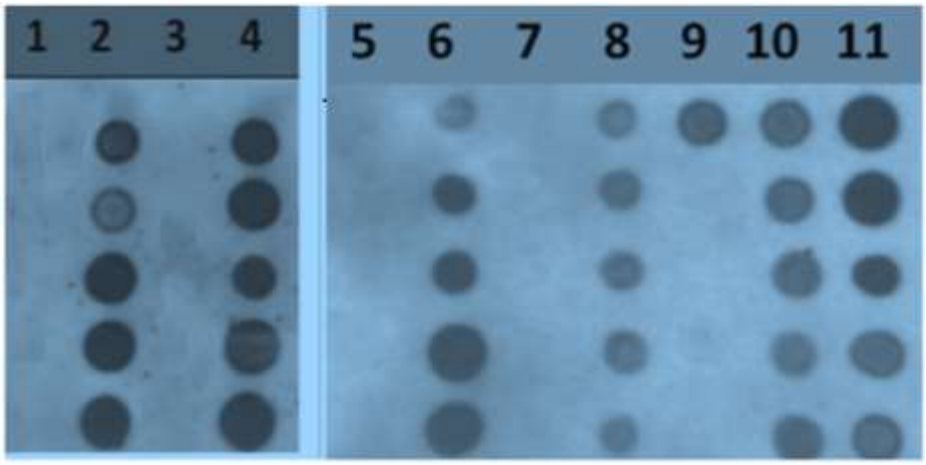

Figure 2. Non-radioactive labeling system dot-blot hybridization for virus detection in the treated plants. 1, pasWmCSV-CP; 2, psWmCSV-CP; 3, pasWmCSV-rep; 4, psWmCSV-rep; 5, pasCYSDV-CP; 6, psCYSDV-CP; 7, pasCYSDV-ORF3; 8, psCYSDV-ORF3; 9, pasCYSDV-Hsp70; 10, psCYSDV-Hsp70; 11, Untreated plants as control.

of sense constructs (ps) which proved the existence of the genome of both viruses in challenging plants (Figures 3 and 4). Infiltrating plants with sense/antisense (pas) constructs gave negative reactions indicating the lack of the viral genome. The obtained results indicate that the pasWmCSV-CP and pasCYSDV-CP constructs succeeded in preventing viral replication and infection in infiltrating plants through the siRNA-mediated resistance.

DISCUSSION

The application of new techniques is becoming a widely used strategy to control diseases caused by plant viruses. Post-transcriptional silencing (PTGS) of viral genes using co-suppression or anti-sense constructs performs a little ratio of silenced individuals (Wesley et al., 2001). There are two hallmarks in PTGS; first, silencing of target miRNAs occurs in the cytoplasm. Secondly, small interfering RNA (siRNA) molecules (21-25 nt) are generated from the silenced target mRNAs. Based on differences in their biogenesis, types of small RNAs (miRNA and siRNA) have been identified (Carthew and Sontheimer, 2009). The second type (siRNA) was used as a tool to have resistance cucurbit plants for CYSDV and WmCSV. The *A. tumefaciens*-mediated transient expression system is a multilateral system to quickly introduce genes into plant tissue. This system enables gene expression within a short period of time and without the demand for regenerating transgenic plants. The *Agrobacterium* mediated expression system has also been used effectively as a way to deliver RNA silencing suppressors and inducers into transgenic plants that express a silencing reporter gene (Johansen and Carrington, 2001).

Data from this study demonstrate clearly the effectiveness of the gene silencing application technique to trigger resistance against CYSDV and WmCSV. Three conserved, un-translated sequences of CYSDV genome were selected; the coat protein gene (CP), heat shock gene (Hsp70) and ORF3. While two conserved, un-translated sequences of WmCSV genome were selected;

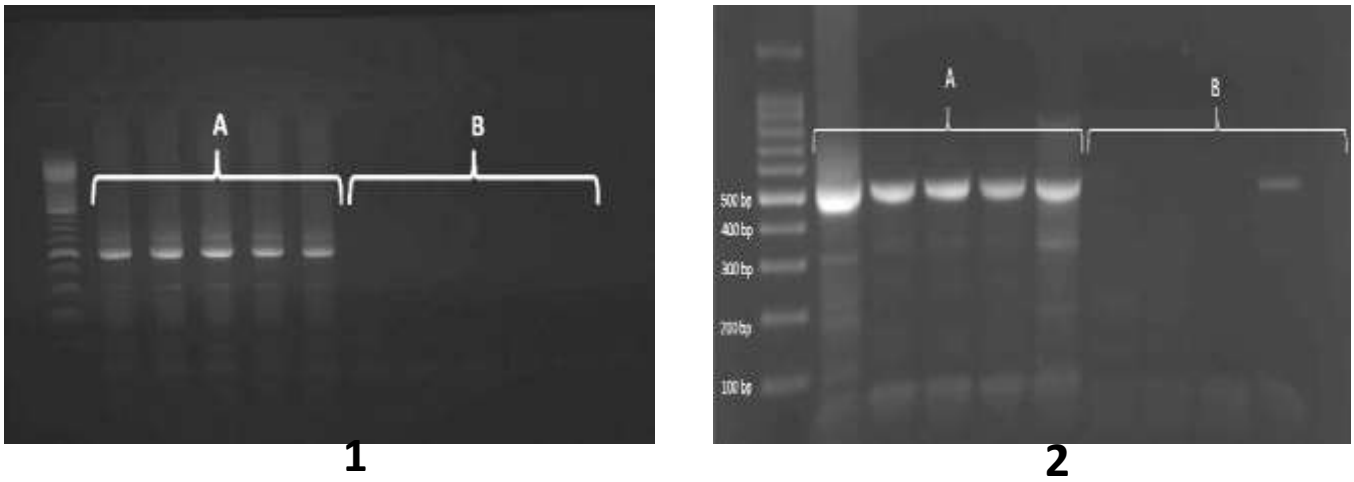

Figure 3. PCR for DNA extracted from different agro-infiltrating plants after 15 days of inoculation with infectious clone, using the primers WmF2 and WmR2. **(1)** A, plants treated with psWmCSV-CP; B, plants treated with pasWmCSV-CP. **(2)** A, plants treated with psWmCSV-rep; B, plants treated with pasWmCSV-rep.

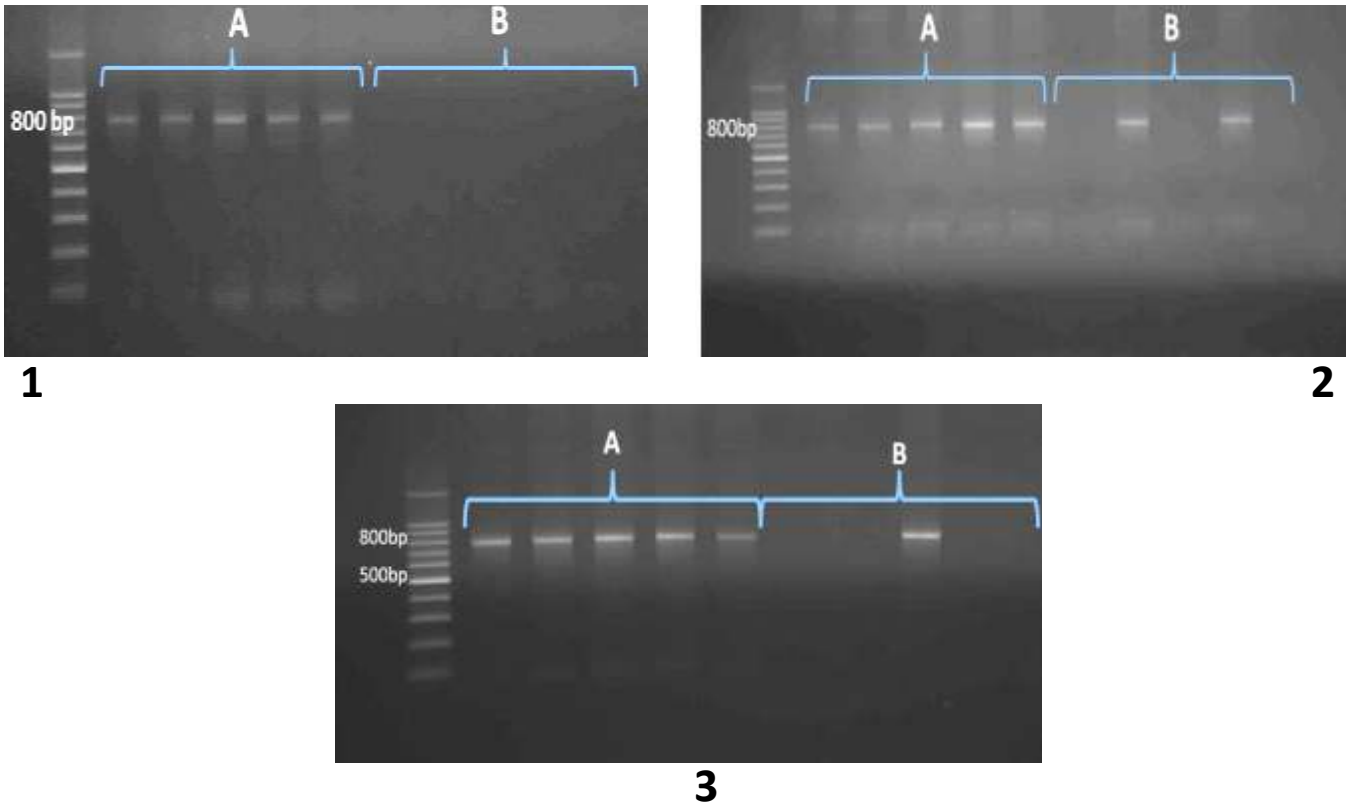

Figure 4. RT-PCR for RNA extracted from different agro-infiltrating plants after 15 days of inoculation with infectious clone, using the primers CYSDV-CP1 and CYSDV-CP1. (1) A, plants treated with psCYSDV-CP; B, plants treated with pasCYSDV-CP. **(2)** A, plants treated with psCYSDV-ORF3; B, pasCYSDV-ORF3. **(3)** A, psCYSDV-Hsp70; B, pasCYSDV-Hsp70.

CP gene and rep gene. In this study, the Syringe-Spotting Technique has been adapted to deliver different constructs into tobacco (*N. benthamiana*) cells. The high efficiency of this technique to convey the constructs may be attributed to the presence of large amount meristematic cells in small leaf tissues of newly evolved

seedlings, which supply the most suitable host-cells for the DNA to be expressed, and the bacterium to be linked (Soliman et al., 2008). Although the transformed plant cells are limited to the spotted region, RNA silencing signals could be systemically transmitted, as supposed by Eckardt (2002). Andrieu et al. (2012) mentioned that, the results of their work indicate that the method is efficient at inducing gene silencing in the agro-infected leaf area.

The transfer of low amounts of siRNA, probably occurring passively through the symplastic pathway from the agro-infected area, seemed sufficient to trigger degradation of target transcripts in the adjacent tissues. Data presented in this study shows that all transformed tobacco plants with empty vector and subsequent inoculated with CYSDV and WmCSV showed viral symptoms after 2 to 3 weeks of inoculation. These results suggest that the binary vector was single-handedly incapable to trigger resistance against CYSDV and WmCSV. In a similar way, all transformed tobacco plants with sense construct were oversensitive (susceptible) to the infection with CYSDV and WmCSV. These results suggest that, the transcription of the sense silencing trigger resulted in a mRNA that lacked the coding for any protein and did not recombine to the viral mRNA during the viral infection cycle.

Plants that had been transformed with antisense construct were all susceptible to the infection with CYSDV and WmCSV. However, these plants developed disease symptoms after two weeks of inoculation with CYSDV and WmCSV. This suggests that the progression rate of disease in these plants was lower than that with other treatments. High level of resistance could be induced in tobacco plants against CYSDV and WmCSV using sense/antisense construct in transformation. No disease symptoms could be observed in plants two and three weeks after inoculation and these plants remained symptomless until the experiment has been terminated (3 weeks after inoculation with CYSDV and WmCSV). These results clearly showed that, dsRNA folding could be produced by the sense/antisense orientation through the complementarities between the sense and the antisense orientations of the silencing triggers after the splicing of the ChaS intron post-transcriptionally. As previously described in the literature review, the dsRNA would be chopped into small temporal RNAs that can guide the host cell RISC protein to degrade the complementary sequence, which is the viral mRNA, in a sequence specific manner. This might explain the reason why plants transformed with sense/antisense construct did not show any disease symptoms during the experiment. The sequence homology of the silencing trigger might guide the RISC protein in tobacco cells to degrade the CYSDV and WmCSV messenger RNA before expressing the replicas and the coat protein, preventing the virus from initiating the replication cycle. Previous studies showed that the 21-23 nucleotides RNA known as siRNA is the main factor of gene silencing (Voinnet, 2002). The siRNA is derived from dsRNA by the action of an RNase III-like enzyme (Dicer). In another study, Llave (2002) showed that the small RNAs, extracted from inflorescent tissues, were accumulated in tissue-specific manner.

Conclusion

Data presented in this study provide evidence that the gene silencing (siRNA) technology could be used as significant virus-control measure. As indicated, high rate of plants was resistant to CYSDV and WmCSV when they were transformed with sense/antisense construct.

CONFLICT OF INTERESTS

The authors have not declared any conflict of interests.

ACKNOWLEDGEMENTS

The authors gratefully acknowledge King Abdulaziz City for Science and Technology (KACST) for financial support of the current research work project No. 10-Bio1096-06. In addition, the authors acknowledge Pest and Plant Diseases Unit (PPDU) team at College of Agricultural and Food Sciences, King Faisal University.

REFERENCES

Abdel-Salam AM, Abdalla Nagla M, Soliman Doaa ZR, Rezk, AA (2006). The incidence of *squash leaf curl begomovirus* (SLCV) in Egypt. Arab J. Biotechnol. 9(2):375-388.

Abhary MK (2003). Pathogen derived resistance for controlling *tomato yellow leaf curl virus* (TYLCV). M. Sc. Thesis, Al-Balqa Applied Univ. Fac. Agric. Tech. Dept. Biotech., Jordan.

Abou-Jawdah Y, Sobh H, Fayad A, Lecoq H, Delécolle B, Trad-Ferré J (2000). *Cucurbit yellow stunting disorder virus* - a new threat to cucurbits in Lebanon. J. Plant Pathol. 82(1):55-60.

Abudy A, Sufrin-Ringwald T, Dayan-Glick C, Guenoune-Gelbart D, Livneh O, Zaccai M, Lapidot M (2010). *Watermelon chlorotic stunt* and *Squash leaf curl begomoviruses* - New threats to cucurbit crops in the Middle East. Israel J. Plant Sci. 58(1):33-42.

Ali-Shtayeh MS, Jamous RM, Hussein EH, Mallah OB, Abu-Zeitoun SY (2014). *Squash leaf curl virus* (SLCV): A serious disease threatening cucurbits production in Palestine. Virus Genes 48(2):320-328.

Al-Musa A, Anfoka G, Al-Abdulat A, Misbeh S, Haj Ahmed F, Otri I (2011). *Watermelon chlorotic stunt virus* (WmCSV): A serious disease threatening watermelon production in Jordan. Virus Genes 43:79-89.

Al-Zahrani Rajaa A (2010). Studies on whiteflies that infect vegetables. M. Sc. Thesis, Girls' College of Education in Jeddah, King Abdulaziz University, Saudi Arabia.

Andrieu A, Breitler JC, Siré C, Meynard D, Gantet P, Guiderdoni E (2012). An *in planta*, *Agrobacterium*-mediated transient gene expression method for inducing gene silencing in rice (*Oryza sativa* L.) leaves. Rice 5:23.

Brown JK, Guerrero JC, Matheron M, Olsen M, Idris AM (2007). Widespread outbreak of *Cucurbit yellow stunting disorder virus* (CYSDV) in melon, squash, and watermelon crops in the Sonoran

Plateau region of the Western USA and Pacific Coast of Mexico. Plant Dis. 91(6):773.

Carthew RW, Sontheimer EJ (2009). Origins and mechanisms of miRNAs and siRNAs. *Cell*, 136(4): 642-655.

Célix A, López-Sése A, Almarza N, Gómes-Guillamón ML, Rodríguez-Cerezo E (1996). Characterization of *Cucurbit yellow stunting disorder virus* a *Bemisia tabaci*-transmitted closterovirus. Phytopathology 86(12):1370-1376.

Ding SW, Voinnet O (2007). Antiviral immunity directed by small RNAs. Cell 130:413-426.

Hassan AA, Duffus JE (1991). A review of yellowing and stunting disorder of cucurbits in the United Arab Emirates. Emir. J. Agric. Sci. 2:1-16.

Idris AM, Abdel-Salam A, Brown JK (2006). Introduction of the new world *Squash leaf curl virus* to squash (*Cucurbita pepo*) in Egypt: A potential threat to important food crops. Plant Dis. 90:1262.

Eckardt NA (2002). RNA Goes Mobile. The Plant Cell 14:1433-1436.

Johansen LK, Carrington JC (2001). Silencing on the Spot. Induction and suppression of RNA silencing in the *Agrobacterium*-mediated transient expression system. Plant Physiol. 126:930-938.

Jones P, Sattar MHA, al Kaff N (1988). The incidence of virus disease in watermelon and sweet-melon crops in the Peoples Democratic Republic of Yemen and its impact on cropping policy. Ann. Appl. Biol. 17:203-207.

Khan AJ, Akhtar S, Briddon RW, Ammara U, Al-Matrooshi AM, Mansoor S (2012). Complete nucleotide sequence of *watermelon chlorotic stunt virus* originating from Oman. Viruses 4:1169-1181.

Kheyr-Pour A, Bananej K, Dafalla GA, Caciagli P, Noris E, Ahoonmanesh A, Lecoq H, Gronenborn B (2000). *Watermelon chlorotic stunt virus* from the Sudan and Iran: Sequence comparisons and identification of a whitefly-transmission determinant. Phytopathology 90:629-635.

Kuo YW, Rojas MR, Gilbertson RL, Wintermantel WM (2007). First Report of *Cucurbit yellow stunting disorder virus* in California and Arizona, in association with *Cucurbit leaf crumple virus* and *Squash leaf curl virus*. Plant Dis. 91(3):330.

Li F, Xu X, Huang C, Gu Z, Cao L, Hu T, Ding M, Li Z, Zhou X (2015). The AC5 protein encoded by *Mungbean yellow mosaic India virus* is a pathogenicity determinant that suppresses RNA silencing-based antiviral defenses. New Phytologist 208:555-569.

Llave C, Kasschau KD, Rector MA, Carrington JC (2002). Endogenous and silencing-associated small RNAs in plants. Plant Cell 14:1605-1619.

Owen CA, Moukarzel R, Huang X, Kassem Mona A, Eliasco E, Aranda MA, Coutts RHA, Livieratos IC (2016). *In Vitro* Synthesized RNA generated from cDNA clones of both genomic components of *cucurbit yellow stunting disorder virus* replicates in cucumber protoplasts. Viruses 8:170.

Papayiannis LC, Hunter SC, Iacofides T, Brown JK (2009). Detection of *Cucurbit yellow stunting disorder virus* in cucurbit leaves using sap extracts and real-time TaqMan® reverse transcription (RT) polymerase chain reaction (PCR). J. Phytopathol. 158:487-495.

Rezk AA, Abdallah Nagla A, Abdel-Salam AM, Nakhla MK, Mazyad HM, Maxwell DP (2006). Transgene-mediated RNA silencing of TYLCV genes affecting the accumulation of viral DNA in plants. Arab J. Biotechnol. 9(1):143-158.

Ruiz-Ferrer V, Voinnet O (2009). Roles of plant small RNAs in biotic stress responses. Ann. Rev. Plant Biol. 60:485-510.

Soliman AM, Barsoum BN, Mohamed GG, Rezk AA, Aboul-Ata AE, Mazyad HM (2008). siRNA silencing of PVX coat protein gene affects the accumulation of viral RNA in potato and tobacco plants. Int. J. Virol. 4(1):14-25.

Sweiss M, Anfoka G, Abou-Jawdah Y (2007). Molecular characterization of Jordanian isolates of Cucurbit yellow stunting disorder virus. J. Phytopathol. 155:557-562.

Voinnet O (2002). RNA silencing: small RNAs as ubiquitous regulators of gene expression. Curr. Opin. Plant Biol. 5:444-451.

Wesley SV, Helliwell CA, Smith NA, Wang M, Rouse DT, Liu Q, Gooding PS, Singh SP, Abbott D, Stoutjesdijk PA, Robinson SP, Gleave AP, Green AG, Waterhouse PM (2001). Construct design for efficient, effect and high throughput gene silencing in plants. Plant J. 27(6):581-590.

academicJournals

Vol. 17(7), pp. 198-205, 14 February, 2018
DOI: 10.5897/AJB2017.16315
Article Number: 84D23C755917
ISSN 1684-5315
Copyright © 2018
Author(s) retain the copyright of this article
http://www.academicjournals.org/AJB

African Journal of Biotechnology

Full Length Research Paper

Tomato yellow leaf curl virus: Diagnosis and metabolites

Ahmed Mohamed Soliman[1,2*] and Maged Elsayed Mohamed[3,4]

[1]Department of Arid Land Agriculture, College of Agriculture and Food Sciences, King Faisal University, P. O. Box 420 Al-Hofuf, Al-Ahsaa 31982, Saudi Arabia.
[2]Department of Virus and Phytoplasma Research, Plant Pathology Research Institute, Agricultural Research Center, Egypt.
[3]Department of Pharmaceutical Sciences, College of Clinical Pharmacy, King Faisal University, Saudi Arabia.
[4]Department of Pharmacognosy, Faculty of Pharmacy, University of Zagazig, Zagazig 44519, Egypt.

Received 11 November, 2017; Accepted 25 January, 2018

The existence of *Tomato yellow leaf curl virus* (TYLCV) was figured out in different locations in Al-Ahsaa of Saudi Arabia. Polymerase chain reaction (PCR) results of samples collected showed that TYLCV existed in all locations. Using AVcore and ACcore primers, begomoviruses family were detected in symptomatic tomato plants and by using TYv2664 and TYc138 (specific primers for the detection of TYLCV), the results proved that the samples were infected with TYLCV. The lipid-soluble fraction of healthy and infected tomato leaves extract was compared using gas chromatography techniques. A total of 46 compounds were identified in both healthy and virus-infected leaf tissues; among which 37 metabolites were common between both samples and increased or decreased in concentration due to the virus attack. Nevertheless, eight compounds were exclusively detected in the infected samples with only one compound consumed and thus recognized only in the healthy samples. The classifications and roles of the identified metabolites were discussed from the point of view of plant defense mechanisms or virus resistance against plant defense.

Key words: Tomato yellow leaf curl virus (TYLCV), begomoviruses, Polymerase chain reaction (PCR), gas chromatography.

INTRODUCTION

Tomato (*Solanum lycopersicum*, L.) is economically important in Saudi Arabia and is one of the most important vegetable crops in the world. It is considered as one of the most popular and widely grown vegetable crops worldwide with the area harvested in Saudi Arabia being 14,902 ha in 2016 (FAOSAT, 2016). The production of tomatoes in Saudi Arabia in 2016 was 503,217 tonnes with most of that production (60%) grown in greenhouses (FAOSTAT, 2016).

Begomoviruses have one (monopartite) or two (bipartite) genomic components, denominated DNA-A and DNA-B, and are transmitted in a persistent manner

*Corresponding author. E-mail: amohamed@kfu.edu.sa, amsma33@hotmail.com.

Author(s) agree that this article remains permanently open access under the terms of the Creative Commons Attribution License 4.0 International License

Figure 1. Healthy **(A)** and TYLCV-infected **(B)** tomato leaves. Picture on the left represent the healthy leaves and picture on the right represent infected leaves by TYLCV. The plant samples were taken from tomato fields and green houses in Al-Ahsaa, Eastern Province, Saudi Arabia.

by whiteflies of the species complex *Bemisia tabaci* Gennadius (Hemiptera: Aleyrodidae) to dicotyledonous plants (Fernandes et al., 2010). *Tomato yellow leaf curl virus* (TYLCV) is one of the most important harmful and invasive members of the genus *begomovirus* (family *Geminiviridae*), which is widespread over the world associated with tomato yellow leaf curl disease (Barboza et al., 2013). TYLCV is transmitted by whiteflies and can spread rapidly; it is also not transmitted through seed or by mechanical transmission. Severe symptoms such as leaf curling, stunting, and yellowing showed on TYLCV-infected tomato plants, which cause serious production loss in tomato cultivation (Kil et al., 2016; Papayiannis et al., 2010). In addition to tomato, other cultivated plants including pepper (*Capsicum* species), common bean (*Phaseolus vulgaris*), cucurbit (*Cucumis* species) and eustoma (*Eustoma grandiflora*) have been reported to be TYLCV hosts (Anfoka et al., 2009; Kil et al., 2016). Polymerase chain reaction (PCR) was applied to detect and establish provisional identity of begomoviruses through amplification of 575 bp fragment of the begomoviral coat protein gene (CP), referred to as the 'core' region of the CP gene (core CP). The core CP fragment contains conserved and unique regions, and was hypothesized to constitute a sequence useful for begomovirus classification (Brown et al., 2001).

Metabolomics is used nowadays as a high potential tool for understanding different metabolic changes in many biological systems and its applications have been recognized in the quality control validations and natural products research (Dai et al., 2010). However, the use of metabolomics in investigating interactions between different organisms is until now infrequent. For example, a metabolic profile for *Catharanthus roseus* leaves infected with phytoplasma has been determined (Choi et al., 2004) and the aromatic metabolite profiles of *Arabidopsis thaliana* infected by *Pythium sylvaticum* has been investigated (Bednarek et al., 2005).

To the knowledge of the authors, the metabolites that resulted from the interaction between the *Tomato yellow leaf curl virus* and its host the tomato plant (*S. lycopersicum*) has never been investigated. The main aim of this study was to explore the type of phytochemicals newly produced, increased or decreased in concentration during the attack of TYLCV on the tomato plant leaves. The study could ascribe to the better knowledge of the plant-virus chemical connection.

MATERIALS AND METHODS

Plant material

Healthy tomato (*S. lycopersicum*, family *Solanaceae)* leaves samples (HTL) were identified and collected from the local fields and greenhouses in Al-Ahsaa, Eastern province, Saudi Arabia. Meanwhile, TYLCV naturally-infected tomato leaves samples (ITL) showing the typical symptoms of TYLCV infection (severe stunting, yellowing, curling of leaves and chlorosis on leaves) were collected from same field greenhouses (Figure 1).

All plants were identified by experts and taxonomists in the College of Agriculture and Food Sciences, King Faisal University, Saudi Arabia with specimens deposited to the herbarium of the college.

Primers for begomoviruses and TYLCV

Two sets of primers were used in this study to identify the TYLCV infection (Table 1). The first set of primers were AVcore and ACcore used for the detection of begomoviruses and the second set of primers were TYv2664 and TYc138 used for the detection of TYLCV (Table 1).

Table 1. The sequences of the primers used to detect the Begomoviruses and TYLCV.

Viruses	Primers' Name	Nucleotide Sequences	Size (bp)	Reference
Begomoviruses	AVcore	5`- GCCHATRTAYAG RAAGCCNAGRAT -3`	575	Brown et al. (2001)
	ACcore	5`- GGRTTDGARGCATGHGTACANGCC -3`		
TYLCV	TYv2664	5`- ATTGACCAAGATTTTTACACTTATCCC -3`	316	Anfoka et al. (2005)
	TYc138	5`- AAGTGGGTCCCACATATTGCAAGAC -3`		

Extraction of total DNA from plant tissues

Total DNA was isolated from the infected tomato plants using DNeasy® Plant Mini Kit obtained from QIAGEN as manufacturer's instruction.

Polymerase chain reaction (PCR)

The extracted DNA was used as a template for PCR using set of primers as shown in Table 1. AVcore and ACcore primers were used as degenerate primers for begomoviruses group to amplify 575 bp while TYv2664 and TYc138 primers were used to amplify 316 bp of IR of TYLCV. PCR reactions were optimized for 25 µl and the final concentrations of reaction components were: 25 µM deoxynucleotide triphosphate (dNTPs), 2.5 µl of 10X PCR buffer, 2.5 mM $MgCl_2$, 5 units *Taq* DNA polymerase, 1 µl of 10 µM of each complementary and viral-sense primers and 3 µl of DNA were used as target templates. PCR cycle parameters for AVcore and AC core primers were as follows: one cycle at 94°C for 2 min; 35 cycles at 94°C for 1 min, 55°C for 2 min, and 72°C for 2 min, followed by one cycle at 72°C for 10 min. PCR cycle parameters for TYv2664 and TYc138 primers were as follows: one cycle at 94°C for 5 min; 30 cycles at 94°C for 1 min, 62°C for 1 min, and 72°C for 1 min, followed by one cycle at 94°C for 1 min, 56°C for 1 min, and 72°C for 10 min. Five microliters aliquots of PCR products were analyzed on 1% agarose gels in 0.5X TBE buffer.

Plant sample preparation for analysis

Three hundred grams of the healthy and TYLCV-infected tomato leaves were isolated directly from the field to make the HTL and ITL samples, respectively. The samples were immediately placed into liquid nitrogen for preservation and enzyme deactivation and then pulverized into a powdered form and kept in -20°C until further analysis.

Metabolites extraction

The powdered samples were extracted by n-hexane (HPLC-grade, Fisher Chemicals) using a Soxhlet apparatus for 3 h (20 cycles, each) according to Shah and Alagawadi (2011). The n-hexane extracts were evaporated under reduced pressure to yield different residues. Twelve plants were used to give six HTL and ITL samples.

Metabolites isolation and identification

The n-Hexane extracts were investigated using gas-chromatography-mass spectrometry (GC-MS) for qualitative analysis and gas chromatography-flame ionization detection (GC/FID) quantitative analysis. The GC conditions involved the use of Shimadzu-QP-2010 machine equipped with a capillary column (DB-5 ms 30 m × 0.25 mm I.D., 0.25 µm). The chromatograph was programmed for an initial temperature of 50°C for 2 min followed by a 5°C/min temperature ramp to 280°C. The final temperature was maintained for 4 min. Injector and detector temperatures are maintained at 250 and 280°C, respectively. The initial head pressure of the carrier gas (He) was 90 kPa and a split injection system (ratio 1:20) was used. In GC/MS, the capillary column was directly coupled to a quadruple mass spectrometer (Shimadzu model QP2010S), the ionization mode was electron impact (EI) and ionization energy was 70 eV.

Components identification and percentage area calculation

Different separated compounds were identified using Kovat's Retention indices (RI) calculated with respect to a set of co-injected homologous series of saturated hydrocarbon standards (C8 to C40, Sigma, UK). Compounds were identified by comparing their spectral data and RI with Wiley Registry of Mass Spectral Data 9th edition/NIST Mass Spectral Library (2011), and literature data (Adams, 2007). Some of the compounds were identified using authentic samples and those compounds are marked in Table 2. Calculations of peak percentage areas, based on FID response, are as follow:

Percent area of peak = (The FID peak area / the sum of all the FID peaks areas) × 100

Most of non-identified components are present as traces with relative abundances of less than 0.1%. The most important constituents identified in the n-hexane fractions analyzed are listed in Table 2. The percent area ratio was calculated for each component and displayed in Table 2. This ratio indicates that this component increased in concentration due to the virus attack (that is, the ratio will be more than 1) or decreased due to the attack (the ratio will be less than 1).

Statistical analysis

Six samples were used for both HTL and ITL (n=6), respectively and each sample was injected in triplicate. Quantitative values are expressed as mean ± standard error of mean of percentage areas and significance difference was determined using unpaired student-sample-t-test performed using SPSS statistical package version (SPSS for Windows, Version 11.5, SPSS Inc., Chicago, IL). $P<0.05$ was considered significant.

RESULTS

Detection of TYLCV

DNA of the expected sizes, 575 and 316 bp of

Table 2. Comparison between the n-hexan extract constituents of healthy tomato leaves (HTL) and infected tomato leaves (ITL) TYLCV. The major 46 compontes the n-hexan fraction were compared. The percentages of infected (ITL) to healthy (HTL) fraction of the same compound of both n-hexan fractions are in the ITL/HTL ratio column. The Quantitative values are expressed as mean ± SEM of six independent infected and healthy leaf samples (n=6).

S/N	Compound name	Rt (min)	RI	Area percentage		Significance difference*	ITL/HTL ratio#
				HTL	ITL		
1	Octane	2.444	801	0.208 ± 0.014	0.692 ± 0.036	Yes	3.327
2	1.3.5-Bisabolatrien-7-ol	21.151	1604	None	0.117 ± 0.014	Yes	Present in ITL only
3	E-Bisabol-11-ol	23.701	1666	None	0.057 ± 0.004	Yes	Present in ITL only
4	Palmitic acid**	24.268	1680	0.195 ± 0.008	0.116 ± 0.007	Yes	0.598
5	2Z.6E-Farnesol	26.012	1723	0.126 ± 0.024	0.162 ± 0.009	Yes	1.289
6	2E.6E-Farnesal	26.268	1729	0.048 ± 0.002	0.131 ± 0.018	Yes	2.711
7	E-β-Santalol	26.493	1735	0.309 ± 0.015	None	Yes	Present in HTL only
8	6R-7R-bisabolone	27.609	1762	0.256 ± 0.047	0.383 ± 0.025	Yes	1.499
9	β-Bisabolenal	27.771	1766	Trace	0.241 ± 0.029	Yes	Present in ITL only
10	2E,6E-Methyl farnesoate	28.38	1781	9.821 ± 0.424	8.379 ± 0.521	Yes	0.853
11	Z-β-Santalol acetate	30.042	1818	0.150 ± 0.024	0.095 ± 0.011	Yes	0.636
12	Phytol	30.953	1837	1.363 ± 0.124	1.645 ± 0.179	No	1.207
13	Linolenic acid methyl ester**	31.275	1843	1.546 ± 0.245	3.786 ± 0.168	Yes	2.449
14	Bisabolatrien-1-ol-4-one	31.377	1845	1.448 ± 0.256	1.643 ± 0.149	No	1.135
15	2E.6E-Farnesyl acetate	31.452	1847	0.925 ± 0.132	1.072 ± 0.087	No	1.159
16	Z.Z-Farnesyl acetone	31.649	1851	0.680 ± 0.055	1.176 ± 0.245	Yes	1.730
17	Stearic acid**	31.857	1855	1.582 ± 0.147	2.288 ± 0.196	Yes	1.446
18	E-β-Santalol acetate	32.243	1863	Trace	0.560 ± 0.084	Yes	Present in ITL only
19	5Z.9E-Farnesyl acetone	33.903	1897	Trace	0.708 ± 0.063	Yes	Present in ITL only
20	cis-9-Hexadecenal	34.775	1915	0.105 ± 0.065	0.095 ± 0.012	No	0.905
21	Isophytol	36.602	1952	None	0.504 ± 0.024	Yes	Present in ITL only
22	E-β-ionone	37.08	1962	0.763 ± 0.054	1.415 ± 0.092	Yes	1.855
23	Stearylaldehyde	37.518	1971	2.089 ± 0.045	0.546 ± 0.013	Yes	0.261
24	Kaur-15-ene	38.994	2001	0.165 ± 0.024	0.095 ± 0.007	Yes	0.578
25	Palmitaldehyde	39.657	2025	0.970 ± 0.057	1.567 ± 0.145	Yes	1.616
26	Kaurene	40.108	2041	0.696 ± 0.049	1.234 ± 0.098	Yes	1.772
27	6Z,10E-Pseudo phytol	40.292	2048	Trace	0.508 ± 0.041	Yes	Present in ITL only
28	6E,10E-Pseudo phytol	40.642	2060	None	0.690 ± 0.036	Yes	Present in ITL only
29	Humulene epoxide	41.524	2092	None	0.067 ± 0.084	Yes	Present in ITL only
30	Methyl linoleate	41.796	2102	0.681 ± 0.009	0.680 ± 0.007	No	0.999
31	Squalene	41.9	2105	0.706 ± 0.062	0.602 ± 0.041	Yes	0.852
32	Stearic acid methyl ester**	42.262	2118	0.757 ± 0.096	1.094 ± 0.112	Yes	1.444
33	linoleic acid**	42.683	2134	1.194 ± 0.145	0.999 ± 0.128	No	0.837
34	Oleic acid**	42.857	2140	Trace	0.486 ± 0.039	Yes	Present in ITL only
35	Abieta-(8(14).13(15)-diene	43.244	2154	6.020 ± 0.341	4.473 ± 0.418	Yes	0.743
36	Phytol acetate	44.951	2215	2.182 ± 0.156	1.808 ± 0.147	Yes	0.829
37	3-β-Stigmast-5-en-3-ol**	46.242	2261	2.104 ± 0.143	3.894 ± 0.221	Yes	1.850
38	Dehydro abietal	46.474	2270	0.844 ± 0.045	0.812 ± 0.061	No	0.962
39	β-Sitosterol**	47.138	2293	25.641 ± 1.597	20.256 ± 1.387	Yes	0.790
40	Abietal	47.459	2305	None	0.629 ± 0.025	Yes	Present in ITL only
41	Campesterol	48.646	2347	None	0.970 ± 0.087	Yes	Present in ITL only
42	Methyl dehydro abietate	48.939	2358	3.997 ± 0.367	3.171 ± 0.278	Yes	0.793
43	4-epi-Abietal	49.646	2383	3.213 ± 0.285	3.346 ± 0.391	No	1.041
44	Stigmast-4-en-3-one	51.642	2566	2.351 ± 0.135	2.282 ± 0.222	No	0.971
45	neo-Abietol	51.997	2605	None	0.566 ± 0.054	Yes	Present in ITL only
46	Lupeol**	52.918	2704	7.266 ± 0.521	6.604 ± 0.428	No	0.909

Table 2. Contd.

Total fraction percentage area	80.400	82.640	
Sesquiterpenes	24.701	25.945	
Fatty acids	9.118	11.656	
Sterols and triterpenes	38.068	34.607	
Abietic acid derivatives	10.938	11.154	
Bisaboline derivatives	1.703	2.440	
Phytol derivatives	3.544	5.155	

Rt, Retention time; RI, retention index. Trace: concentration less than 0.1%. *Significance difference is between H and I percentage area for each component, determined using unpaired student-sample-t-test (p<0.05). ** identified using standards compounds. #The ITL/HTL ratio indicate if this component increased in concentration due to TYLCV attack (implying the ratio is more than 1) or decreased due to the attack (implying the percentage is less than 1).

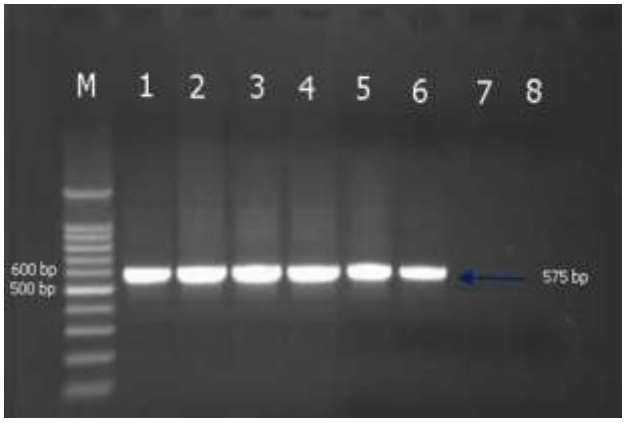

Figure 2. Agarose gel electrophoresis of PCR products using the degenerate primers AVcore/ACcore. M, 100 bp DNA ladder (Promega); from 1 to 6, six tomato samples showed symptoms of TYLCV infection; 7, healthy tomato sample; 8, negative control.

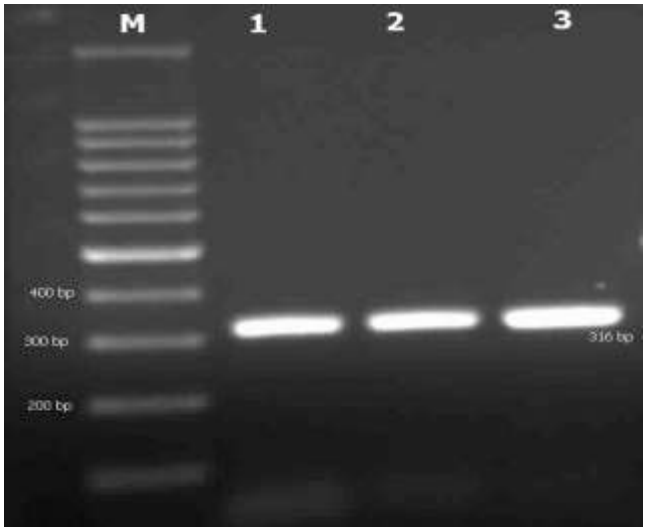

Figure 3. Agarose gel electrophoresis of PCR products using the primers TYv2664/TYc138. M, 100 bp DNA ladder (Promega); from 1 to 3, three tomato samples showed symptoms of TYLCV infection and gave positive reaction with degenerate primers AVcore/ACcore.

begomoviruses and TYLCV, respectively, were amplified from symptomatic tomato plants using the primer pairs AVcore/ACcore (Figure 2) and TYv2664/TYc138 (Figure 3), respectively.

Analysis of n-hexane fraction

This study was performed to compare the lipid-soluble metabolic pool of compound in healthy tomato leaves to that of the TYLCV-infected leaves, which allows the identification of the newly synthesized metabolites, or those, which differ in concentration because of the virus attack.

The gas chromatographic analysis of the n-hexane fraction (Figure 4 and Table 2) resulted in the separation of 84 components, 46 of which were identified, representing 80.40 and 82.64% of the total fraction contents of the HTL and ITL sample, respectively. Thirty-seven common compounds were identified between the two extracts; however eight compounds were produced uniquely in the infected tissue extracts and a compound was identified in the healthy samples only indicating its total consumption during the virus infection process. Similarly, five compounds were found in trace in the healthy tissues indicating that 14 compounds were more or less produced due to the virus infection (Table 2). The concentrations of the 12 compounds increased in the infected tissues in relation to the healthy ones. Nevertheless, ten common compounds decreased in concentration when the tissue was infected and both cases can be recognized from ITL/HTL ratio in Table 2. The change in concentration in ten common compounds was considered insignificant, and thus those compounds are considered to have no change in concentration due to the virus infection.

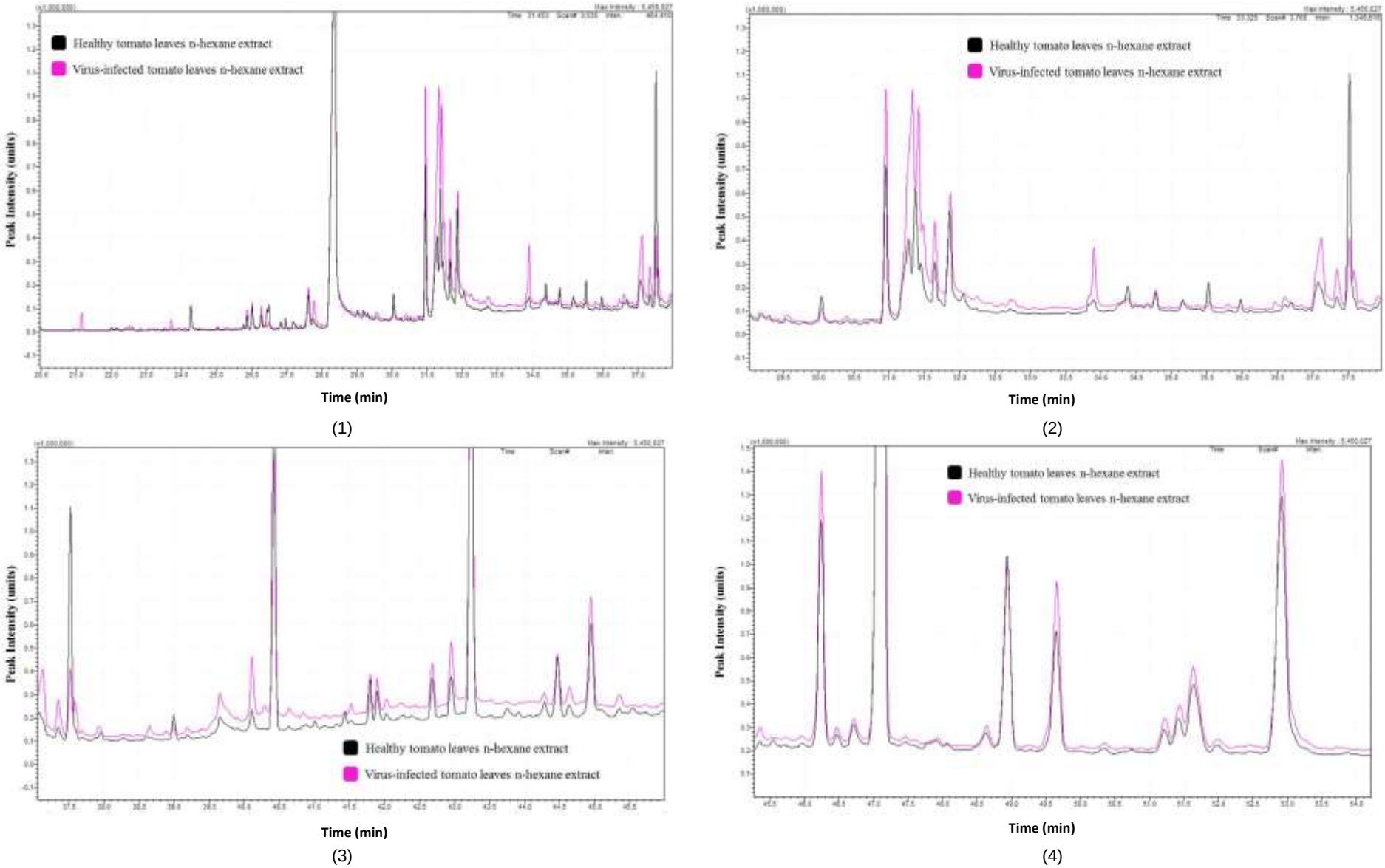

Figure 4. Aligned and expanded GC-MS chromatograms of the n-hexane fraction extracted from healthy Tomato leaves (HTL, lower in black) and TYLCV-infected leaves (ITL, upper in pink). To follow up the retention time on the chromatograms (from 1 to 55 min), follow the numbers from 1 to 4.

DISCUSSION

In the present study, the detection of begomoviruses in tomato was done and the results agreed with that of Alhudaib et al. (2014) and Rezk (2016) who used the degenerate primers of AVcore and ACcore to detect the begomoviruses in infected tomato samples in Saudi Arabia. Also, a leaf curl disease with symptoms typical of begomoviruses was observed in bean (*P. vulgaris*) at the Main Research Farm of the Indian Institute of Pulses Research, Kanpur, India (Kamaal et al., 2015) whereas Herrera-Vásquez et al. (2016) detected begomoviruses in commercial tomato plots using both production systems (open field and greenhouse) in Panama with different degenerate primers.

Just et al. (2014) stated that, imported tomato fruits infected with *Tomato yellow leaf curl virus* (TYLCV) were identified on the market in northern Europe using paper-based FTA Classic Cards (Whatman), PCR and partial DNA sequence analysis.

Impact of the metabolites pool changes due to the virus attack

Analysis of Table 2 discloses many classes of lipid-soluble components in the healthy and infected tissues of tomato leaves with different ratios. Sterols and triterpenes are the main class of compounds, which can be identified in the metabolites of both healthy and virus-infected leaves (Table 2). Although there was total decline in sterols and triterpenes concentration, 3-β-Stigmast-5-en-3-ol increased by 1.85 folds due to the virus infection. The concentration of β-Sitosterol represents nearly 25% of the total lipid-soluble fraction and it declined in the virus-infected leaves to reach 0.7 of its amount in healthy tissues. Accumulation of stigmasterol is a characteristic for plants during pathogens infection (Griebel and Zeier, 2010). Stigmasterol is chemically produced from β-sitosterol through C22 desaturation and this can explain the consumption of β-sitosterol and the increase in stigmasterol concentration due to the virus attack. Campesterol is produced uniquely in the virus-infected tomato leaves tissues. Campesterol are the precursor of steroidal phytohormones called brassinosteroids (Schaller, 2003), which are of vital role in plant defense mechanism against any pathogen attack (Choudhary et al., 2012). The increase in Campesterol concentration due to the virus attack might indicate an effect applied by the virus to weaken the plant defense through prevention of the production of brassinosteroids. On the other hand, a low ratio of Campesterol to sitosterol is needed for high plant cell membrane integrity and functionality (Schaeffer et al., 2001), though this ratio was affected by the production of Campesterol in the virus infected tissues which could lead to interruption and weakness of cell member, that is, the curling effect.

Sesquiterpenes are another class of compounds which are found in high ratio in the lipid soluble metabolic pool of tomato leaves. Although the total sesquiterpene compounds concentration insignificantly changed due to the virus infection, many individual components were produced exclusively or showed meaningful increase in concentration due to infection. Sesquiterpenes in tomato leaves metabolic pool can be divided into three main classes; Fernesols, bisabolines and abietic acid derivatives. Fernesols represent around 11.6% of the total lipid-soluble fraction of tomato leaves and although this whole ratio did not change due to the virus infection, many compounds were individually increased or decreased. The most abundant fernesol-type sequitepene in tomato leaf is methyl farnesoate, which represents 9.82% in healthy tissue, and this percentage decreased to 8.37 in the infected tissues. Fernesols are insect hormones (Nagaraju, 2007) and prevent fungal mycelia development with slight anti-fungal properties (Hornby et al., 2001). Bisabolene-type compound are another type of component that belong to the sesquiterpenes pool. Bisabolenes are recognized as sexual pheromones (Brézot et al., 1994; Lu and Teal, 2001) and thus they, together with Fernesols could be emitted by the plant to attract insects (War et al., 2012) as a way to resist the virus attack. Abietic acid derivatives is another class of sesquiterpenes, which is represented in the total lipid-soluble fraction tomato leaves extract by nearly 11%. This ratio did not change significantly between the infected and non-infected leave tissues. Abietic acid and its derivatives are diterpenes which are known for their role in plant defense mechanisms and are recognized for their tissue healing properties and pathogen trapping capabilities (Costa et al., 2016).

Phytols are acyclic diterpene alcohols, which decreased due to the virus attack on the plant. Although phytol and phytol acetate concentration decreased, isophytol was produced uniquely in the attacked tissues. The production of isophytol can explain the decrease in concentrations in phytol and its acetate. The role of isophytol as a production in the virus infected tissues is not clear and needs further investigation. Fatty acids have been identified in both the HTL and ITL samples with 9.11 and 11.6%, respectively. The main fatty acids found in both extracts was stearic acids and its derivative; stearylaldehyde and its methyl ester. The concentration of stearylaldehyde has dramatically decreased in ITL tissues to reach 0.2% of its original concentration in HTL. However, the concentration of stearic acid and its methyl ester has increased by 1.4% for both compounds due to the virus attack and this could explain the decline in stearylaldehyde concentration.

Conclusion

TYLCV has been identified in local area of Al-Ahsaa region, Eastern province of Saudi Arabia using means of

specific PCR primers. The fat-soluble metabolites resulting from the virus attack on the tomato plants has been revealed using means of GC/MS and quantified using GC/FID. Forty-six compounds were separated in both healthy and virus-infected leaf tissues, among which eight compounds were exclusively detected in the infected samples and only one compound was consumed and thus recognized only in the healthy samples.

CONFLICT OF INTERESTS

The authors have not declared any conflict of interests.

ACKNOWLEDGEMENT

The authors are thankful to Dr. Mohamed S. Al-Saikhan, the Supervisor of Central Labs, College of Agricultural and Food Sciences, King Faisal University for assistance during scientific experiments.

REFERENCES

Adams, RP (2007). Identification of Essential Oil Components by Gas Chromatography/Mass Spectrometry, 4th Edition ed. Allured Publishing corporation, Chicago, Illinois, USA.

Alhudaib K, Alaraby W, Rezk AA (2014). Molecular characterization of tomato yellow leaf curl disease associated viruses in Saudi Arabia. Int. J. Virol. 10, 180-191.

Anfoka G, Haj Ahmad F, Abhary M, Hussein A (2009). Detection and molecular characterization of viruses associated with tomato yellow leaf curl disease in cucurbit crops in Jordan. Plant Pathol. 58:754-762.

Barboza N, Blanco-Meneses M, Hallwass M, Moriones E, Inoue-Nagata AK (2013). First Report of Tomato yellow leaf curl virus in Tomato in Costa Rica. Plant Dis. 98:699-699.

Bednarek P, Schneider B, Svatos A, Oldham NJ, Hahlbrock K (2005). Structural complexity, differential response to infection, and tissue specificity of indolic and phenylpropanoid secondary metabolism in Arabidopsis roots. Plant Physiol. 138:1058-1070.

Brézot P, Malosse C, Mori K., Renou M (1994). Bisabolene epoxides in sex pheromone innezara viridula (L.) (Heteroptera: Pentatomidae): Role ofcis isomer and relation to specificity of pheromone. J. Chem. Ecol. 20:3133.

Brown JK, Idris AM, Torres-Jerez I, Banks GK, Wyatt SD (2001). The core region of the coat protein gene is highly useful for establishing the provisional identification and classification of begomoviruses. Arch. Virol. 146:1581-1598.

Choi YH, Tapias EC, Kim HK, Lefeber AWM, Erkelens C, Verhoeven JTJ, Brzin J, Zel J, Verpoorte R, (2004). Metabolic Discrimination of Catharanthus roseus Leaves Infected by Phytoplasma Using 1H-NMR Spectroscopy and Multivariate Data Analysis. Plant Physiol. 135:2398-2410.

Choudhary SP, Yu JQ, Yamaguchi-Shinozaki K, Shinozaki K, Tran LS (2012). Benefits of brassinosteroid crosstalk. Trends Plant Sci. 17:594-605.

Costa MS, Rego A, Ramos, V, Afonso TB, Freitas S, Preto M, Lopes V, Vasconcelos V, Magalhães C, Leão PN (2016). The conifer biomarkers dehydroabietic and abietic acids are widespread in Cyanobacteria. Sci. Rep. 6:23436.

Dai H, Xiao C, Liu H, Tang H (2010). Combined NMR and LC-MS Analysis Reveals the Metabonomic Changes in Salvia miltiorrhiza Bunge Induced by Water Depletion. J. Proteome Res. 9:1460-1475.

Food and Agriculture Organization of the United Nations (FAOSTAT) (2016). Food and Agricultural Organization of United Nations, Crop (Tomatoes).

Fernandes FR, Albuquerque LCd, Inoue-Nagata AK (2010). Development of a species-specific detection method for three Brazilian tomato begomoviruses. Trop. Plant Pathol. 35, 043-047.

Griebel T, Zeier J (2010). A role for beta-sitosterol to stigmasterol conversion in plant-pathogen interactions. The Plant J. Cell Mol. Biol. 63:254-268.

Herrera-Vásquez JA, Ortega D, Romero AB, Davino S, Mejía LC, Panno S, Davino M (2016). Begomoviruses Infecting Tomato Crops in Panama. J. Phytopathol. 164:102-113.

Hornby JM, Jensen EC, Lisec AD, Tasto JJ, Jahnke B, Shoemaker R, Dussault P, Nickerson KW (2001). Quorum sensing in the dimorphic fungus Candida albicans is mediated by farnesol. Appl. Environ. Microbiol. 67:2982-2992.

Just K, Leke WN, Sattar MN, Luik A, Kvarnheden A (2014). Detection of *Tomato yellow leaf curl virus* in imported tomato fruit in northern Europe. Plant Pathol. 63(6):1544-1460.

Kamaal N, Akram M, Agnihotri A K (2015). Molecular evidence for the association of Tomato leaf curl Gujarat virus with curl disease of *Phaseolus vulgaris* L. J. Phytopathol. 163(1):58-62.

Kil EJ, Kim S, Lee YJ, Byun HS, Park J, Seo H, Kim CS, Shim JK, Lee JH, Kim JK, Lee KY (2016). Tomato yellow leaf curl virus (TYLCV-IL): a seed-transmissible geminivirus in tomatoes. Scientific reports. 6:19013.

Lu F, Teal PEA (2001). Sex pheromone components in oral secretions and crop of male caribbean fruit flies, *Anastrepha suspensa* (Loew). Arch. Insect Biochem. Physiol. 48:144-154.

Nagaraju GPC (2007). Is methyl farnesoate a crustacean hormone? Aquaculture 272:39-54.

Papayiannis LC, Katis NI, Idris AM, Brown JK (2010). Identification of weed hosts of tomato yellow leaf curl virus in cyprus. Plant Dis. 95:120-125.

Rezk AA (2016). Molecular characterization of tomato yellow leaf curl virus (TYLCV) infecting pepper and common bean. Int. J. Virol. 12(1-3):1-9.

Schaeffer A, Bronner R, Benveniste P, Schaller H (2001). The ratio of campesterol to sitosterol that modulates growth in Arabidopsis is controlled by sterol methyltransferase 2;1. Plant J. Cell Mol. Biol. 25:605-615.

Schaller H (2003). The role of sterols in plant growth and development. Prog. Lipid Res. 42, 163-175.

Shah AS, Alagawadi KR (2011). Anti-inflammatory, analgesic and antipyretic properties of *Thespesia populnea* Soland ex. Correa seed extracts and its fractions in animal models. J. Ethnopharmacol. 137:1504-1509.

War AR, Paulraj MG, Ahmad T, Buhroo AA, Hussain B, Ignacimuthu S, Sharma HC (2012). Mechanisms of plant defense against insect herbivores. Plant Signal. Behav. 7:1306-1320.

academicJournals

Vol. 17(7), pp. 206-212, 14 February, 2018
DOI: 10.5897/AJB2017.15989
Article Number: AD002BD55919
ISSN 1684-5315
Copyright © 2018
Author(s) retain the copyright of this article
http://www.academicjournals.org/AJB

African Journal of Biotechnology

Full Length Research Paper

Polymerase chain reaction amplification of 16S rDNA from three nosocomial bacterial isolates in Kaduna State, Northern Nigeria

Richard, R.[1*], Denwe, S. D.[2]., Yerima, M. B.[3] and Olatunde, S. K.[4]

[1]Department of Biological Science, Faculty of Science, Federal University Gashua, P.M.B 1005, Yobe State, Nigeria.
[2]Department of Biological Science, Faculty of Science, Nigerian Defence Academy, Kaduna State, Nigeria.
[3]Department of Microbiology and Biotechnology, Faculty of Science, Federal University Dutse, Jigawa State, Nigeria.
[4]Department of Pure and Applied Biology, Faculty of Pure and Applied Sciences, Ladoke Akintola University of Technology, P. M. B. 4000 Ogbomoso, Oyo State, Nigeria.

Received 15 March, 2017; Accepted 13 July, 2017

A wide variety of opportunistic pathogens has been detected in hospital surfaces. Medical center surfaces can serve as reservoirs of pathogenic bacteria. Among this pathogens, *Pseudomonas* species are one of the leading causes of nosocomial infections, frequently found in hospital environments. Polymerase chain amplification system remains one of the best methods for the rapid detection of low numbers of pathogenic bacteria with core references to nucleic Acid content. However, there is a limited researches focusing on these techniques to examine the molecular content of nosocomial bacteria. The present investigation examines types and strains of bacteria present in indoor air of wards, fomites and surgical tools of three prominent hospitals namely, Ahmadu Bello University Teaching Hospital Zaria, Hajiya Gambo Sawaba Hospital Zaria City and Barau Dikko Teaching Hospital Kaduna using standard methods. Preliminary Grams reaction and biochemical characterization was done according to standard methods, DNA extraction precede PCR amplification, probable organisms include *Pseudomonas aeruginosa*, *Corynebacterium* sp., *P. aeruginosa, Bacillus* sp., *Klebsiella pneumonia, Neisseria* sp., *Staphylococcus aureus* and *Staphylococcus epidermidis.* Out of all the isolates that were of public health concern, *Neisseria* sp., *S. aureus* and *P. aeruginosa* are the most prevailing isolates. A strain of *P. aeruginosa* was observed to give a DNA sequence. *P. aeruginosa* was the bacteria isolates sequenced and it showed 100% similarity having the id query: 86603, when blast using National Center for Biotechnology Information (NCBI). In general, patterns were specific at either the genus level or the species level. This research has been able to show that PCR is a promising fast method for the identification of nosocomial microorganisms.

Key words: Polymerase chain reaction, nosocomial bacterial, hospital and DNA.

INTRODUCTION

Nosocomial infection is one of the most common complications within health care facilities, certain studies have reported outbreaks resulting from contaminated hospital environments, it is called nosocomial infection if it develops 72 h after admission to the hospital (Akihiro et al., 2017). These infections are more dangerous than

other infections because they are caused by bacteria with a high resistance to antibiotics.

Health care facilities provide an environment conducive to exposure and transmission of bacteria; infections caused by these bacteria are an important cause of increased morbidity, mortality and health care costs worldwide (Daniel and Michael, 2015). Nowadays, although modern antibiotics have improved; still sometimes the treatment is difficult and causes morbidity and mortality to patients. Many outbreaks of nosocomial infections have come from reservoirs of pathogens in the inanimate hospital surfaces. The contribution of the environment surfaces remains an important factor in nosocomial infection. It has been reported that majority of the patient acquire this infection while staying in hospital (Ananthan et al., 2011).

The major causative agents in the Western world comprise Gram-positive *Staphylococcus aureus*, *Enterococcus* spp., *Streptococcus* spp., Gram-negative *Escherichia coli*, *Enterobacter* spp., *Proteus mirabilis*, *Klebsiella* spp. In Africa, *P. aeruginosa* are in increasing proportions due to intensive care treatment (Souza et al., 2015). *Pseudomonas* sp. are considered opportunistic pathogens that causes opportunistic infection, they are commonly found in nature (soils, water, plants and animals) and water treatment systems, thus demonstrating their adaptation to environments with low nutrient concentration and over a large temperature range (between 4 and 42°C) (Frickmann et al., 2013). Conventional examination of a bacterial infection mainly relies on culture-based techniques. These cultivations usually yield diagnostic results in days or in some cases up to a week after sampling. Furthermore, cultivation of bacteria is not always successful under laboratory conditions (Kerremans et al., 2008; Yoshimura et al., 2011). Such failures may occur due to unsuitable culturing conditions and methods for the bacterial species under study. Alternatively, the particular patient under investigation may have received antimicrobial therapy before sampling.

Molecular methods based on nucleic acid amplification and hybridization aim to circumvent these problems and hasten diagnostic procedures. In such methods, the pathogen is simultaneously detected and identified, which results in more rapid diagnosis than those obtained by conventional culturing methods and obviates the need for additional culture tests (Akihiro et al., 2017). The purpose of this research was to use molecular techniques as alternative methods for strains level identification of nosocomial bacterial found in indoor air of wards, fomites and surgical tools of three prominent hospitals namely, Ahmadu Bello University Teaching Hospital Zaria, Hajiya Gambo Sawaba Hospital Zaria City and Barau Dikko Teaching Hospital Kaduna, Northern Nigeria.

MATERIALS AND METHODS

Synopsis of the study location

Kaduna with location Coordinates 10°20'N 7°45'E, and 10.333°N 7.750°E usually referred to as Kaduna state to distinguish it from the city of Kaduna, is a state in Northwest Nigeria. It is the capital of Kaduna with a population of over 6,066,562 (2006 Census). The selected hospitals are the three major government hospitals in the state and the justification for selection of these hospitals was based on high patronization.

Isolation and molecular characterization of bacteria

Bacteria were isolated from indoor air of wards, fomites and surgical tools of Ahmadu Bello University Teaching Hospital Zaria, Hajiya Gambo Sawaba Hospital Zaria City and Barau Dikko Teaching Hospital Kaduna using standard methods described by Kerremans et al. (2008) and Cheesbrough (2006). The bacteria from bed sheets, pillow cases, nurses' desk and surgical tools were isolated using sterile swab sticks while those from the air in surgical wards and main wards were isolated using exposed plate technique.

Media preparation

All the media used in this research work (nutrient agar, nutrient broth, mannitol salt agar and blood agar) were prepared according to manufacturer's instructions.

Sample collection

Sampling sterile swab sticks were immediately introduced into nutrient broth and taken to Kaduna State University Microbiology Laboratory for incubation and further bacteriological analysis. In the exposed plate technique, the agar plates were opened and exposed to the indoor air of the wards for about 5 min. After 5 min of exposure the plates were covered again and taken to Microbiology laboratory for incubation. Both the agar plates and the broth were incubated at 37°C for 24 h. After incubation, the bacterial colonies that showed positive growth were sub-cultured, gram stained and viewed under the microscope using oil immersion x100 objectives lens (Kerremans et al., 2008).

Biochemical characterization and identification of the nosocomial isolate

Bacteria isolates extracted were characterized and identified after studying their Gram reaction as well as cell micro morphology. Other tests performed were spore formation, motility and catalase production, citrate utilization, fermentative utilization of glucose, indole production, methyl red- Voges Proskauer reaction, urease and coagulate production, starch hydrolysis, production of H_2S from triple sugar iron (TSI) agar and sugar fermentation. The test were carried out according to the methods described (Cheesbrough, 2006; Adeoye, 2007; Agwung-Fobellah and Kemajou, 2007; Ochei

*Corresponding author: E-mail: beckycool4u@gmail.com. Tel: +2347068360103.

Author(s) agree that this article remains permanently open access under the terms of the Creative Commons Attribution License 4.0 International License

and Kolhatkar, 2008). Microbial identification was performed using the keys provided in Barrow and Feltham (1993) and Bergey's Manual of Determinative Bacteriology (1994).

Molecular characterization of species of bacteria

The bacteria species characterized using biochemical methods were subjected to strain level identification using molecular approach. These involve extracting the DNA using standard protocols, amplifying the DNA using PCR, sequencing the gene of interest using next generation sequencing (NGS).

DNA extraction using phenol chloroform method

DNA was extracted using phenol chloroform standard method as described by Psifidi et al. (2010). 200 µl of the bacterial cells were added in a 1.5 ml Eppendorf tube, 400 µl of lysis buffer (Tris-HCL) and 10 µl of proteinase k was added to the 1.5 ml tube. The tube was vortexed and placed on heat block at 65°C for 1 h while vortexing at interval. 400 µl of phenol chloroform was added and vortexed briefly, it was centrifuged for 10 min at 13,000 rpm to separate the phases. The upper layer was carefully removed with a micro pipette, 400 µl of chloroform was added and vortexed, and was then centrifuged for 5 min at 13,000 rpm. The upper layer was carefully removed, 1000 µl of absolute ethanol and 40 µl of 3 M sodium acetate and mixed by inverting the tube several times.

The tubes containing pure DNA were incubated at -20°C overnight. The tubes were centrifuged for 5 min at 14,000 rpm using cool centrifuge, the upper layer was carefully removed using micro pipette, 400 µl of 70% ethanol was added to the precipitate, the tubes were centrifuged for 5 min at 14,000 rpm using cold centrifuge, the upper layer was carefully removed using micro pipette in order to remove all traces of ethanol, the DNA was then allowed to dry by leaving the tubes open for 20 min at room temperature and 50 µl of sterile water was added, vortexed and kept at -20°C.

PCR amplification of 16S rDNA using conventional PCR

The extracted DNA from different species of bacteria was quantified using Nano drop. Thereafter, the quantified genomic DNA was placed in a tube containing master mix and primer and the tube was spined for 30 s and introduced into a thermocycler. The thermocycler was operated based on initial denaturation (95°C for 5 min), 25 cycles of denaturation (94°C for 1 min), annealing (52°C for 1 min), extension (72°C for 1 min) and final extension (72°C for 7 min) according to Psifidi et al. (2010). 16S rDNA forward sequence 5^1 GGACTACGGGTATCTAAT 3^1 and reverse sequence 3^1 AGAGTTTGATCCAGG 5^1 after the PCR in the thermocycler, the amplified PCR products of expected size 789 bp were confirmed by agarose gel electrophoresis system. The amplified PCR products was run in 1.5% agarose gel electrophoresis stained with ethidium bromide and was viewed under ultra violet (UV) light (Smith et al., 2003; Black and Foarde, 2007).

Sequencing of the gene

The amplified genes of interest were documented, cut and freeze dried. The freeze dried samples of DNA were sent to Macrogen U.S.A laboratory for sequencing. The genomic sequence data was appropriately analyzed using bioinformatics tools, sequence identification was performed using NCBI Basic Local Alignment Search Tool (BLAST) algorithm, similar sequences were down-loaded and aligned while phylogenetic tree was drawn with MEGA 7 software (Kumar et al., 2016).

RESULTS

A total number of 66 bacteria were isolated from three hospitals in Kaduna State namely; Ahmadu Bello University Teaching Hospital, Zaria, Hajiya Gambo Sawaba Hospital, Zaria City and Barau Dikko Teaching Hospital, Kaduna (Table 1). Twenty-two (22) samples were collected from each of the hospitals for preliminary antibiotic resistance potency. Observation shows that only 20 of the bacterial isolates were recorded as multi drugs resistant which includes six (6) from Ahmadu Bello University Teaching Hospital, Zaria, eight (8) from Hajiya Gambo Sawaba Hospital, Zaria City and six (6) from Barau Dikko Teaching Hospital, Kaduna. The morphological and biochemical characterization of nosocomial bacterial isolates from hospital environments was presented in Table 1. Investigation revealed that *S. aureus* occurred as the highest predominant bacterial isolate with the percentage occurrence of 10 (50%) followed by *P. aeruginosa* with 4 (20%) and *Bacillus* sp. had 2 (10%), *Corynebacterium* sp., *Klebsiella pneumoniae, Neisseria* sp. and *Staphylococcus epidermidis* all recorded 1 (5%) appearances (Table 1).

DISCUSSION

A number of morphological and biochemical parameters have been used to facilitate the determining of the identities of nosocomial bacteria and other hospital acquired infections (Ateba and Mbewe, 2011). Even though selective and differential media has been used to aid the identification of the bacterial species, yet the sensitivity of these protocols might not be very reproducible between laboratories. Generally, selective and differential media rely on some structural or metabolic property of the species that is preferentially selected. It is highly recommended that they should be combined with confirmatory biochemical and morphological tests.

Table 1 show the morphological and biochemical characteristics of the 20 isolated multidrug resistant nosocomial bacterial (MDRNB). The present study (morphological observation) revealed the cell shapes of 40.00% of the overall isolated microorganisms possessed rod shape under the microscope while 60.00% were found to be cocci in shapes. This is a good characteristic of some organisms but not enough to categorize, hence, all isolates were subjected to grams staining test. About 25.00% of the isolated microorganism from analyzed samples stained pink to red, indicating them to be Gram negative organisms, while 75.00% of the overall isolates stained blue to purple by retaining the crystal violet dye indicating them to be Gram positive organisms (Bergey et al., 1994).

Table 1. Morphological and biochemical features of the selected examined Multi-Drugs Resistant (MDRI) isolate.

Isolate code	Cell shape	Gram reaction	Catalase	TSI reaction	SIM reaction 1 M H_2S	C-U	MR	VP	GL	MAL	MNT	SU	LAC	OF OR H L	N-R	*Probable organisms*
HSP-ABU	LR	-	+	NCNCNC	- + -	+	-	-	NC	NC	NC	NC	NC	OX	+	*Pseudomonas aeruginosa*
HSP-AGS	MLR	+	-	YGY+	+ + -	-	+	-	YG	YG	YG	YG	YG	F(G)	+(G)	*Corynebacterium* sp.
HSP-BDT	SR	-	+	NCNCNC	- + -	+	-	-	NC	NC	NC	NC	NC	OX	+	*Pseudomonas aeruginosa*
HSP-ABU	MLR	-	+	NCNCNC	- + -	+	-	-	NC	NC	NC	NC	NC	OX	+	*Pseudomonas aeruginosa*
HSP-AGS	LR	+	+ +	YGY+	+ + +	+	+	-	YG	YG	YG	YG	YG	F(G)	+(G)	*Bacillus* sp.
HSP-BDT	LR	-	+ +	YGNCNC	+ - -	+	+	-	YG	YG	YG	YG	YG	F	+	*Klebsiella pneumoniae*
HSP-AGS	CC	-	+	YGNCNC	+ + -	-	+	-	YG	YG	YG	YG	YG	F(G)	+	*Neisseria* sp.
HSP-BDT	MLR	-	+	NCNCNC	- + -	+	-	-	NC	NC	NC	NC	NC	OX	+	*Pseudomonas aeruginosa*
HSP-AGS	LR	+	+ +	YGY+	+ + +	+	+	-	YG	YG	YG	YG	YG	F(G)	+(G)	*Bacillus* sp.
HSP-ABU	CC	+	+ + +	YGNCNC	+ - -	+	+	-	YG	Y	Y	Y	Y	NC	+	*Staphylococcus aureus*
HSP-AGS	CC	+	+ + +	YGNCNC	+ - -	+	+	-	YG	Y	Y	Y	Y	NC	+	*Staphylococcus aureus*
HSP-BDT	CC	+	+ + +	YGNCNC	+ - +	+	+	-	YG	Y	Y	Y	Y	NC	+	*Staphylococcus aureus*
HSP-BDT	CC	+	+ + +	YGNCNC	+ - -	+	+	-	YG	Y	Y	Y	Y	NC	+	*Staphylococcus aureus*
HSP-BDT	CC	+	+ +	YGNCNC	+ - +	+	+	-	YG	Y	Y	Y	Y	NC	+	*Staphylococcus aureus*
HSP-ABU	CC	+	+ + +	YGNCNC	+ - -	-	+	-	YG	Y	Y	Y	Y	NC	+	*Staphylococcus aureus*
HSP-AGS	CC	+	+ +	YGNCNC	+ + -	+	+	-	YG	Y	Y	Y	Y	NC	+	*Staphylococcus aureus*
HSP-ABU	CC	+	+ + +	YGNCNC	+ - -	+	+	-	YG	Y	Y	Y	Y	NC	+	*Staphylococcus aureus*
HSP-ABU	CC	+	+ + +	YGNCNC	+ - -	+	+	-	YG	Y	Y	Y	Y	NC	+	*Staphylococcus aureus*
HSP-AGS	CC	+	+ +	YGNCNC	+ + +	-	+	-	YG	Y	Y	Y	Y	NC	+	*Staphylococcus aureus*
HSP-AGS	CC	+	+ +	YGNCNC	+ - -	+	+	-	YG	Y	Y	Y	Y	NC	+	*Staphylococcus epidermidis*

CC, Cocci shape; SR, short rod; MLR, medium long rod; LR, long rod; YG, acid and gas production; Y, acid production only; TSI, triple sugar ions; SIM, sulphide,indole,motility tests; CU, citrate utilization test; MR/VP, methyl red and Voges, Proskaur test; GL, glucose; NC, No change; F, fermentative; OX, oxidative; I, indole production; M, motility; H_2S, hydrogen sulphide production; MAL, maltose; MNT, mannitol; SU, sucrose; LAC, lactose; nitrate reduction test; OF, oxidation,fermentation Test; HSP, hospital; ABU, Ahmadu Bello University; HGS, Hajiya Gambo Sawaba; BDT, Barau Dikko Teaching Hospital Kaduna.

PCR amplification of 16S rDNA from the three highest prevailing nosocomial bacterial isolates in Kaduna State

Organisms of concern in this study are *P. aeruginosa, S. aureus* and *Neisseria* sp. Figure 1 shows the amplified 16S rDNA gene with band size of 789 bp bands from *Neisseria* sp., *P. aeruginosa* and *S. aureus* obtained from some selected hospitals in Kaduna State. To test whether we can discriminate between these isolates, *Neisseria* sp., *P. aeruginosa* and *S. aureus* strains were examined for their electrophoretic mobility patterns in PCR amplification (Figure 1). Although the observed differences were small, PCR amplification was capable of distinguishing all the isolates from one and other (Lee et al., 2009). For the *Pseudomonas* species, the observed electrophoretic mobility patterns showed light differences between *Staphylococcus* and *Neisseria* sp. (Figure 1). Because of the closed mobility relativity of all these on electrophoresis gel, these data suggest species-specific patterns for identification. To evaluate the applicability of PCR amplification as a general tool for the identification of bacteria, the amplified 16S rDNA products from the three nosocomial bacterial isolates were sequenced according to Cole et al. (2009) and the result obtained is shown in Figure 2. Out of the three bacterial isolates analyzed, only one which is *P. aeruginosa* gave a DNA sequence. *P. aeruginosa* was the bacterial isolates sequenced and it showed 100% similarity

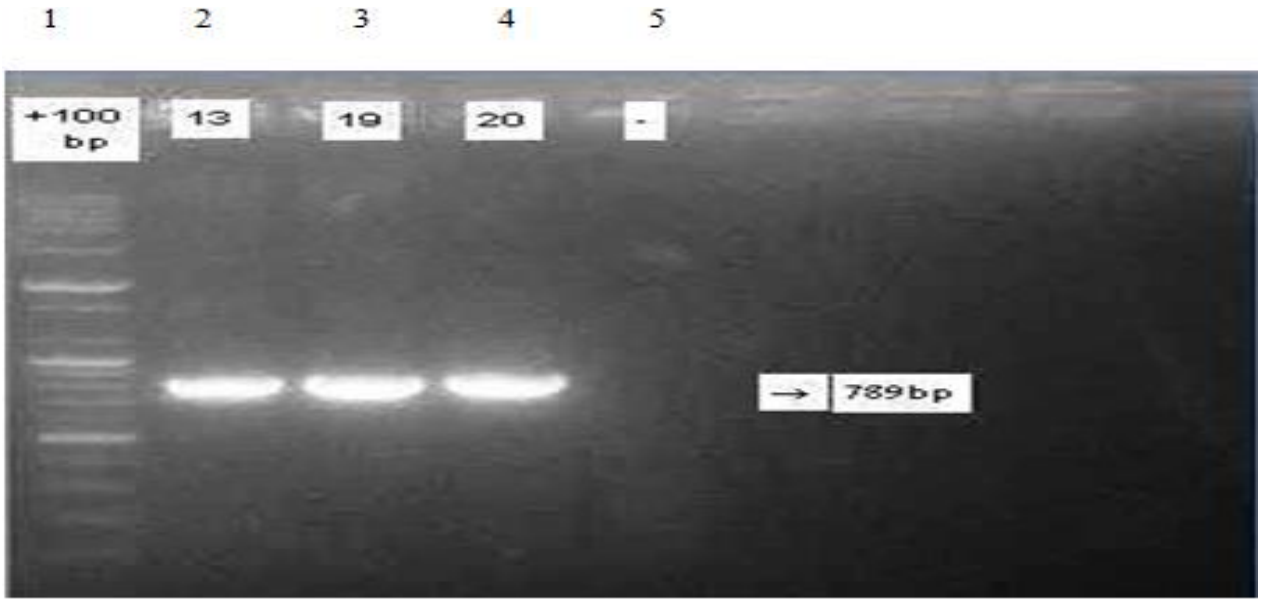

Figure 1. PCR amplification of 16S rDNA gene in three nosocomial bacterial isolates from some selected hospitals in Kaduna State. Lane 1, DNA marker; lane 2, *Neisseria* sp.; lane 3, *P. aeruginos;* lane 4, *S. aureus*; lane 5, negative control.

5[1]_CTCTCTTGGCGGCGAGTGGCGGACGGGTGAGTAATATATCGGAACGTGCCCAGTAGCGGGGGA
TAACTACTCGAAAGAGTGGCTAATACCGCATACGCCCTACGGGGGAAAGGGGGGGATCGCAAGACC
TCTCACTATTGGAGCGGCCGATATCGGATTAGCTAGTTGGTGGGGTAAAGGCTCACCAAGGCAACG
ATCCGTAGCTGGTTTGAGAGGACGACCAGCCACACTGGGACTGAGACACGGCCCAGACTCCTACGG
GAGGCAGCAGTGGGGAATTTTGGACAATGGGGGGAACCCTGATCCAGCCATCCCGCGTGTATGATG
AAGGCCTTCGGGTTGTAAAGTACTTTTGGCAGAGAAGAAAAGGTATCCCCTAATACGGGATACTGCT
GACGGTATCTGCAGAATAAGCACCGGCTAACTACGTGCCAGCAGCCGC _3[1]

Figure 2. Sequence of bacteria isolate (*Pseudomonas aeruginosa*).

having the id query: 86603, when using BLAST National Center for Biotechnology Information (NCBI). The red bullet indicates the sequenced *P. aeruginosa* (Figure 3). In general, patterns were specific at either the genus level or the species level.

However, we opined that in order to overcome lane-to-lane and gel-to-gel differences, PCR resolution was improved by the addition of an internal DNA marker for each sample lane. This makes it feasible to precisely compare relative migration times. This research has been able to show that PCR is a promising fast method for the identification of microorganisms. Also, the use of PCR with universal primers and Single Strand Conformational Polymorphism (SSCP) patterns as an identification method can generally be applied to a wide range of nosocomial bacteria without the need of a large panel of probes.

In order to intensify our research, we added an option for molecular identification of methicillin resistant S. species by including the methicillin resistance gene *mecA* in the assay. The identification was based on PCR amplification as shown in Figure 4. *mecA* gene was amplified in *S. aureus* which showed no visible band size. The presence of coagulase negative staphylococcal DNA other than that associated with *S. epidermidis* was then detected by genus-specific probes.

Conclusion

Molecular and genotypic characterization of bacteria is advantageous when compared to biochemical and phenotypic methods of characterization and identification of nosocomial bacterial. The latter require a prolonged cultivation period for the suspected bacteria and pure bacterial cultures for various biochemical assays. It is therefore concluded that broad-range PCR amplification with subsequent hybridization on a microarray is a rapid diagnostic tool in identifying causative agents of bacterial infections in various specimens from normally sterile site of the hospital environment to medical and surgical tool surfaces.

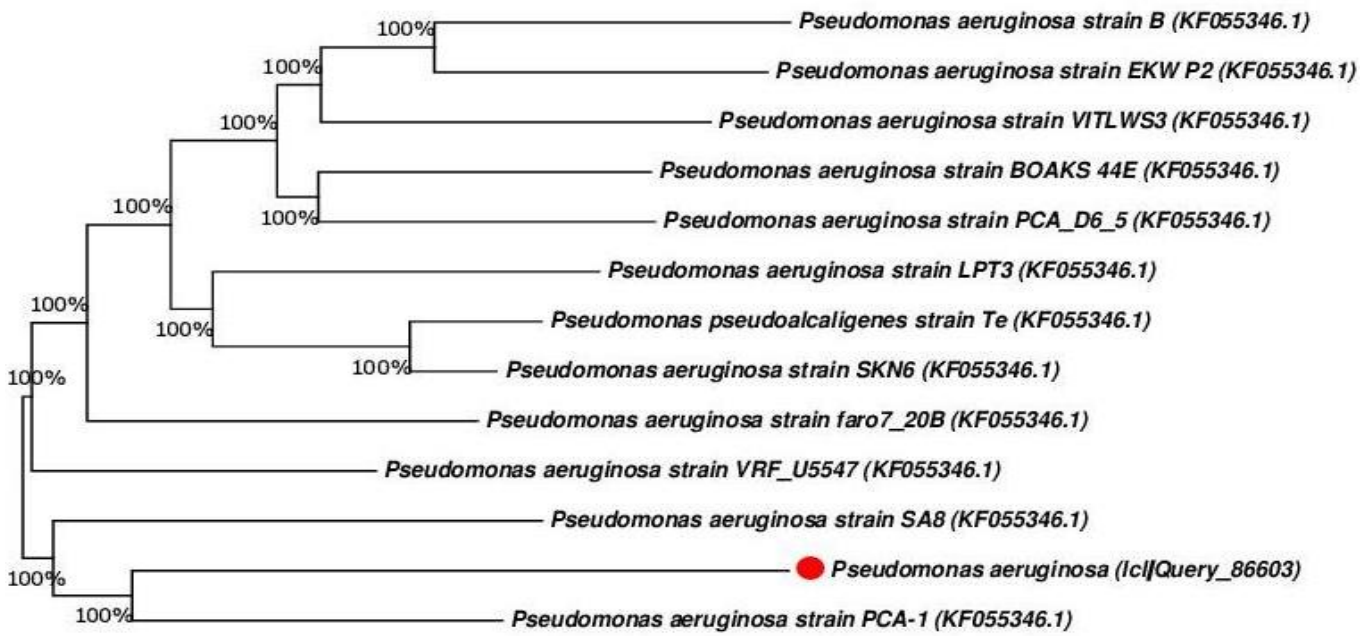

Figure 3. Phylogenetic tree of isolate with query id: 86603 Made by MEGA 7.0 showing percentage similarity of coding regions.

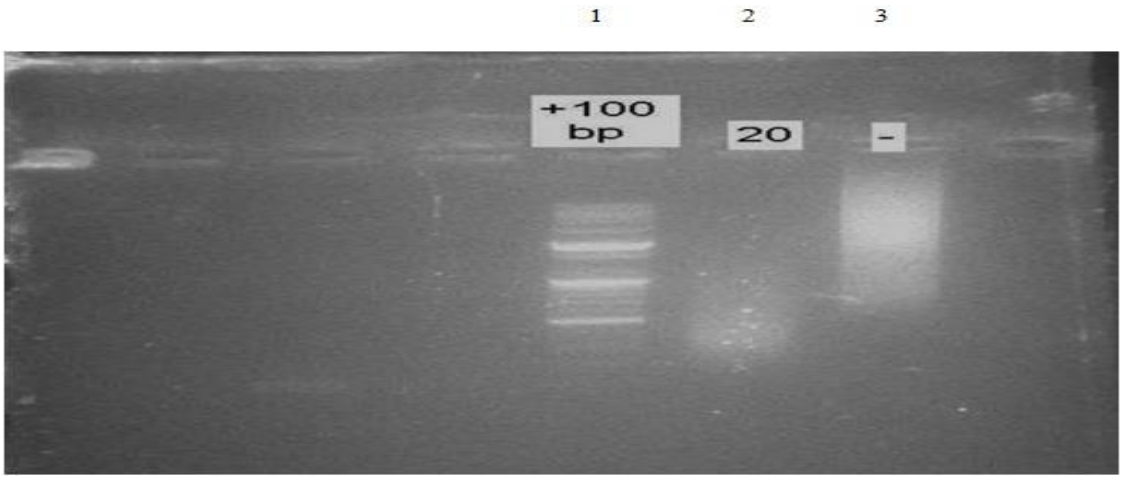

Figure 4. PCR amplification of mecA Gene in *S. aureus* showing no band. Lane 1, DNA marker; lane 2, *S. aureus;* lane 3, negative control.

CONFLICT OF INTERESTS

The authors have not declared any conflict of interests.

ACKNOWLEDGEMENT

The authors are grateful to DNA laboratory No. Q5 Danja Road, Off Katuru Road, Unguwar Sarki Kaduna state Nigeria for the technical support throughout the molecular aspect of the work and to Mallam Sani Mohammed of Microbiology Laboratory Kaduna State University for his contributions during the bacterial isolation and characterization.

REFERENCES

Adeoye A (2007). Medical Laboratory Practice 1st edition, FEMCO Publishers Limited, Lagos, Nigeria, P 153.

Agwung-Fobellah D, Kemajou ST (2007). Laboratory Microbiology and Activity Manual, Ark of Wisdom Publishers, Aba, Nigeria. pp. 12-37.

Akihiro Ma, Yutaka T, Masami M (2017). Comparison of 16S ribosomal RNA gene sequence analysis and conventional culture in the

environmental survey of a hospital. J. Pharm. Health Care Sci. 3(1):8.
Ananthan G, Sivaperumal P, Hussain SM (2011). Antibacterial potential of marine ascidian *Phallusia Arabica* against isolated urinary tract infections bacterial pathogens. Asian J. Anim. Sci. 5(3):208-212.
Ateba CN, Mbewe M (2011). Detectionof *Escherichia coli* O157:H7 virulence genes in isolates from beef, pork, water, human and animal species in the Northwest Province, South Africa: Public health implications. Res. Microbiol. 162:240-248.
Bergey's Manual of Determinative Bacteriology (1994). 9th edition, Holt, J.D. (Ed.), Williams Wilkins CO. Baltimore, P.783.
Black JA, Foarde KK (2007). Comparison of four different methods for extraction of Stachybotrys chartarum spore DNA and verification by real-time PCR. J. Microbiol. Methods 70:75-81.
Barrow GH, Feltham, RKA (1993). *Cowan and Steel's Manual for Identification of Medical bacteria*. Third edition. Cambridge University Press. Cambridge, Great Britain. pp. 245-247.
Cheesbrough M (2006). District laboratory practice in Tropical Countries Part 2 (5th Edition), Cambridge University Press. Cambridge. pp. 132-143.
Cole JR, Wang Q, Cardenas E, Fish J, Chai B, Farris RJ, Kulam-Syed-Mohideen AS, McGarrell DM (2009). The Ribosomal Database Project: improved alignments and new tools for rRNA analysis. Nucleic Acids Res. 37:141-145.
Daniel JD, Michael AP (2015). Prevention of health care-associated infections. In. James HJ, Michael AP, Karen CC, Guido F, Marie LL, Sandra SR, David WW, editors. Manual of Clinical Microbiology. 11th ed. Washington: American Society for Microbiology. pp. 106-119.
Frickmann H, Dekker D, Boahen K, Acquah S, Sarpong N, Adu-Sarkodie Y (2013). Increased detection of invasive enteropathogenic bacteria in pre-incubated blood culture materials by real-time PCR in comparison with automated incubation in Sub-Saharan Africa. Scand. J. Infect. Dis. 45:616-622.
Kerremans JJ, Verboom P, Stijnen T, Hakkaart-van Roijen L, Goessens W, Verbrugh HA, Vos MC (2008). Rapid identification and antimicrobial susceptibility testing reduce antibiotic use and accelerate pathogen-directed antibiotic use. J. Antimicrob. Chemother. 61:428-435.
Kumar S, Stecher G, Tamura K (2016). MEGA7: Molecular Evolutionary Genetic Analysis Version 7.0. Mol. Evol. 33(7):1870-1874.
Lee YA, Sung AN, Liu TF, Lee YS (2009). Combination of chromogenic differential medium and *estA*-specific PCR for isolation and detection of phytopathogenic *Xanthomonas* spp. Appl. Environ. Microbiol. 75:6831-6838.
Ochei JO, Kolhatkar AA (2008). Medical Laboratory Science: Theory and Practice. Tata McGraw-Hill Publishing Company Limited, New York, pp. 311-347.
Psifidi A, Dovas CI, Banos G (2010). A comparison of six methods for genomic DNA extraction suitable for PCR-based genotyping applications using ovine milk samples. Mol. Cell Probes 24:93-98.
Smith K, Diggle MA, Clarke SC (2003). Comparison of commercial DNA extraction kits for extraction of bacterial genomic DNA from whole-blood samples. J. Clin. Microbiol. 41:2440-2443.
Souza C, Faria YV, Sant'Anna LO, Viana VG, Seabra SH, Souza MC, Vieira VV, Hirata JR, Moreira LO, Mattos-Guaraldi AL (2015). Biofilm production by multiresistant Corynebacterium striatum associated with nosocomial outbreak. Mem. Inst. Oswaldo Cruz. 10(2):242-248.
Yoshimura K, Morotomi N, Fukuda K, Nakano M, Kashimura M, Hachisuga T, Tanigychi H (2011). Intravaginal microbial flora by the 16S rRNA gene sequencing. Am. J. Obstet. Gynecol. 205(3):235-e1.

academicJournals

Vol. 17(7), pp. 213-225, 14 February, 2018
DOI: 10.5897/AJB2017.16289
Article Number: 9CFD65F55921
ISSN 1684-5315
Copyright © 2018
Author(s) retain the copyright of this article
http://www.academicjournals.org/AJB

African Journal of Biotechnology

Full Length Research Paper

The nitrogen-fixing *Frankia* significantly increases growth, uprooting resistance and root tensile strength of *Alnus formosana*

Jung-Tai Lee* and Sung-Ming Tsai

Department of Forestry and Natural Resources, College of Agriculture, National Chiayi University, Taiwan.

Received 19 October, 2017; Accepted 18 January, 2018

Restoration of *Alnus formosana* (Burk.) Makino on landslide areas is important for agroforestry, forestry and soil erosion control in Taiwan. To ensure successful reforestation, *A. formosana* seedlings have to develop strong root system for nutrient and water acquisition as well as anchorage. Inoculating of *A. formosana* with symbiotic nitrogen-fixing actinobacteria *Frankia* may help mitigate drought and nutrient deficiencies on landslide sites. However, the effects of *Frankia* inoculation on growth, root architecture and mechanical properties of *A. formosana* seedlings are not well understood. In this research, a *Frankia* strain AF1 was isolated from actinorhizal nodules of local *A. formosana* and recognized as *Frankia* species, and its influences on growth performance and root mechanical properties of *A. formosana* seedlings were examined and analyzed. The results showed that the inoculated seedlings had significantly larger height and root biomass, longer root length, and more root tip number than that of the non-inoculated controls. Consistently, the inoculated seedlings had statistically significant higher uprooting resistance, root tensile resistance force and tensile strength than the controls. The results reveal that this native *Frankia* strain can promote growth performance, root system architecture, anchorage ability and root tensile strength of *A. formosana*.

Key words: Actinorhiza, Betulaceae, inoculation, root morphology, tensile strength, uprooting resistance.

INTRODUCTION

Landslide hazards and their large negative impacts on human lives, economies and infrastructure have become a growing challenge globally (Dai et al., 2002). Due to the fragile geology, steep terrain and torrential rains brought by typhoons, landslides have become one of the most severe disasters in Taiwan. Vegetation landslide engineering has become increasingly important for landslide prevention and rehabilitation in recent years (Chen et al., 2014). In general, trees and forests can play an important role in preventing and rehabilitating landslides. Actinorhizal trees are pioneer species and can improve tree growth and survival on degraded landslide soils (Diagne et al., 2013). *Alnus formosana* (*Alnus formosana* (Burk.) Makino), belonging to the family Betulaceae, is a native nitrogen-fixing actinorhizal woody species, widely distributed throughout the island of

*Corresponding author. E-mail: jtlee@mail.ncyu.edu.tw.

Author(s) agree that this article remains permanently open access under the terms of the Creative Commons Attribution License 4.0 International License

Taiwan in landslide sites (Liao, 1996). It has high potential for agroforestry, forestry, lumber production and landslide restoration. It can establish symbiosis with nitrogen-fixing *Frankia* and form actinorhizal root nodules in which *Frankia* provides fixed nitrogen to the host plant for growth and development (Lee, 1986; Lin, 1992). Several previous studies have demonstrated that *Frankia* can improve the establishment and growth of *Alnus* in degraded lands (Lefrançois et al., 2010; Santi et al., 2013; Bissonnette et al., 2014; Põlme et al., 2014). Inoculation with *Frankia* significantly increases seedling growth, biomass and root nodules of *Alnus crispa* and *Alnus sieboldiana* (Yamanaka et al., 2005; Quoreshi et al., 2007).

Morphological types of tree root system architecture have been classified into heart system, plate system and taproot system (Stokes and Mattheck, 1996). Stokes et al. (2009) indicated that taproot length, amount of lateral roots and root architecture affects uprooting resistance of plants. Orfanoudakis et al. (2010) showed that inoculation of *Alnus glutinosa* with *Gigaspora rosea* and *Frankia* improves ramous root. Past studies on root morphological characteristics and biomechanical properties of *Alnus* species were focused on *Alnus subcordata* and *Alnus viridis*. In *A. viridis*, the maximum root area ratio (RAR) values were located in the upper 30 cm soil layer and the maximum rooting depth was about 1 m, whereas the root tensile strength decreased with diameter (Bischetti et al., 2005). In *A. subcordata*, the root density, root number and RAR decreased with increasing depth and the maximum rooting depth was 1 m, while the root tensile strength decreased with increasing root diameter (Naghdi et al., 2013). However, there were few studies that tried to investigate the effects of inoculation of *Frankia* on growth, root morphological characteristics and mechanical properties of *A. formosana*. Therefore, the purposes of this research were: (1) to isolate the *Frankia* strain from *A. formosana*, and (2) to examine the influences of *Frankia* inoculation on growth performance, uprooting resistance and tensile strength of *A. formosana* seedlings in order to provide strategy for landslide prevention and erosion control practices. This study focused on the application of nitrogen-fixing *Frankia* to alder seedling production in order to improve seedling growth performance and enhance root mechanical properties, which is important in prevention of landslide hazards.

MATERIALS AND METHODS

Sample collection

An elite tree of *A. formosana* was selected from the natural forest stand located at Fenqihu Township, Chiayi County, Taiwan (219417.59E, 2599775.50N, TWD 97) in October 2014. Actinorhizal nodules were gathered from roots at 6 to 30 cm deep in soil, kept in sealed plastic bags and transported to laboratory in a cold box for *Frankia* strain isolation (Lin, 1992). Cones were also collected from upper crown of the same tree. Cones were sun-dried in trays for seed release. Seeds were extracted, cleaned and freeze-stored in polyethylene bags at -20°C.

Frankia strain isolation and purification

Actinorhizal root nodules were washed in distilled water to remove soil particles. Single nodule lobes were cut 2 mm from the tip with scalpel, ultrasonically cleaned, surface-sterilized with 75% ethanol for 10 min, 15% NaOCl for 10 min, and 30% hydrogen peroxide for 10 min. The endosymbiont *Frankia* in nodule lobes were isolated aseptically on QMOD medium (Lalonde and Calvert, 1979).

DNA extraction, sequencing, and gene sequence similarity analysis

Frankia genomic DNA was extracted with Puregene DNA Purification Kit (QIAGEN, Pleasanton, CA, USA), and subsequently subjected to 1.2% agarose gel electrophoresis. The primers used for PCR of rDNA were primer FGPL2054 (5'-CCGGGTTTCCCCATTCGG-3') and primer FGPS989e (5'-GGG GTC CTT AGG GGC T-3') (Daniel et al., 1999). Then, the amplified samples were analyzed by gel electrophoresis and the particular PCR products were sequenced. The DNA sequences were submitted to NCBI to access GenBank for sequence similarity analysis of the *Frankia* rDNA gene sequences.

Seedling preparation

Seeds of *A. formosana* were surface cleaned with tap water, sterilized 2 times with 10% NaOCl solution for 5 min and washed with sterile water, and then germinated in autoclaved peat moss and vermiculite mixtures (1:1, v/v) in October 2015. The wooden boxes ($l \times w \times h$, 30 cm × 30 cm × 60 cm) were used for transplanting. The boxes were sterilized with 10% NaOCl solution, and the sandy loam soils collected from the same natural forest stand were autoclaved and then fumigated with 200 g Basamid fumigant per cubic meter of soil, and the soil surface was sealed with polyethylene sheets for 14 days to prevent the toxic gas from escaping. Then, the boxes were filled with the sterilized soils. When seedlings attained a height of 5 cm, they were individually transplanted to the boxes, and watered regularly. Twenty-eight seedlings in boxes were arranged randomly into two individual plastic houses.

Inoculum preparation

The isolated *Frankia* strain was successively cultured twice for 30 days. Inocula were prepared by concentrating *Frankia* cultures in sterile 1 ml tubes (15,000 rpm for 10 min at 4°C) using a Hitachi centrifuge (HIMAG Centrifuge CR 15T, Rotor RT15A, Tokyo, Japan). The pellets were then homogenized with glass tissue homogenizer (Wheaton 25802a, Millville, NJ, USA) in sterile BAP medium and sonicated for 1 min using an ultrasonicator (Biologics 150VT, Manassas, VA, USA) on ice, and used as inoculum. The protein concentration of the homogenized inoculum was assayed with the Bradford method (Bradford, 1976). The protein concentration of the *Frankia* inoculum was 2.8±0.02 μg ml^{-1}.

Inoculation test

Four weeks after transplanting, 14 plants in one plastic house were inoculated with the isolated *Frankia* strain. A 5 ml suspension of the

strain (protein concentration 2.8±0.02 µg ml^{-1}) was dripped into five small holes near the seedling. The process was duplicated after fourteen days for ensuring high rate of root colonization. Another 14 non-inoculated control seedlings were treated with sterilized water. The boxes of inoculated and control seedlings were placed individually in two separate plastic houses. The seedlings were grown at 26±4°C during daytime and 18±5°C at night time, with 60 to 80% relative humidity, and 1000±200 µmoles photon m^{-2} s^{-1} photosynthetic photon flux density during daytime. Eight months later, the seedlings were sampled for measurements of growth performance, root morphological characteristics, uprooting resistance and tensile strength.

Plant growth performance and root morphological characteristics

After 8 months of cultivation, seven inoculated and seven non-inoculated control plants were randomly chosen, separately. The height and stem-base diameter of seedlings were measured with ruler and caliper. The root systems were carefully excavated by hand with trowel (Böhm, 1979). The root length and root numbers were recorded. Images of seedling roots were captured for analysis of root architecture and morphological characteristics. The root morphological characteristics analysis was conducted using a WinRHIZO*Pro* analysis system (Regent Instruments, Quebec, QC, Canada) (Bouma et al., 2000). However, root volume was evaluated with water displacement technique due to large quantity of roots (Pang et al., 2011). Biomass of leaf, root, stem and root nodule was estimated by drying in a hot air oven at 75°C until a constant weight was obtained. Root functional characteristics, that is, root mass density (g dm^{-3}), root length density (m dm^{-3}), tissue mass density (g cm^{-3}), specific root length (m g^{-1}), and root to shoot ratio were computed (Stokes et al., 2009; Burylo et al., 2012; Gould et al., 2016). Live roots were also collected from sampled seedlings and prepared for subsequent tensile testing.

Vertical uprooting test

After 8 months of cultivation, 7 inoculated and 7 non-inoculated control seedlings were randomly sampled for vertical uprooting test, respectively. The soil material was categorized as sandy loam soil (containing 65.2% sand, 27.4% silt and 7.4% clay). At first, seedling height and stem-base diameter were recorded. The seedling stem was removed from 15 cm above the stem base and the bark was peeled away to prevent slide of the pulling fixture. The uprooting test was conducted using an *in situ* pullout instrument (U-Soft USPA-003, U-Soft Technology Co., Taiwan) fitted with a 5T load cell (Kyowa, Tokyo, Japan) attached to loading recorder and constant control unit, and erected on a triangular steel frame. Then, the instrument was attached to the pulling fixture. The uprooting force was applied perpendicular to the soil surface at a constant rate of 2 mm min^{-1}. The data of uprooting resistance force and displacement were recorded with load cell and displacement transducer, and stored on a laptop computer. The uprooting test was terminated once the resisting force dropped sharply.

Root tensile test

After root excavation, live roots of different diameter classes (0 to 1, 1 to 2, 2 to 5, and 5 to 10 mm) at a depth of 30 cm below the soil surface were collected randomly from the sampled seedlings, respectively. The roots were kept in separate sealed plastic bags to prevent drying of root tissues (De Bates et al., 2008) and transported with a cold box (Bischetti et al., 2005). Root samples were then immersed in a 15% ethanol solution at 4°C in order to conserve root tensile strength (Bischetti et al., 2009). Tensile tests were performed in the laboratory using a tensile-testing machine (U-Soft USPT-003, U-Soft Technology Co., Taipei, Taiwan). The load cell (Kyowa LCN-A, Tokyo, Japan; sensor resolution 0.1 N, maximum force 500 N) was connected to a loading recorder and control unit. The data of tensile force and displacement were compiled on a portable computer. A total of 110 root segments were randomly sampled from the inoculated seedlings. Another 110 root segments were also randomly collected from the non-inoculated seedlings. All root segments were washed and cut to 60 mm in length, and the root segments were clamped with sand paper during testing to prevent slippage. Then, the root segments were pulled vertically at a constant speed of 4.7 mm min^{-1} until the resisting force dropped sharply. The root tensile strength (T_s, MPa) was calculated using the following formula (De Baets et al., 2008; Osman et al., 2011; Zhang et al., 2012):

$$T_s = 4F_{max}/\pi d_i^2$$

where F_{max} is the maximum force (N) at rupture and d_i is the mean root segment diameter (mm) measured at three points, that is, near the upper clamp, halfway and near the bottom clamp, using a digital caliper (accuracy of 0.01 mm).

Data analysis

T-test in SPSS 22.0 software (Chicago, IL., USA) was used for analyzing variations in growth performance and morphological characteristics data between inoculated and non-inoculated control seedlings. The relationships between uprooting resistance, root tensile resistance, tensile strength and morphological characteristics were evaluated using Microsoft Excel regression analysis.

RESULTS

Actinobacterial strain isolation and sequencing

The actinobacterial strain was isolated and purified on QMOD medium and classified as AF1. Molecular analysis showed that the rDNA gene sequence of the isolated AF1 has 100% similarity to that of *Frankia* species genus (Figure 1). The local strain was recognized as *Frankia* spp. AF1. Inoculation test showed that the isolated *Frankia* strain can induce nodule development in the roots of *A. formosana* (Figure 2).

Growth performance

Results of statistical analysis showed that *Frankia* inoculation significantly promoted growth performance characteristics of *A. formosana* seedlings. Generally, seedlings inoculated with *Frankia* developed significantly larger height (50%), tap root length (60%), root biomass (60%), and shoot biomass (46%) than the non-inoculated ones (Table 1).

Root system architecture

Results of the investigation revealed that inoculated *A.*

Score	Expect	Identities	Gaps	Strand
429 bits (232)	3e-117	232/232(100%)	0/232 (0%)	Plus/Plus

```
Query 1        TGAGATGTTGGGTTAAGTCCCGCAACGAGCGCAACCCTTGTCCTATGTTGCCAGCGAGTC 60
               ||||||||||||||||||||||||||||||||||||||||||||||||||||||||||||
Sbjct 1275970  TGAGATGTTGGGTTAAGTCCCGCAACGAGCGCAACCCTTGTCCTATGTTGCCAGCGAGTC 1276029

Query 61       ATGTCGGGGACTCATAGGAGACTGCCGGGGTCAACTCGGAGGAAGGTGGGGATGACGTCA 120
               ||||||||||||||||||||||||||||||||||||||||||||||||||||||||||||
Sbjct 1276030  ATGTCGGGGACTCATAGGAGACTGCCGGGGTCAACTCGGAGGAAGGTGGGGATGACGTCA 1276089

Query 121      AGTCATCATGCCCCTTACGTCCTGGGCTGCACACATGCTACAATGGCCGGTACAATGGGC 180
               ||||||||||||||||||||||||||||||||||||||||||||||||||||||||||||
Sbjct 1276090  AGTCATCATGCCCCTTACGTCCTGGGCTGCACACATGCTACAATGGCCGGTACAATGGGC 276149

Query 181      TGCGATACCGCGAGGTGGAGCGAATCCCAAAAAGCCGGTCTCAGTTCGGATC 232
               ||||||||||||||||||||||||||||||||||||||||||||||||||||
Sbjct 1276150  TGCGATACCGCGAGGTGGAGCGAATCCCAAAAAGCCGGTCTCAGTTCGGATC 1276201
```

Figure 1. Partial sequence of strain AF1 rDNA gene (query), compared to that of *Frankia* spp. genus (subject).

Figure 2. Actinorhizal nodules formed on the roots of *A. formosana* inoculated with *Frankia* strain (bar = 3 cm).

Table 1. Growth performance of *A. formosana* seedlings inoculated and non-inoculated with *Frankia* after 8 months of cultivation.

***Frankia* inoculation**	**Height (cm)**	**Stem-base diameter (mm)**	**Taproot length (cm)**	**Root biomass (g)**	**Shoot biomass (g)**
Inoculated	218.8±5.5[a]	21.9±3.0[a]	43.0±7.5[a]	68.6±11.1[a]	162.6±26.8[a]
Non-inoculated	145.2±4.3[b]	18.2±2.4[a]	26.4±3.1[b]	42.8±14.0[b]	111.2±20.8[b]

All values are the mean ± standard error of 7 replicates. Values in the same column followed by different superscript letters significantly differ at 5% significant level.

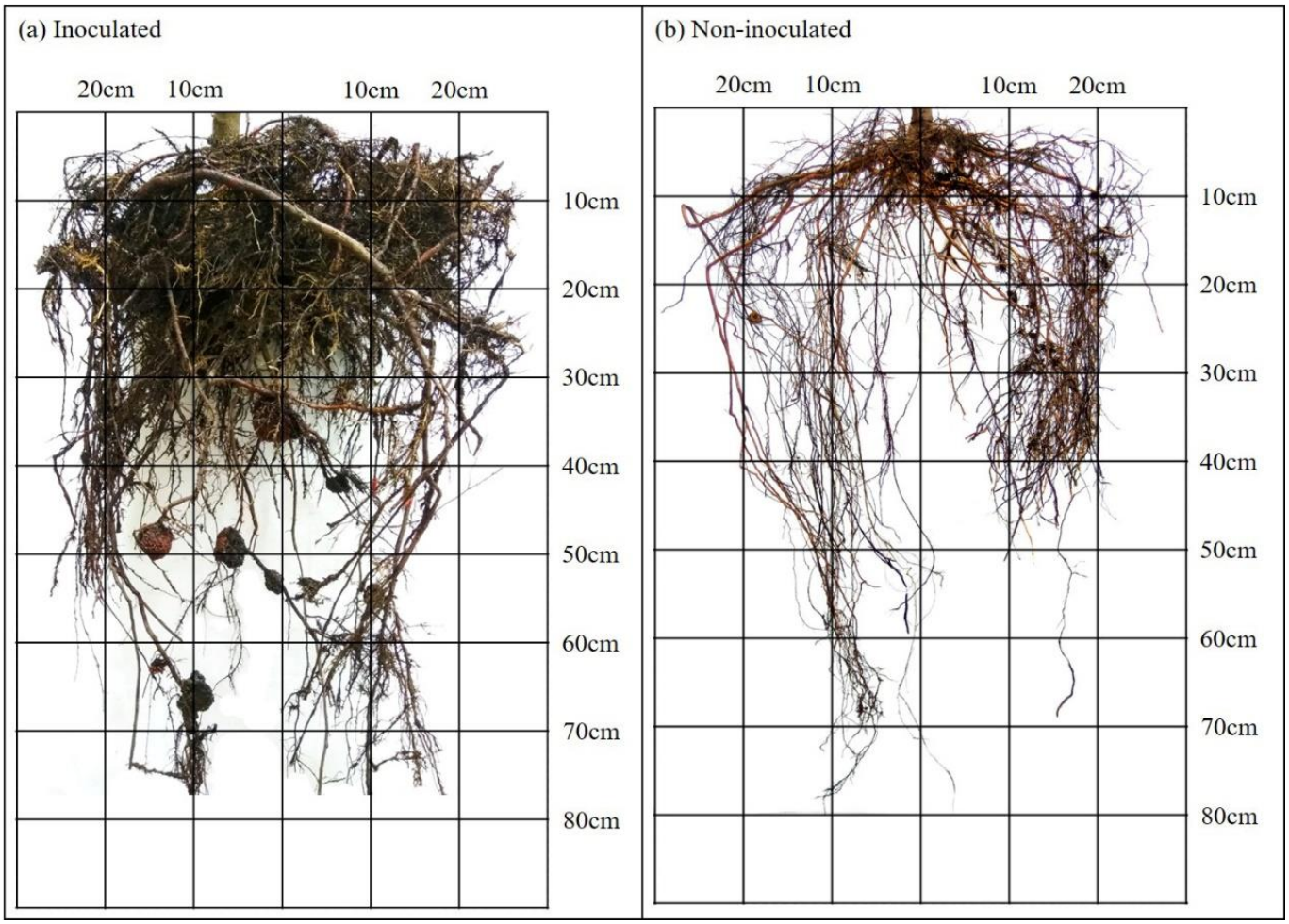

Figure 3. Root morphologies of *A. formosana* seedlings after 8 months of cultivation: (a) inoculated with *Frankia* strain; (b) non-inoculated.

formosana plants developed larger root systems than the non-inoculated ones (Figure 3). The taproots of inoculated plants grew to 43 cm deep. In addition, the inoculated plants developed about 85% of the root matrix in the top 40 cm soil, and its lateral roots extended profusely, with many nodules (Figure 3a). Conversely, the taproots of non-inoculated ones grew only to 20 cm deep. Also, the non-inoculated plants developed about 90% of the root matrix in the top 30 cm soil, and its lateral roots grew sparsely, without any nodules (Figure 3b). The types of root architecture of inoculated and non-inoculated *A. formosana* seedlings were categorized to the heart root system according to Stokes and Mattheck (1996).

WinRHIZO analysis of root morphological characteristics revealed that *Frankia* inoculation significantly influenced all morphological characteristics. Generally, the inoculated plants developed larger total

Table 2. Root morphological characteristics of *A. formosana* seedlings inoculated and non-inoculated with *Frankia* after 8 months of cultivation.

***Frankia* inoculation**	**Total root length (cm)**	**Root surface area (cm^2)**	**Root volume (cm^3)**	**Root tip number**
Inoculated	5217.4±379.1[a]	3120.8±162.0[a]	498.3±53.9[a]	6570±265 [a]
Non-inoculated	3254.2±585.0[b]	1939.9±153.2 [b]	322.3±16.6[b]	3823±229 [b]

All values are the mean ± standard error of 7 replicates. Values in the same column followed by different superscript letters significantly differ at 5% significant level.

Table 3. Root functional characteristics of *A. formosana* seedlings inoculated and non-inoculated with *Frankia* after 8 months of cultivation.

***Frankia* inoculation**	**Root density ($kg\ m^{-3}$)**	**Root length density ($km\ m^{-3}$)**	**Root tissue density ($g\ cm^{-3}$)**	**Specific root length (mg^{-1})**	**Root shoot ratio**
Inoculated	1.27±0.21[a]	0.97±0.26[a]	0.14±0.02[a]	0.76±0.14[a]	0.42±0.09[a]
Non-inoculated	0.79±0.19[b]	0.58±0.30[b]	0.12±0.02[a]	0.85±0.16[a]	0.39±0.07[a]

All values are the mean ± standard error of 7 replicates. Values in the same column followed by different superscript letters significantly differ at 5% significant level.

Table 4. Uprooting resistances of inoculated and non-inoculated *A. formosana* seedlings after 8 months of cultivation.

***Frankia* inoculation**	**Uprooting resistance (kN)**
Inoculated	1.09± 0.40[a]
Non-inoculated	0.60± 0.17[b]

All values are the mean ± standard error of 7 replicates. Values in the same column followed by different superscript letters significantly differ at 5% significant level.

root length (60%), root surface area (61%), root volume (55%), and root tip number (72%) than the non-inoculated ones (Table 2).

Statistical analysis of root functional characteristics exhibited that the root density and root length density of inoculated plants were higher than the controls. Generally, the inoculated *A. formosana* seedlings had higher root density (60%) and root length density (67%) than the non-inoculated ones (Table 3).

Uprooting resistance

In this study, seven uprooting tests were conducted to examine the uprooting resistance of the inoculated and non-inoculated seedlings. The results revealed that the average maximum uprooting resistance of the inoculated seedlings (1.09±0.40 kN) was significantly higher than the non-inoculated ones (0.60±0.17 kN) (Table 4). The uprooting resisting force increased with displacement up to the peak and then decreased sharply as the roots broke (Figure 4). Regression analysis exhibited the significant linear positive correlations between the maximum uprooting resistance force and morphological characteristics, that is, tree height, stem-base diameter, taproot length, root biomass, and shoot biomass (Figures 5, 6, 7, 8, and 9).

Root tensile strength

In total, 220 tests were performed to investigate the root tensile strength of the inoculated and non-inoculated *A. formosana* seedlings. Among them, 86 root tensile tests of the inoculated seedlings and 102 root tensile tests of the non-inoculated controls were successful. The average root tensile resistance force of inoculated seedlings (81.1±19.0 N) was significantly higher than that of the controls (68.0±23.5 N). The mean value of root tensile strength of inoculated seedlings (17.45±3.36 MPa) was significantly higher than that of the non-inoculated controls (11.42±1.83 MPa). On the other hand, the average root diameter of non-inoculated seedlings (2.88±1.28 mm) was significantly higher that the inoculated ones (2.42±1.20 mm) (Table 5). Regression analysis revealed that root tensile resistance force increased with increasing root diameter in accordance with a positive power function correlation (Figure 10), whereas the root tensile strength decreased with increasing root diameter in accordance with negative logarithmic function correlation (Figure 11). Furthermore, the maximum root tensile resistance and tensile strength of inoculated seedlings were significantly higher than that of the non-inoculated controls.

DISCUSSION

The results showed that the native symbiotic

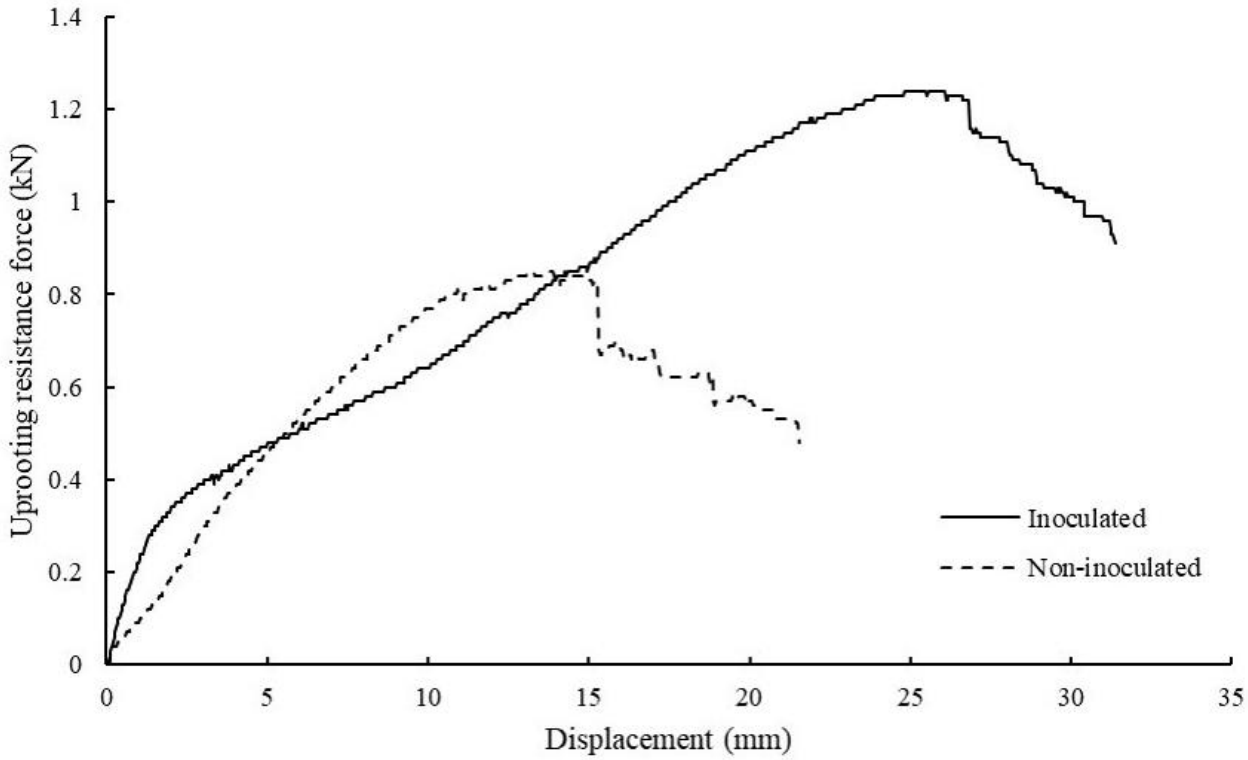

Figure 4. Uprooting resistance force-displacement curves for *A. formosana* seedlings inoculated (—) and non-inoculated (--) with *Frankia*..

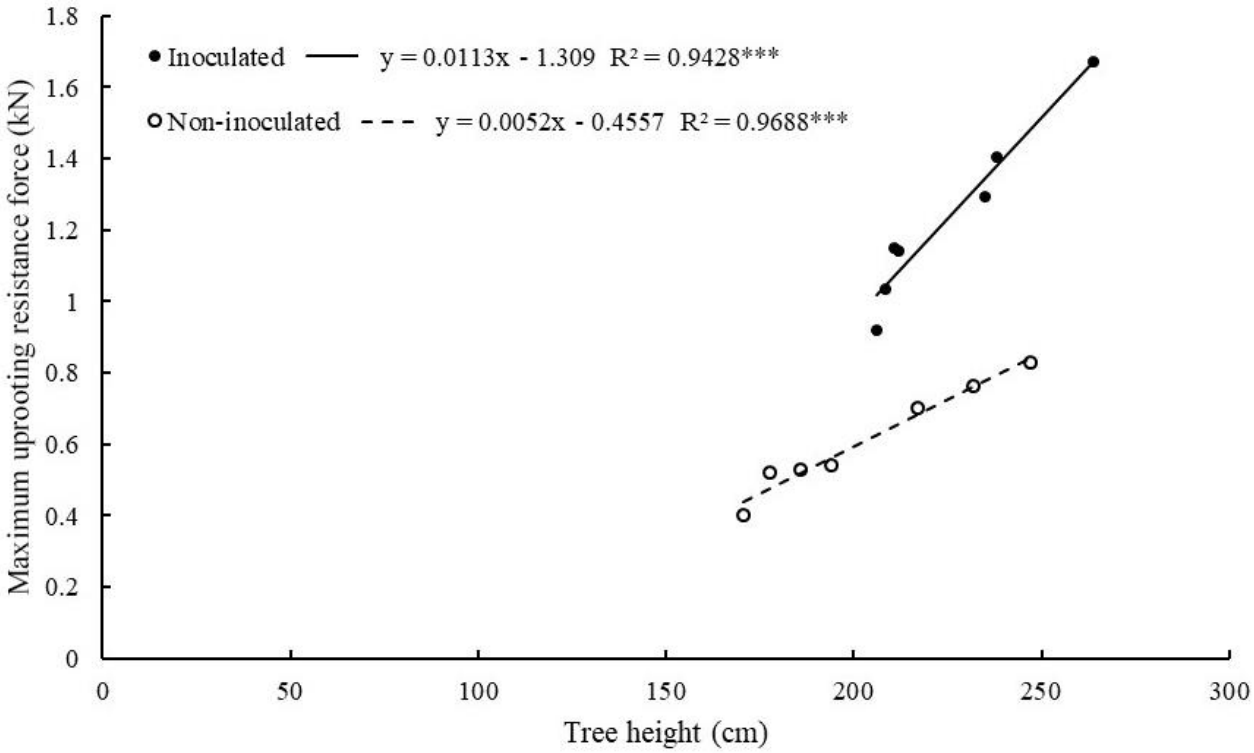

Figure 5. Maximum uprooting resistance force-tree height relationship for *A. formosana* seedlings inoculated (—) and non-inoculated (- -) with *Frankia*. N = 7.

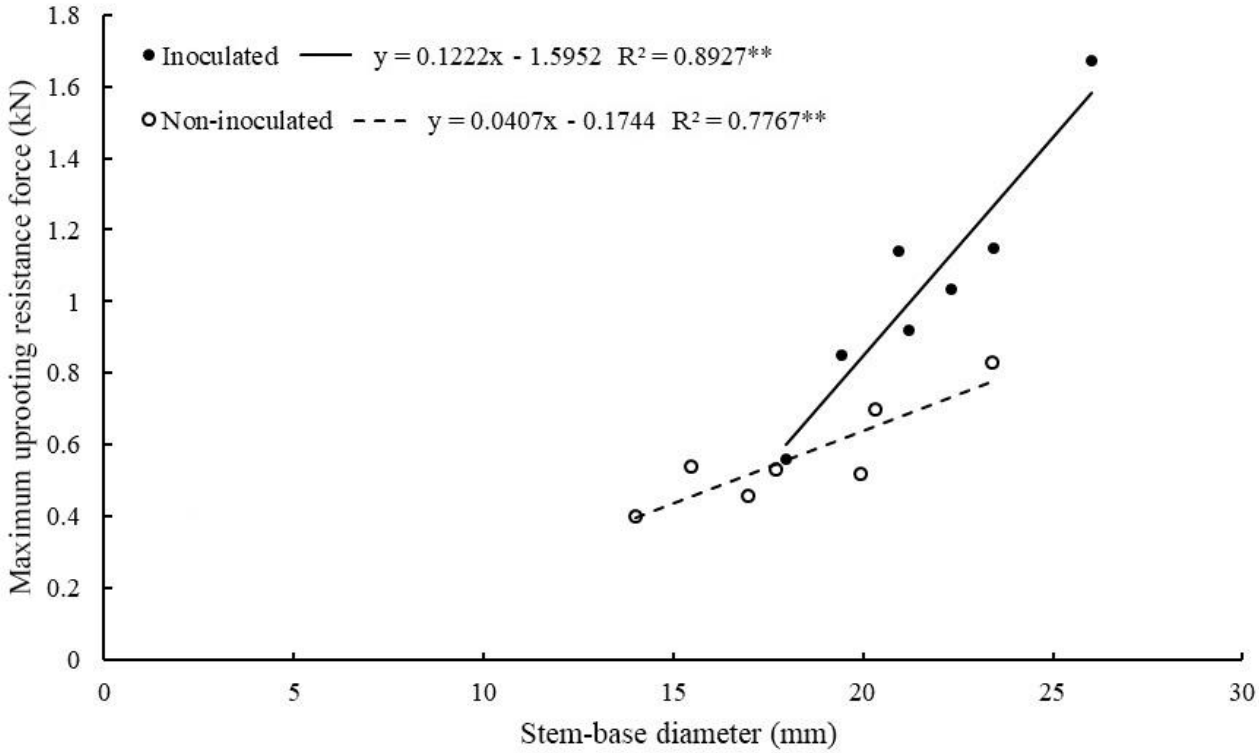

Figure 6. Maximum uprooting resistance force-stem base diameter relationship for *A. formosana* seedlings inoculated (—) and non-inoculated (- -) with *Frankia*. N = 7.

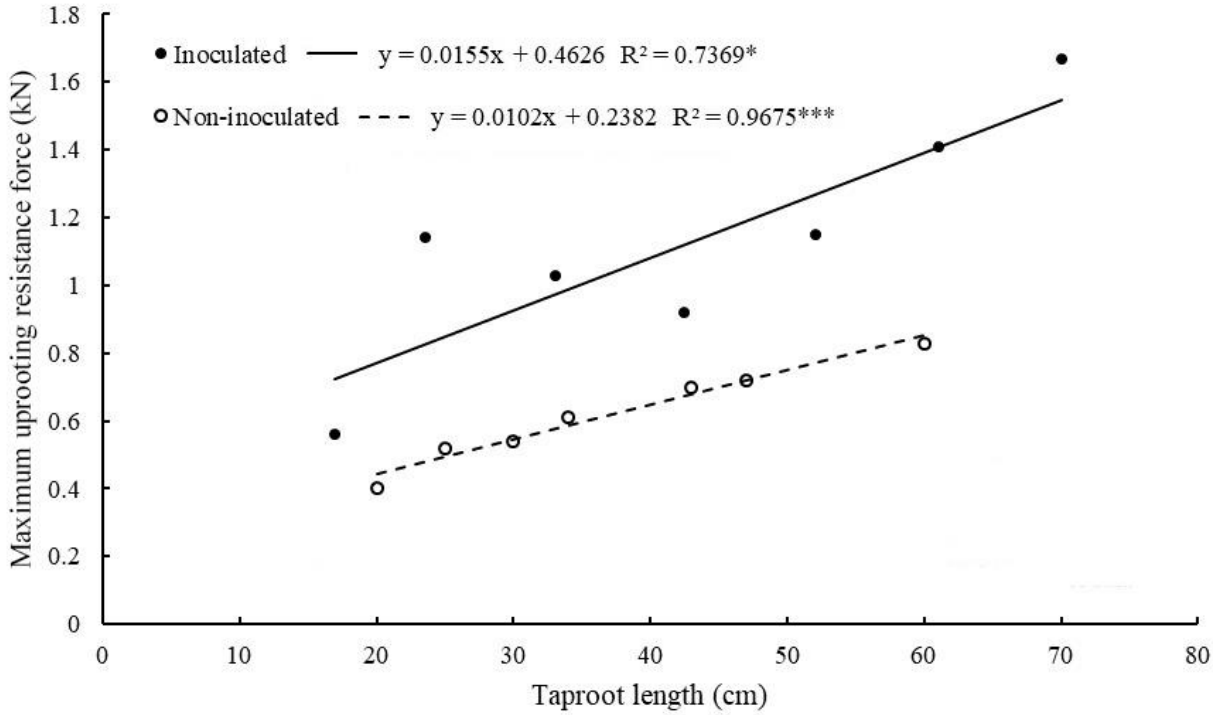

Figure 7. Uprooting resistance force-taproot length relationship for *A. formosana* seedlings inoculated (—) and non-inoculated (- -) with *Frankia*. N = 7.

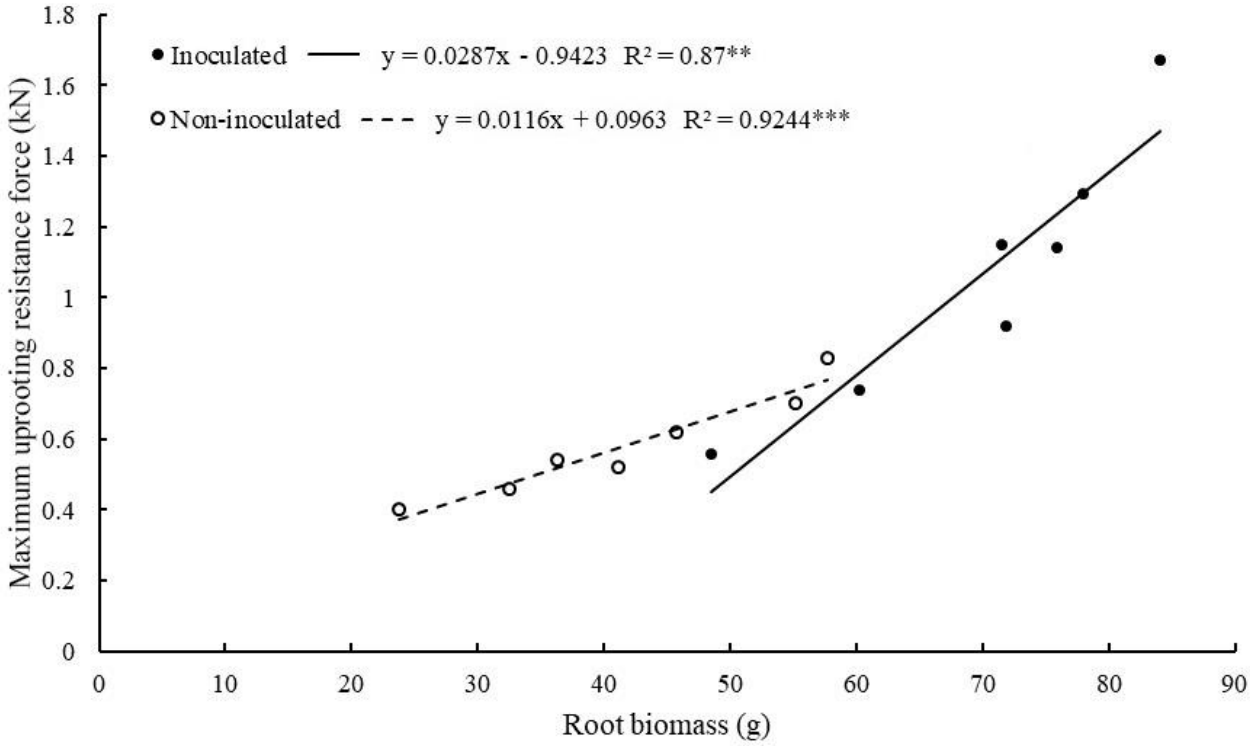

Figure 8. Maximum uprooting resistance force-root biomass relationship for *A. formosana* seedlings inoculated (—) and non-inoculated (- -) with *Frankia*. N = 7.

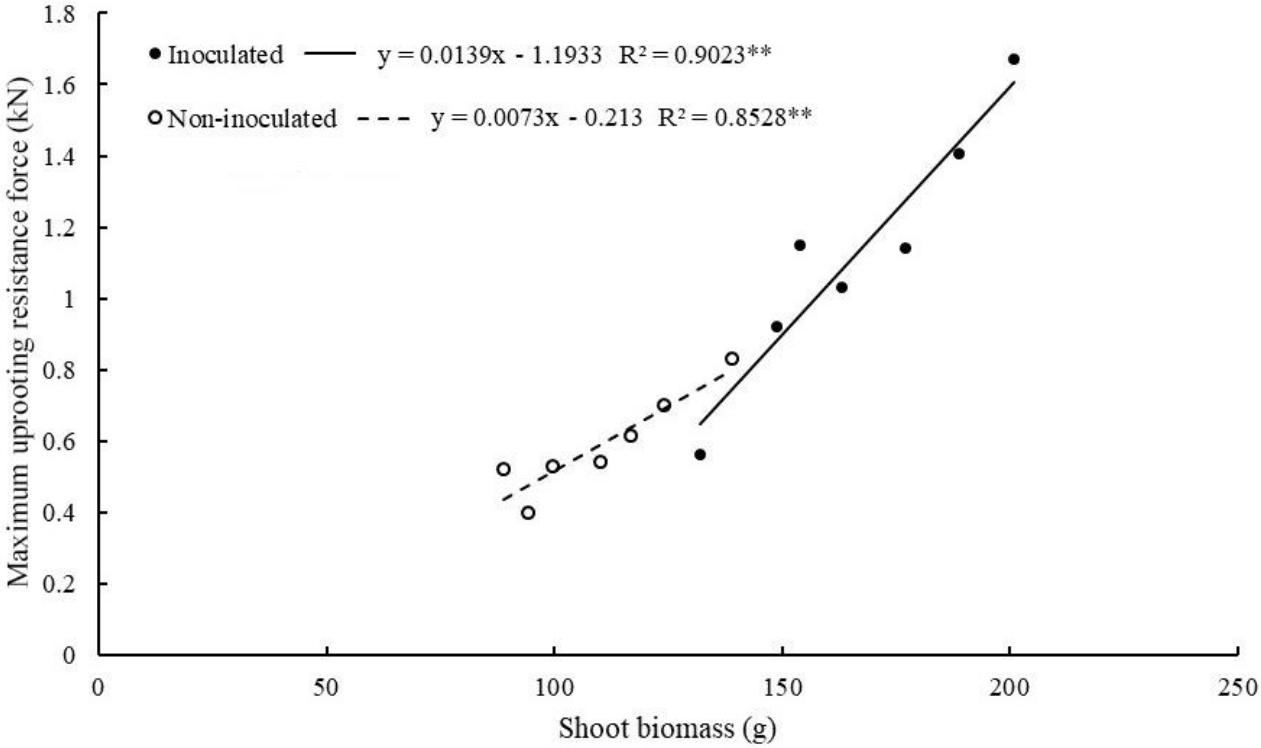

Figure 9. Maximum uprooting resistance force-shoot biomass relationship for *A. formosana* seedlings inoculated (—) and non-inoculated (- -) with *Frankia*. N = 7.

Table 5. Average root diameter, tensile resistance force and tensile strength of inoculated and non-inoculated *A. formosana* seedlings after 8 months of cultivation.

***Frankia* inoculation**	**Average root diameter (mm)**	**Tensile resistance force (N)**	**Tensile strength (MPa)**
Inoculated	2.42±1.20[b]	81.1±19.0[a]	17.45±3.36[a]
Non-inoculated	2.88±1.28[a]	68.0±23.5[b]	11.42±1.83[b]

All values are the mean ± standard error of 86 root segments and 102 root segments of inoculated and non-inoculated *A. formosana*, respectively. Values in the same column followed by different superscript letters significantly differ at 5% significant level.

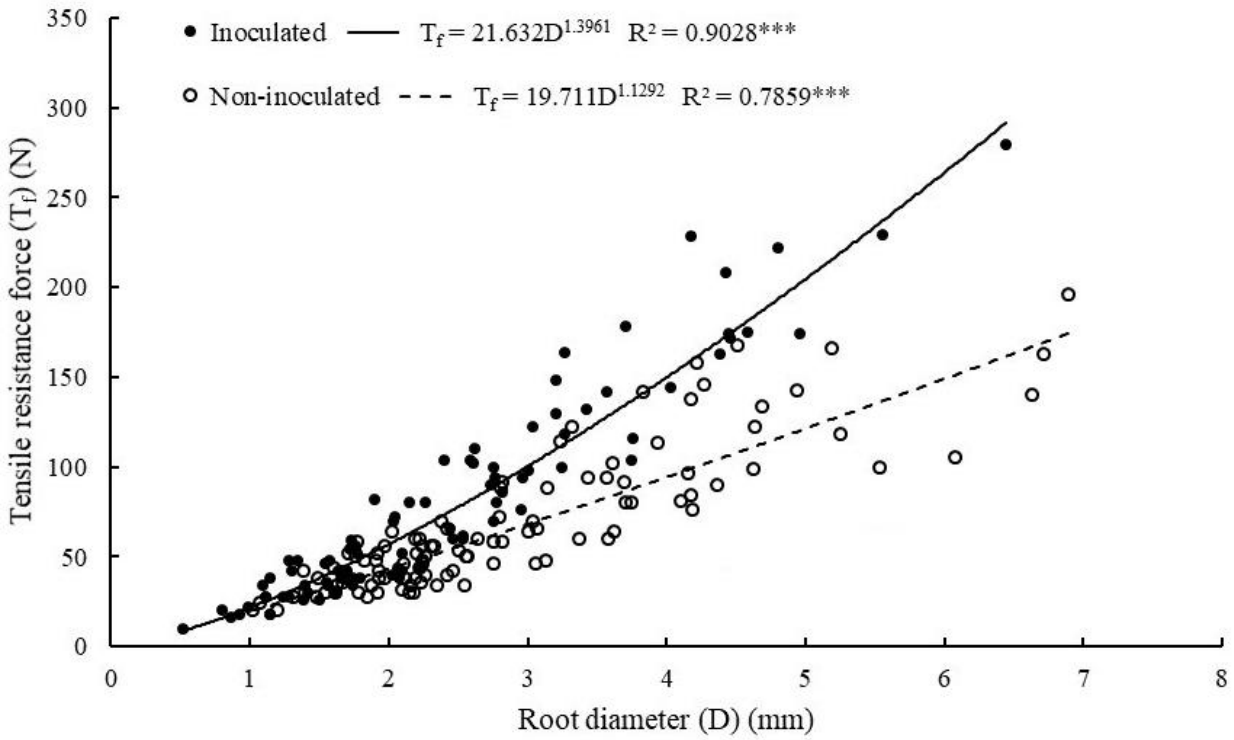

Figure 10. Root tensile resistance force-root diameter relationship for *A. formosana* seedlings inoculated (●—) and non-inoculated (○- -) with *Frankia*.

actinobacterium strain in nodules of *A. formosana* was isolated and recognized as *Frankia* by 16S rDNA gene similarity analysis. Inoculation test showed that this *Frankia* strain can induce actinorhizal nodule development in the roots of *A. formosana* seedlings. A number of studies indicated that *Frankia* strains associate with *Alnus* spp. (that is, *Alnus acuminata, A. crispa*, *A. glutinosa*, *Alnus nepalensis*, *Alnus rubra* and *Alnus sieboldiana*, respectively) (Benson, 1982; Carlson and Dawson, 1985; Hooker and Wheeler, 1987; Vendan et al., 1999; Carú et al., 2000; Oliveira et al., 2005; Yamanaka et al., 2005). Faure-Raynaud et al. (1991) analyzed the diversity of *Frankia* strains isolated from single nodules of *A. glutinosa* and showed no divergence among strains isolated from the same nodule. McEwan et al. (2015) also demonstrated that a single ribotype of *Frankia* is the major bacterium in single lobe from a nodule of *A. glutinosa*.

The research revealed that *A. formosana* seedlings inoculated with the native *Frankia* had significantly higher growth performance than the non-inoculated ones. Many previous studies have shown that inoculation with *Frankia* strains could significantly increase growth and development of alder seedlings (Prat, 1989; Wheeler et al., 1991; Kendall et al., 2003; Martin et al., 2003; Schrader and Graves, 2008; Bissonnette et al., 2014; Yamanaka et al., 2009). Lumini et al. (1994) showed that inoculation of selected *Frankia* strains and arbuscular mycorrhizal fungi along with sterilized media developed significantly higher shoot biomass than the non-inoculated controls. Quoreshi et al. (2007) demonstrated that *A. crispa* inoculated with *Frankia* had significantly

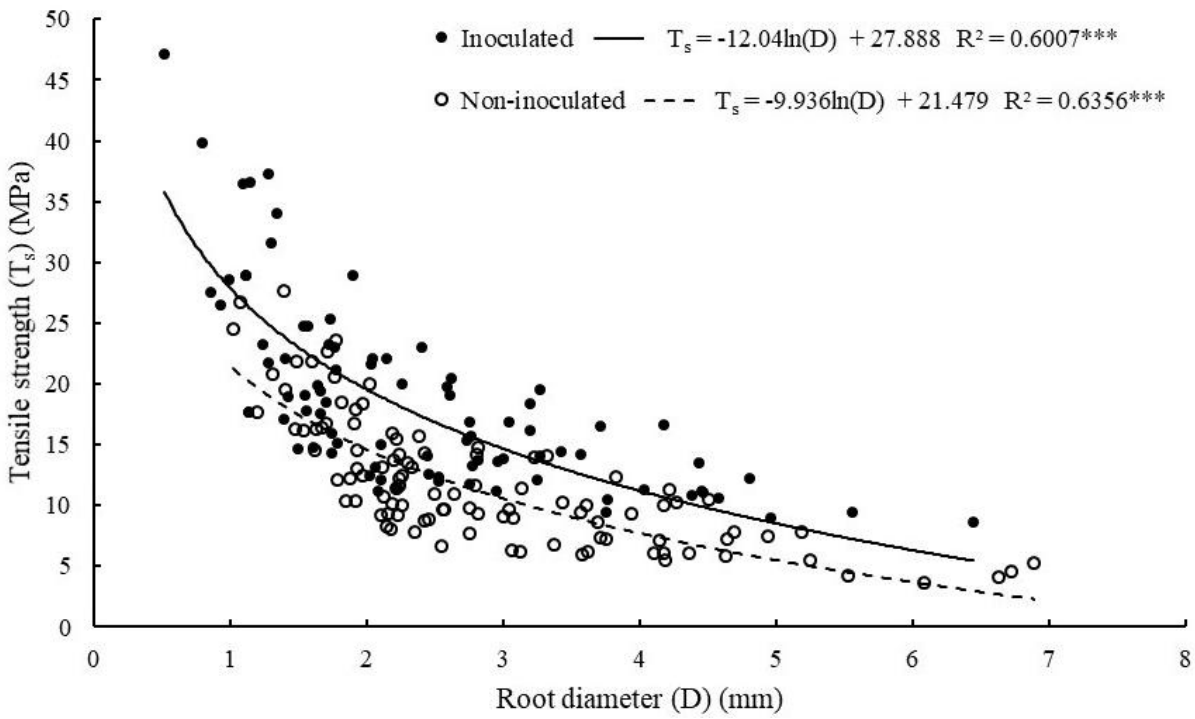

Figure 11. Root tensile strength-root diameter relationship for *A. formosana* seedlings inoculated (●—) and non-inoculated (○- -) with *Frankia*.

higher biomass, nodule lobes, and nodule weight than the controls. Moreover, Vendan et al. (1999) showed that Nepalese alder (*A. nepalensis*) plants inoculated with *Frankia* have a higher shoot length, root length, and biomass, while the *Frankia* strain AVC-II exhibited better infectivity and productivity of Nepalese alder than other strains tested. They also clearly indicated the potentiality of utilizing the *Alnus-Frankia* specificity for higher productivity through effective symbiosis. Schrader and Graves (2008) demonstrated that alder seedlings inoculated with species-specific *Frankia* strain grew larger, and gained more biomass than the cross-inoculated ones. Consistently, the study also demonstrated the positive effect of local *Frankia* strain on growth performance of *A. formosana* seedlings.

The root system architecture of *A. formosana* seedlings inoculated and non-inoculated with *Frankia* were similar to the heart root system (Stokes and Mattheck, 1996). The seedlings inoculated with *Frankia* had deeper taproot and more profuse roots than the non-inoculated ones. The inoculated seedlings had significantly higher total root length, root surface area, root volume, and root tip number than the controls. Moreover, seedlings inoculated with *Frankia* also had significantly higher root density and root length density than the non-inoculated ones. Wheeler et al. (1979) demonstrated that alder inoculated with *Frankia* developed more lateral root primordia than the non-inoculated ones, suggesting that *Frankia* can induce lateral root formation. De Bates et al. (2006) indicated that root density is a pertinent parameter to estimate the erosion-reducing efficacy. Stokes et al. (2009) also showed that higher root length density increases the uprooting resistance of plants.

This study demonstrates that *A. formosana* seedlings inoculated with *Frankia* have significantly higher uprooting resistance than the controls, indicating a higher anchorage capability in roots of the inoculated seedlings. Also, there were strong linear positive correlations between uprooting resistance and tree height, stem-base diameter, taproot length, root biomass and shoot biomass. Additionally, the inoculated *A. formosana* seedlings have longer taproot and more profuse lateral roots than the non-inoculated ones. Hence, inoculation with *Frankia* significantly augmented the numbers of lateral roots, which consequently stimulate seedling anchorage capability and uprooting resistance. Stokes et al. (2005) also indicated that heart root system is more resistant to uprooting than taproot system and plate root system.

The results of root tensile tests showed that the root tensile resistance force increased with increasing root diameter, whereas the root tensile strength decreased with increasing diameter. The findings are congruent with many other studies (Bischetti et al., 2005; Genet et al., 2005; De Baets et al., 2007; Normaniza et al., 2011; Nyambane et al., 2011; Abdi et al., 2014; Mohammed and

Normaniza, 2014; Capilleri et al., 2016). Root chemical components, such as cellulose, lignin, hemicellulose and holocellulose, are closely related to root mechanical properties. Genet et al. (2005) found that root cellulose content increased with increasing root diameter and increasing tensile strength in both *Pinus pinaster* and *Castanea sativa*. Several studies have shown that the root cellulose content increases and lignin content decreases with an increase in root diameter, and decrease in tensile strength (Lv et al., 2013; Zhang et al., 2014; Yang et al., 2016). In addition, the results from the present study also demonstrated that the average root tensile resistance force and tensile strength of inoculated seedlings were significantly higher than that of the non-inoculated controls. This suggests that inoculation with *Frankia* promotes root tensile resistance force and tensile strength of *A. formosana* seedlings.

Conclusions

Collectively, results of the present study clearly show that the native *Frankia* strain significantly enhances growth performance, root system architecture, uprooting resistance and root tensile strength of *A. formosana* seedlings. The findings of this study are of great importance in the application of *Frankia* in alder seedling production for landslide reforestation and soil conservation practices. This is the first report to demonstrate that inoculation with *Frankia* can significantly enhance growth, root system architecture, anchorage capability and root tensile strength of *A. formosana* seedlings. Additionally, further studies on the diversity of native *Frankia* strains and its symbiotic compatibility with alder species are needed for seedling production. Also, researches on the effects of alder roots on hillslope stability and erosion control are useful in ecological restoration and soil conservation in landslide areas.

CONFLICT OF INTERESTS

The authors have not declared any conflict of interests.

ACKNOWLEDGEMENS

The authors gratefully appreciate the financial support provided by the Ministry of Science and Technology, Taiwan and National Chiayi University.

REFERENCES

Abdi E, Azhdari E, Abdulkhani A, Mariv HS (2014). Tensile strength and cellulose content of Persian ironwood (*Parrotia persica*) root as bioengineering material. J. For. Sci. 60(10):425-430.

Benson DR (1982). Isolation of *Frankia* strains from alder actinorhizal root nodules. Appl. Environ. Microbiol. 44:461-465.

Bischetti GB, Chiaradia EA, Epis T, Morlotti E (2009). Root cohesion of forest species in the Italian Alps. Plant Soil 324:71-89.

Bischetti GB, Chiaradia EA, Simonato T, Speziali B, Vitali B, Vullo P, Zocco A (2005). Root strength and root area ratio of forest species in Lombardy (Northern Italy). Plant Soil 278:11-22.

Bissonnette C, Fahlman B, Perub KM, Khasa DP, Greer CW, Headley JV, Roy S (2014). Symbiosis with *Frankia* sp. benefits the establishment of *Alnus viridis* ssp. *crispa* and *Alnus incana* ssp. *rugosa* in tailings sand from the Canadian Oil Sands Industry. Ecol. Eng. 68:167-175.

Böhm W (1979). Methods of Studying Root Systems. Springer-Verlag, Heidelberg.

Bouma TJ, Nielsen KL, Koutstaal K (2000). Sample preparation and scanning protocol for computerized analysis of root length and diameter. Plant Soil 218:185-196.

Bradford MM (1976). A rapid and sensitive method for the quantitation of microgram quantities of protein utilizing the principle of protein-dye binding. Anal. Biochem. 72:248-254.

Burylo M, Rey F, Mathys N, Dutoit T (2012). Plant root trais affecting the resistance of soils to concentrated flow erosion. Earth Surf. Process. Landforms 37:1463-1470.

Capilleri PP, Motta E, Raciti E (2016). Experimental study on native plant root tensile strength for slope stabilization. Procedia Eng. 158:116-121.

Carlson, PJ, Dawson JO (1985). Soil nitrogen changes, early growth, and response to soil internal drainage of a plantation of *Alnus jorullensis* in the Colombian highlands. Turrialba 35:141-150.

Carú M, Becerra A, Sepúlveda DA, Cabello A (2000). Isolation of infective and effective *Frankia* strains from root nodules of *Alnus acuminata* (Betulaceae). World J. Microbiol. Biotechnol. 16:647-651.

Chen YC, Wu CF, Lin SH (2014) Mechanisms of forest restoration in landslide treatment areas. Sustainability 6: 6766-6780.

Dai FC, Lee CF, Ngai YY (2002). Landslide risk assessment and management: an overview. Eng. Geol. 64: 65-87.

Daniel G, Jaffre T, PrinY (1999). Occurrence of both *Casuarina*-infective and *Elaeagnus*-infective *Frankia* strains within actinorhizae of *Casuarina collina*, endemic to New Caledonia. Eur. J. Soil Biol. 35(1):9-15.

De Bates S, Poesen J, Gyssels G, Knapen A (2006). Effects of grass roots on the erodibility of topsoils during concentrated flow. Geomorphology 76:54-67.

De Baets S, Poesen J, Knapen A, Barberá GG, Navarro JA (2007). Root characteristics of representative Mediterranean plant species and their erosion-reducing potential during concentrated runoff. Plant Soil 294:169-183.

De Baets S, Poeson J, Reubens B, Wemans K, Baerdemaeker JD, Muys B (2008). Root tensile strength and root distribution of typical Mediterranean plant species and their contribution to soil shear strength. Plant Soil 305:207-226.

Diagne N, Arumugam K, Ngom M, Nambiar-Veetil M, Franche C, Narayanan KK, Laplaze L (2013). Use of *Frankia* and actinorhizal plants for degraded lands reclamation. Biomed. Res. Int. doi.org/10.1155/2013/948258.

Faure-Raynaud M, Daniere C, Moiroud A, Capellano A (1991). Diversity of *Frankia* strains isolated from single nodules of *Alnus glutinosa*. Plant Soil 132:207-211.

Genet M, Stokes A, Salin F, Mickovski SB (2005). The influence of cellulose content on tensile strength in tree roots. Plant Soil 278:1-9.

Gould IJ, Quinton JN, Weigelt A, de Deyn GB, Bardgett RD (2016). Plant diversity and root traits benefit physical properties key to soil function in grasslands. Ecol. Lett. 19:1140-1149.

Hooker JE and Wheeler CT (1987). The effectivity of *Frankia* for nodulation and nitrogen fixation in *Alnus rubra* and *A. glutinosa*. Physiol. Plant. 70:333-341.

Kendall JM, Tanaka Y, Myrold DD (2003). Dual inoculation increases plant growth with *Frankia* on red alder (*Alnus rubra* Bong.) in fumigated nursery beds. Symbiosis 34(3):253-260.

Lalonde M, Calvert HE (1979). Production of *Frankia* hyphae and spores as an infective inoculant for *Alnus* species. In: Gordon JC, Wheeler CT, Perry DA (eds), Symbiotic Nitrogen Fixation in the Management of Temperate Forests. Oregon State University,

Corvallis, OR, USA. pp. 95-110.
Lee MJ (1986). Seasonal variation of actinorhizal root nodule biomass and symbiotic nitrogen fixation in natural stands of Formosan alder. Q. J. Chin. For. 19(3):13-23.
Lefrançois E, Quoreshi A, Khasa D, Fung M, Whyte LG, Roy S, Greer CW (2010). Field performance of alder-*Frankia* symbionts for the reclamation of oil sands sites. Appl. Soil Ecol. 46:183-191.
Liao JC (1996). Betulaceae. In: Flora of Taiwan, 2nd Ed., Vol. 2, Editorial Committee of Flora of Taiwan (eds). Editorial Committee of Flora of Taiwan, Taipei, Taiwan, pp. 44-46.
Lin LP (1992). The ecological significance of *Frankia* isolated from *Alnus formosana* root nodules in northern Taiwan. In: Chiang CH, Wang YN (eds), Proceedings of the 1992 Joint International Symposium on Air Pollution, Soil Microbiology and Biotechnology of Forestry. Taipei, Taiwan, pp. 199-213.
Lumini E, Bosco M, Puppi G, Isopi R, Frattegiani M, Buresti E, Favilli F (1994). Field performance of *Alnus cordata* Loisel (Italian alder) inoculated with Frankia and VA-mycorrhizal strains in mine-spoil afforestation plots. Soil Biol. Biochem. 26(5):659-661.
Lv CJ, Chen LH (2013). Relationship between root tensile mechanical properties and its main chemical components of typical tree species in North China. Trans. Chin. Soc. Agri. Eng. 29(3):69-78.
Martin KJ, Tanaka Y, Myrold DD (2003). Dual inoculation increases plant growth with *Frankia* on red alder (*Alnus rubra* Bong.). Symbiosis 34:253-260.
McEwan NR, Snelling TJ, Collins T, Girdwood SE, Wilkinson T, Dougal K, Jones DL, Godbold DL (2015). Lobes on *Alnus glutinosa* nodules contain a single major ribotype of *Frankia*. J. Endocyt. Cell Res. 25:83-86.
Mohammed S, Normaniza O (2014). Evaluation of hydro-mechanical properties and root architecture of plants for soil reinforcement. Curr. Sci. 107(5):845-852.
Naghdi R, Maleki S, Abdi E., Mousavi R, Nikooy M (2013). Assessing the effect of *Alnus* roots on hillslope stability in order to use in soil bioengineering. J. For. Sci. 59(11):417-423.
Normaniza O, Mohamad NA, Che HA (2011). Pullout and tensile strength properties of two selected tropical trees. Sains Malays. 40(6):577-585.
Nyambane OS, Mwea SK (2011). Root tensile strength of 3 typical plant species and their contribution to soil shear strength: a case study: Sasumua Backslope, Nyandarua District, Kenya. J. Civ. Eng. Res. Prac. 8(1):57-73.
Oliveira RS, Castro PM, Dodd JC, Vosátka M (2005).Synergistic effect of *Glomus intraradices* and *Frankia* spp. on the growth and stress recovery of *Alnus glutinosa* in an alkaline anthropogenic sediment. Chemosphere 60(10):1462-1470.
Orfanoudakis M, Wheeler CT, Hooker JE (2010). Both the arbuscular mycorrhizal fungus *Gigaspora rosea* and *Frankia* increase root system branching and reduce root hair frequency in *Alnus glutinosa*. Mycorrhiza 20(2):117-126.
Osman N, Abdullah MN, Abdullah CH (2011). Pull-out and tensile strength properties of two selected tropical trees. Sains Malays. 40(6):577-585.
Pang W, Crow WT, Luc JE, McSorley, Giblin-Davis RM (2011). Comparison of water displacement and WinRHIZO software for plant root parameter assessment. Plant Dis. 95:1308-1310.
Põlme S, Bahram M, Kõljalg U, Tedersoo L (2014). Global biogeography of *Alnus*-associated *Frankia* actinobacteria. New Phytol. 204:979-988.
Prat D (1989). Effect of some pure and mixed *Frankia* strains on seedling growth in different *Alnus* species. Pant Soil 113(1):31-38.
Quoreshi AM, Roy S, Greer CW, Beaudin J, McCurdy D, Khasa DP (2007). Inoculation of green alder (*Alnus crispa*) with *Frankia*-ectomycorrhizal fungal inoculant under commercial nursery production conditions. Native Plants J. 8:271-281.
Santi C, Bogusz D, Franche D (2013). Biological nitrogen fixation in non-legume plants. Ann. Bot. 111:743-767.
Schrader JA, Graves WR (2008). Nodulation and growth of *Alnus nitida* and *Alnus maritima* inoculated with species-specific and nonspecific *Frankia*. J. Environ. Hort. 26(1):29-34.
Stokes A, Atger C, Bengough AG, Fourcaud T, Sidle RC (2009). Desirable plant root traits for protecting natural and engineered slopes against landslides. Plant Soil 324:1-30.
Stokes A, Mattheck C (1996). Variation of wood strength in tree roots. J. Exp. Bot. 47:693-699.
Stokes A, Salin F, Kokutse AD, Berthier S, Jeannin H, Mochan S, Dorren L, Kokutse N, AbdGhani M, Fourcaud T (2005). Mechanical resistance of different tree species to rockfall in the French Alps. Plant Soil 278:107-117.
Vendan RT, Rajeshwari T, Narayanan R (1999). Studies on strain specificity of *Frankia* in *Alnus nepalensis*. Trop. Agric. Res. Ext. 2(2):124-125.
Wheeler CT, Henson IE, McLaughlin ME (1979). Hormones in plants bearing actinomycetes nodules. Bot. Gaz.140 (Suppl.):52-57.
Wheeler CT, Hollingsworth MK, Hooker JE, McNeill JD, Mason WL, Moffat AJ, Sheppard LJ (1991). The effect of inoculation with either cultured *Frankia* or crushed nodules on nodulation and growth of *Alnus rubra* and *Alnus glutinosa* seedlings in forest nurseries. For. Ecol. Manage. 43:153-166.
Yamanaka T, Akama A, Li CY, Okabe H (2005). Growth, nitrogen fixation and mineral acquisition of *Alnus sieboldiana* after inoculation of *Frankia* together with *Gigaspora margarita* and *Pseudomonas putida*. J. For. Res. 10(1):21-26.
Yamanaka T, Kobayashi H, Okabe H (2009). Effect of *Frankia* inoculation on the growth of *Alnus siebolaiana* on unsterilized soil. J. For. Res. 14(3):183-187.
Yang Y, Chen L, Li N, Zhang Q (2016). Effect of root moisture content and diameter on root tensile properties. PLoS ONE 11(3):e0151791.
Zhang CB, Chen LH, Liu YP, Ji XD, Liu XP (2012). Triaxial compression test of the soil-root composites to evaluate the influence of roots on soil shear strength. Ecol. Eng. 36:19-26.
Zhang CB, Chen LH, Jiang J (2014). Why fine tree roots are stronger than thicker roots: The role of cellulose and lignin in relation to slope stability. Geomorphology 206:196-202.
Zhang CB, Chen LH, Liu YP, Ji XD, Liu XP (2012). Triaxial compression test of the soil-root composites to evaluate the influence of roots on soil shear strength. Ecol. Eng. 36:19-26.

academicJournals

Vol. 17(7), pp. 226-231, 14 February, 2018
DOI: 10.5897/AJB2015.15126
Article Number: FABDF5655923
ISSN 1684-5315
Copyright © 2018
Author(s) retain the copyright of this article
http://www.academicjournals.org/AJB

African Journal of Biotechnology

Full Length Research Paper

Characterization of biodiesel obtained from atemoya (*Annona squamosa* × *A. cherimola*) seed oil

Luciana Soares Da Cruz[1], Bárbara Lemes Outeiro Araújo[2], Luiz Roberto Marques Albuquerque[1], Pedro Castro Neto[2], Angelita Duarte Corrêa[1] and Luciana de Matos Alves Pinto[1*]

[1]Departamento de Química, Universidade Federal de Lavras (UFLA), Campus Universitário, Caixa Postal 3037, CEP 37200-000, Lavras - MG, Brazil.
[2]Departamento de Engenharia Agrícola, Universidade Federal de Lavras (UFLA), Campus Universitário, Caixa Postal 3037, CEP 37200-000, Lavras - MG, Brazil.

Received 25 November, 2015; Accepted 30 September, 2016

Biodiesel is derived from renewable sources, such as vegetable oils, by means of a transesterification process in which triacylglycerols are transformed into smaller molecules of esters of fatty acids and glycerol. The transesterification reactions of 'Gefner' atemoya (*Annona squamosa* × *A. cherimola*) seed oil extracted by pressing (physical) and solvent (chemical) processes were studied, with analysis of the methyl esters produced. The reactions were monitored using gas chromatography coupled to mass spectrometry (GC-MS), as well as by hydrogen nuclear magnetic resonance spectroscopy (^{1}H-NMR). The methyl esters formed during the transesterification reaction with methanol were determined for each oil. The major methyl esters (16:0, 18:0, 18:1 and 18:2) formed during 50 min of reaction were similar to those reported in the literature for other biodiesels; the peak areas and retention times were also similar. No changes in signal intensity over time were observed for the oils obtained by the two extraction methods. It was also noted that the extraction method had no influence on the types of methyl esters formed during biodiesel production.

Key words: Annona, oil extraction, transesterification.

INTRODUCTION

Biodiesel consists of mono-alkyl esters of long-chain fatty acids derived from renewable sources such as vegetable oils, obtained by a transesterification process in which triglycerides are transformed into smaller molecules of fatty acid esters and glycerol. Its use is intended to replace fossil fuels in diesel engines. It has promising potential, not only for its important contribution to reducing environmental pollution, but also for the generation of renewable energy as a replacement for fossil diesel and other petroleum products (Pinto et al., 2005).

In 2013, Brazil was the world's second largest biodiesel

*Corresponding author. E-mail: luca@dqi.ufla.br.

Author(s) agree that this article remains permanently open access under the terms of the Creative Commons Attribution License 4.0 International License

consumer, only behind the United States, which had a demand of 5.2 million m^3. In terms of production, the USA is the global leader, with production of 5.1 million m^3 in 2013, followed by Germany and Brazil, with production of 3.6 and 3.0 million m^3 of biodiesel, respectively (Agência Nacional do Petróleo (ANP), 2013).

In 2004, the Brazilian government launched the National Program for Biodiesel Production (PNPB). Biodiesel can be used to partially or totally replace mineral diesel for light vehicles, trucks, tractors, and generators. In Brazil, the biodiesel mixture has been regulated by law since 2008. At first, the mandatory mixture was 2%, and it has been progressively increased to 5% (Kohlhepp, 2010).

Biodiesel is registered by the United States Environmental Protection Agency as a fuel and as an additive for fuels (Ferrari et al., 2005). After transesterification, biodiesel can be used neat at 100% (B100) or at proportions of 5% upwards in mixtures whose use is intended to replace fossil fuels in diesel cycle engines, without any need for modification of the engine. Various vegetable oils have been successfully tested in transesterifications with methanol or ethanol for the production of biodiesel. The seeds of peanuts, sunflowers, and soybeans, with oil contents of 41.3, 60.2, and 24.5 g 100 g^{-1}, respectively, are widely used for biodiesel production (Constantino et al., 2014). Oils extracted from different fruits have also been explored for biodiesel production (Adekunle et al., 2016; Alexandre et al., 2015), offering non-conventional sources of this biofuel.

Atemoya is an interspecific hybrid of cherimoya (*Annona cherimola*) and sugar-apple (*Annona squamosa*). It was introduced to Brazil in the 1980s and is mainly grown in the south and southeast of the country. In the 1990s, the 'Gefner' hybrid variety was successfully introduced in the northeast of Brazil. The cultivated area now exceeds 1,500 hectares, spread over the States of São Paulo and Paraná, as well as the northeast region (Braga-Sobrinho, 2014).

Atemoya seeds represent around 8.4% of the weight of the fruit and have potential as a source of biodiesel, since the lipid content is 27.3 g 100 g^{-1} (Cruz et al., 2013). This content is close to that of other seeds such as soybeans, which are widely used for biofuel. The use of atemoya seeds to produce biodiesel can add value to the fruit.

The objective of this study was to analyze methyl esters produced during the transesterification reaction of the oil from 'Gefner' atemoya seeds, obtained by physical (pressing) and chemical (solvent) extraction.

MATERIALS AND METHODS

The atemoya was obtained during the 2010/2011 agricultural cycle in an orchard situated in the municipality of Jaíba, in northern Minas Gerais State, Brazil (14°33'-15°28'S, 43°29'-44°06'W, altitude of 500 m). The fruits were harvested at the appropriate stage of maturity and transported overland to Universidade Federal de Lavras. In the laboratory, the fruits were selected considering size, maturity, and absence of defects. Each replicate employed 82 fruits, totaling 902 fruits.

The seeds were separated and washed with distilled water, weighed, and dried in a forced-air circulation oven at 60 to 65°C until they reached humidity lower than 6%. The seeds were then vacuum-packed in plastic bags and stored at around -10°C in a cold chamber until oil extraction (AOAC, 2012).

Oil extractions

Oil extractions were performed by pressing (physical) and solvent (chemical) methods, as described by Cruz et al. (2015). Oil pressing was performed in a continuous expeller press, while chemical extraction employed a Soxhlet extractor with hexane as solvent at 68°C. Humidity determination was performed by dehydration of the oil until constant weight in an oven at 105°C, (Lutz, 2008).

Biodiesel production

Transesterification reactions were performed for 40 min at 50°C in a jacketed reactor, to which 200 ml of vegetable oil and 50 ml of methanol were added. This mixture was heated to a temperature of 50°C under mechanical stirring for 20min. After this time, 6 ml of sodium methoxide (30%) were added, maintaining the temperature and stirring for 40min. The solution was then transferred to a separation funnel for separation of the phases (biodiesel and glycerin) (Silva, 2005). Aliquots were removed at 0, 10, 20, 30, 40, and 50min of reaction. Subsequently, 1ml of each of the six aliquots was treated with 5ml of chloroform, 0.5ml of sulfuric acid, and 10ml of saturated sodium chloride solution. The organic phase obtained was dried with magnesium sulfate, the solvent was removed in a rotary evaporator, and the product was dried with a flow of nitrogen gas. The samples obtained were analyzed using gas chromatography-mass spectrometry (GC-MS), as well as by hydrogen nuclear magnetic resonance spectroscopy (^{1}H-NMR). For the GC-MS analyses, the samples were resuspended in 0.1 ml of hexane.

Chromatographic analysis

The samples were analyzed using a gas chromatograph coupled to a GC-MS QP2010 Plus mass spectrometer (Shimadzu, Japan) equipped with an AOC-5000 autosampler for liquids and gases (Shimadzu, Japan). A 30 m × 0.25 mm × 0.25 µm RTX-5MS column (5% phenyl to 95% dimethylsiloxane) was used for separation and identification of the compounds. The injector was operated at 220°C in split mode, with a split ratio of 1:20. The carrier gas used was He 5.0, at a flow rate of 1.18 ml min^{-1}. The oven temperature was programmed from 60 to 240°C, with a heating ramp of 5°C min^{-1}, and then from 240 to 270°C, with a heating ramp of 10°C min^{-1}, followed by a final hold at 270°C for 7min. An electron impact mass spectrometer (70 eV) was used in scan mode (45 to 500 Da), with solvent cutting at 3.5min. The detector interface and ion source temperatures were kept at 240°C and 200°C, respectively. The compounds were identified by comparing the mass spectra with library spectra (Wiley 8 and FFNSC 1.2 libraries).

Nuclear magnetic resonance analysis

The ^{1}H-NMR analyses employed an EFT-60 spectrometer (Anasazi Instruments, Indianapolis, USA), with one-dimensional spectra acquired for the biodiesel samples obtained by both methods.

Table 1. Methyl esters obtained from transesterification of the seed oil from 'Gefner' atemoya (% peak area), using two oil extraction methods: physical (P) and chemical (C).

Methyl esters of fatty acids	Number of carbons from the fatty acid: unsaturation number	Retention time (1st identification)	Reaction time (min)											
			1		10		20		30		40		50	
			P	C	P	C	P	C	P	C	P	C	P	C
Methyl octadecanoate	18:0	24.45	25.46	24.65	19.95	20.74	18.50	21.31	20.95	19.96	22.85	21.86	20.64	23.42
Methyl nonanoate	9:0	26.57	0.09	-	-	-	0.02	-	-	-	-	-	0.04	-
Methyl eicosenoate	20:0	28.10	0.07	8.95	0.08	-	0.12	3.5	3.05	2.83	0.03	-	0.06	-
Methyl hexadecanoate	16:0	28.62	27.39	29.39	21.26	21.49	20.47	22.85	22.72	21.61	24.54	23.85	22.2	24.30
Methyl (9z)-9-octadecenoate	18:1	30.09	41.95	24.31	56.62	29.96	32.89	27.95	29.2	29.82	25.06	26.13	28.69	25.26
Methyl heptadecanoate	17:0	30.53	0.64	1.77	0.66	0.47	0.39	0.64	0.62	0.44	0.87	0.64	0.44	-
Methyl nonadecanoate	19:0	34.16	0.14	0.61	0.14	-	-	-	-	-	0.19	0.14	-	-
Methyl eicosanoate	21:0	35.86	3.25	-	-	2.92	1.76	-	-	-	4.58	3.78	2.96	6.25
Methyl docosanoate	10:0	38.62	0.56	1.64	0.48	0.49	0.25	0.47	0.51	0.48	0.79	0.58	0.51	0.98
Methyl tetracosanoate	24:0	41.04	0.34	0.9	0.31	-	0.16	0.34	0.32	0.31	0.47	0.29	0.3	0.51
Methyl tetradecanoate	14:0	24.45	-	0.49	0.19	-	0.06	0.24	0.19	0.16	0.3	-	-	-
Methyl (9z)-9-hexadecenoate	16:1	28.19	-	1.31	0.3	0.45	0.3	0.94	-	0.36	1.56	0.94	0.5	1.65
Methyl (9z,12z)-9,12-octadecadienoate	18:2	31.86	-	3.73	-	23.08	24.86	21.12	22.04	23	17.72	21.03	22.81	15.32
Methyl (11e)-11-eicosenoate	20:1	35.45	-	1.53	-	-	0.14	-	-	0.44	0.84	0.59	0.42	1.15

Previously treated biodiesel samples (0.1ml) were dissolved in 0.1ml of chloroform deuterated with 99.8% deuterium ($CDCl_3$), in 5 mm NMR tubes. Tetramethylsilane (0.1 ml) was used as an internal reference standard.

RESULTS AND DISCUSSION

The yield of the transesterification reaction for the oil obtained by pressing of atemoya seeds was 89% methyl esters and 11% glycerin. The biodiesel yield for the chemical extraction was 91% methyl esters and 9% glycerin. These values differed from the results obtained for soybean biodiesel by Ferrari et al. (2005), who reported 57.26% ethyl esters, 22.29% glycerin, 10.04% recovered ethanol, and 10.41% losses. The concentration of glycerin in the biodiesel obtained from atemoya seeds was approximately half that obtained from soybeans, so the concentration of biodiesel was much higher, and losses were not observed.

Table 1 shows the profile of methyl esters for the transesterification reaction of the oil from 'Gefner' atemoya seeds. The major esters found in the atemoya biodiesel were 16:0, 18:0, 18:1, and 18:2.

The ester area percentages obtained for the physical and chemical extractions, after a reaction time of 50min, at which the biodiesel was decanted, were 22.2 and 24.3 (16:0), 20.64 and 23.42 (18:0), 28.7 and 25.26 (18:1), and 22.81 and 15.32 (18:2), respectively. Comparison of the results obtained here with the findings of Urioste et al. (2008) revealed the presence of one additional ester (18:2).

In chromatographic, determination of the esters of fatty acids was obtained in transesterification reactions of babassu oil with ethanol, propanol, and butanol. Urioste et al. (2008) reported the following areas (%) for ethyl, propyl, and butyl esters, respectively: 24.82, 22.82, and 23.52 (16:0); 21.56, 22.14, and 23.28 (18:0); and 24.60, 22.50, and 24.56 (18:1). It appears that there was virtually no difference between the areas of the three ethyl, propyl and butyl esters formed in babassu biodiesel.

In their study with soybean oil, Ferrari et al. (2005) observed the following areas (%) for ethyl esters of fatty acids: 11.29 (16:0), 3.54 (18:0), 22.45 (18:1), 54.62(18:2), and 8.11 (18:3), with a predominance of unsaturated fatty acids. These esters were the same as those obtained in the transesterification of atemoya seed oil, with the exception of the 18:3 ester, which was not found in atemoya oil. The 18:2 methyl ester of the atemoya seed oil extracted by the pressing and solvent methods showed areas of 22.81% and

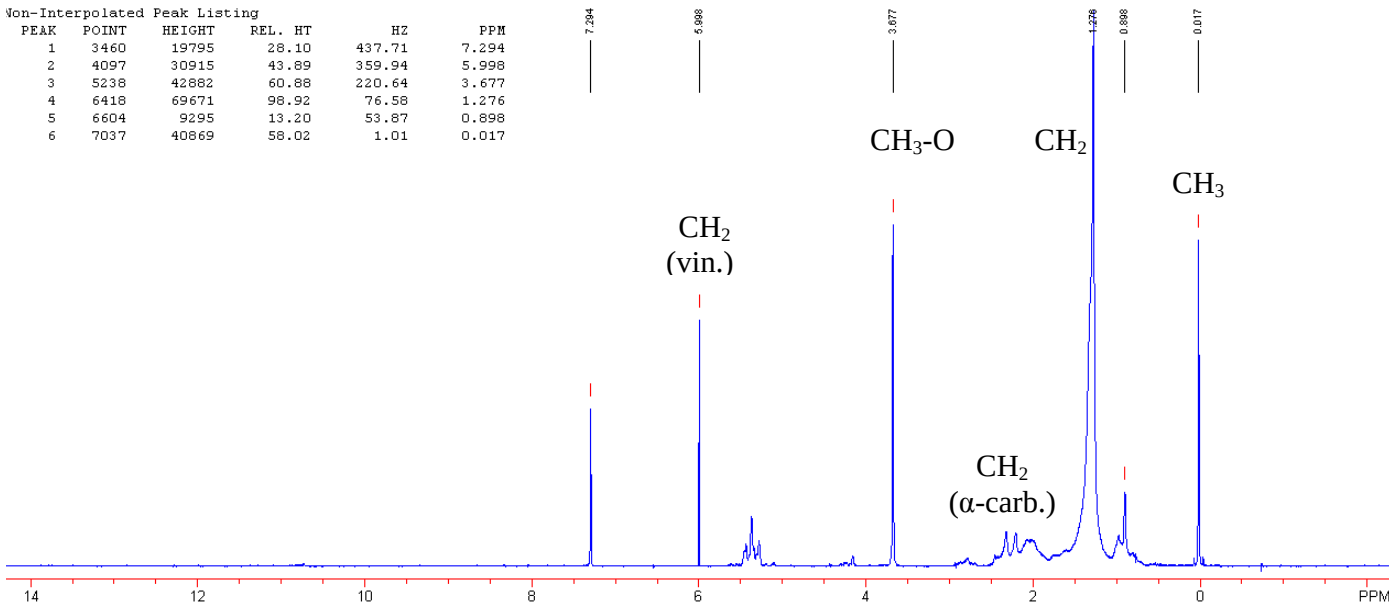

Figure 1.^{1}H-NMR spectrum of methyl esters obtained in the transesterification of the 'Gefner' atemoya seed oil extracted physically (by pressing), at 50 min reaction time.

15.32%, respectively, which were smaller than the value obtained for soybean oil. On the other hand, the 18:0 and 18:1 esters of atemoya oil had greater areas, compared to the soybean oil, with values of 20.64% (pressed) and 23.42% (solvent extracted), and 28.69% (pressed) and 25.26% (solvent extracted), respectively. These data show that the predominant esters in current biodiesels are 16:0, 18:0, 18:1, 18:2, and 18:3.

Marques et al. (2010) emphasized the importance of considering instrumental precision when evaluating major peak areas, in order to increase the accuracy of determination of esters of fatty acids formed during transesterification reactions. Barbosa et al. (2010) reported the following areas (%) for ethyl esters of soybean seed oil: 16.0 (16:0), 2.4 (18:0), 23.5 (18:1), and 51.2 (18:2). In the present work, greater areas were obtained for 16:0, 18:0, and 18:1 esters in the atemoya oil biodiesel obtained using both forms of oil extraction (press and solvent), while the value obtained for the 18:2 ester was smaller. Benito et al. (2014) studied the biodiesel potential of Annona diversifolia seed oil and reported the following areas (%) for methyl esters: 16.4 (16:0), 5.22 (18:0), 70.4 (18:1), and 7.97 (18:2). The areas obtained for the 16:0, 18:0, and 18:2 methyl esters were greater for the decanted biodiesel from atemoya oil extracted by both techniques (physical and chemical), while the area was smaller for the 18:1 ester.

Methanol is the main alcohol used in transesterification in many countries (Pinto et al., 2005). In Brazil, several research groups and small producers use the methyl pathway for the production of biodiesel, because methanol is more reactive, while ethanol causes greater dispersion of glycerin in the biodiesel, making separation difficult (Lôbo et al., 2009). A reaction time of 30min was required for the formation of methyl esters in the biodiesel, similar to the duration of 25min reported by Urioste et al. (2008) for biodiesel from Babassu, where the major esters formed were 16:0, 18:0, and 18:1.

Encinar et al. (2002) observed that the transesterification reaction was very fast, with conversion into ethyl esters close to the maximum value after only 5 to 10min of reaction, and stabilization at a maximum value after 20 to 30min. These values were similar to those found for the formation of biodiesel from atemoya oil, which occurred after 20 to 30min of reaction. However, in the study of Ferrari et al. (2005), chromatographic monitoring of the products formed after various reaction times showed that a time of 5min was sufficient for the conversion of neutral and dried oil into ester. The conversion of fatty acids into methyl esters in the atemoya oil occurred between 5 and 10min of reaction, stabilizing at a maximum value after 20 to 30min. The physical extraction (pressing) of atemoya seed oil is economically advantageous and provides a high oil extraction efficiency of 88.9g 100 g^{-1} (dry mass basis) (Cruz et al., 2015).

Furthermore, in comparison with chemical extraction using solvent, a disadvantage of the latter has greater oxidation of the extracted oil. The profile of the methyl esters identified by GC-MS was confirmed by ^{1}H-NMR. Figures 1 and 2 show the major chemical shifts characterizing the esters, formed after 50 min of reaction. No changes in signal strength or in the hydrogen chemical shifts with time were observed after the

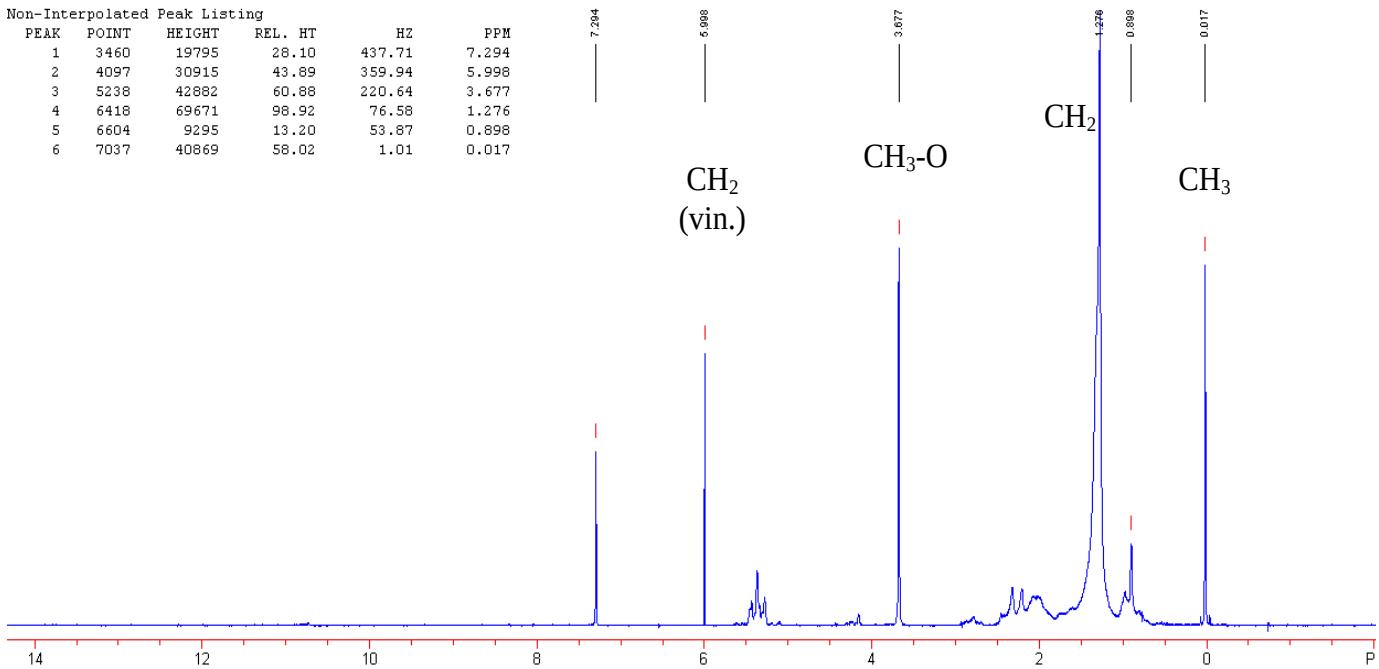

Figure 2. ^{1}H-NMR spectrum of methyl esters obtained in the transesterification of the 'Gefner' atemoya seed oil extracted chemically (using solvent), at 50 min reaction time.

Table 2. Chemical shifts (ppm) obtained by ^{1}H-NMR (60 MHz) of biodiesel in $CDCl_3$ at 25°C (physical extraction).

H	δ_H	
	Atemoya biodiesel	**Paiva et al. (2010)**
CH_3	0.89	0.90
CH_2	1.27	1.2 – 2.5
CH_2 (α-carbonyl)	2.40	2.1 – 2.5
CH_3-O	3.68	3.5 – 4.8
CH_2 (vinylic)	5.99	4.5 – 7.0

Table 3. Chemical shifts (ppm) obtained by ^{1}H-NMR (60 MHz) of biodiesel in $CDCl_3$ at 25°C (chemical extraction).

H	δ_H	
	Atemoya biodiesel	**Paiva et al. (2010)**
CH_3	0.89	0.90
CH_2	1.27	1.2 – 2.5
CH_2 (α-carbonyl)	2.40	2.1 – 2.5
CH_3-O	3.68	3.5 – 4.8
CH_2 (vinylic)	5.99	4.5 – 7.0

transesterification reactions of the atemoya oils obtained by the two extraction methods (physical and chemical). This suggests that the extraction method had no influence on the characteristics of the oil obtained, or, therefore, on the product (biodiesel). Tables 2 and 3 show the ^{1}H-NMR data (60 MHz) for the biodiesel (in $CDCl_3$), compared with the literature. There was a good correlation of the chemical shifts in the spectra with the data reported by Paiva et al. (2010).

Conclusions

The methyl esters formed from the 16:0, 18:0, 18:1, and 18:2 fatty acids during the transesterification reaction were similar to those present in other current biodiesels. The method used for oil extraction had no influence on the types of methyl esters formed during biodiesel production.

The oil from atemoya seeds has potential for use as biodiesel, with advantages including addition of value to the fruit and a use for unwanted biomass (the seeds) that might otherwise be treated as waste.

CONFLICT OF INTERESTS

The authors have not declared any conflict of interests.

ACKNOWLEDGMENTS

The authors would like to thank CAPES and FAPEMIG

for financial support, and the Center for Analysis and Chemical Prospecting (CAPQ) at the Chemistry Department of UFLA for the use of equipment.

REFERENCES

Adekunle AS, Oyekunle JAO, Obisesan OR, Ojo OS, Ojo OS (2016). Effects of degumming on biodiesel properties of some non-conventional seedoils. Energy Rep. 2:188-193.

Agência Nacional do Petróleo (ANP)(2013). Brazilian National Agency of Petroleum, Natural Gas and Biofuels – ANP. Gás Natural e Biocombustíveis. Resolução nº 30. Biocombustíveis. Available at: <http://anp.gov.br/?pg=60467&m=&t1=&t2=&t3=&t4=&ar=&ps=&cachebust=1412632 744151>. Accessed: March 3rd, 2015.

Alexandre ACF, Silveira EV, Castro CFS, Sales JF, Oliveira LCS, Viana LH, Barbosa LCA (2015). Synthesis, characterization and study of the thermal behavior of methylic and ethylic biodiesel produced from tucumã (*Astrocaryum huaimi* Mat.) seed oil. Fuel 161:233-238.

Association of Official Analytical Chemistry (AOAC) (2012). Official Methods of Analysis. 19th ed. Gaithersburg, 3000p.

Barbosa CD, Serra TM, Meneghetti SMP, Meneghetti MR (2010). Biodiesel production by ethanolysis of mixed castor and soybean oils. Fuel 89:3791-3794.

Benito RT, Ramírez DG, Prada HZ, Sánchez JAC, Lino Reyes L, Chumacero AR, Salazar JAR (2014). *Annona diversifolia* seed oil as a promising non-edible feedstock for biodiesel production. Ind. Crops Prod. 52:400-404.

Braga-Sobrinho R (2014). Integrated production of *Annonaceae* in Brazil. Rev. Bras. Fruticult. 36(SPE1):102-107.

Constantino AF, Lacerda JRV, Santos RB, Greco SJ, Silva RC, Neto AC, Barbosa LL, Castro EVR, Freitas JCC (2014). Análise do teor e da qualidade dos lipídeos presentes em sementes de oleaginosas por RMN de baixo campo. Quím. Nova 37(1):10-17.

Cruz LS, Corrêa AD, Bastos VA, Neto PC, Pinto LMA (2015). Chemical and physicochemical characterization of the seed oil from 'Gefner' atemoya. Afr. J. Biotechnol. 14(2):143-148.

Cruz LS, Lima RZ, Abreu CMP, Corrêa AD, Pinto LMA (2013). Physical and chemical characterization of fractions of fruit atemoya Gefner. Ciênc. Rural 43(12):2280-2284.

Encinar JM, González JF, Rodríguez JJ, Tejedor A (2002). Biodiesel fuels from vegetables oils: transesterification of *Cynara cardunculus* L. oils with ethanol. Energ. Fuels 19:443-450.

Ferrari RA, Oliveira VS, Scabio A (2005). Biodiesel de soja: taxa de conversão em ésteres etílicos, caracterização físico-química e consumo em gerador de energia. Quím. Nova 28(1):19-23.

Kohlhepp G (2010). Análise da situação da produção de etanol e biodiesel no Brasil. Estud. Av. 24(68):223-253.

Lôbo IP, Ferreira SLC, Cruz RS (2009). Biodiesel: Parâmetros de qualidade e métodos analíticos. Quím. Nova 32(6):1596-1608.

Lutz IA (2008). Métodos químicos e físicos para análise de alimentos. 4th edition. IMESP, São Paulo. 1020p.

Marques MV, Naciuk FF, Mello MAS, Seibel NM, Fontoura LAM (2010). Determinação do teor de ésteres graxos em biodiesel metílico de soja por cromatografia gasosa utilizando oleato de etila como padrão interno. Quím. Nova 33(4):978-980.

Paiva DL, Lampman GM, Kriz GS, Vyvyan JRS (2010). Introdução à Espectroscopia. 4th edition. Cengage Learning, São Paulo. pp.150-152.

Pinto AC, Guarieiro LLN, Rezende MJC, Ribeiro NM, Torres EA, Lopes WA, Pereira PAP, Andrade JB (2005). Biodiesel, an overview. J. Braz. Chem. Soc. 16:1313-1330.

Silva CLM (2005). Obtenção de ésteres etílicos a partir da transesterificação do óleo de andiroba com etanol. Dissertation. Universidade Estadual de Campinas, Instituto de Química, Campinas, SP. 64p.

Urioste D, Castro MBA, Biaggio FC, de Castro HF (2008). Síntese de padrões cromatográficos e estabelecimento de método para dosagem da composição de ésteres de ácidos graxos presentes no biodiesel a partir do óleo do babaçu. Quím. Nova 31(2):407-412.

African Journal of Biotechnology

Related Journals Published by Academic Journals

- *Biotechnology and Molecular Biology Reviews*
- *African Journal of Microbiology Research*
- *African Journal of Biochemistry Research*
- *African Journal of Environmental Science and Technology*
- *African Journal of Food Science*
- *African Journal of Plant Science*
- *Journal of Bioinformatics and Sequence Analysis*
- *International Journal of Biodiversity and Conservation*

academicJournals